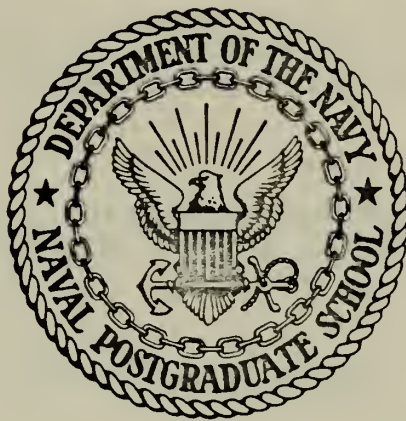


IMPLEMENTATION AND TESTING OF A
PROPOSED DIFFERENTIAL OMEGA SYSTEM

Robert Lawrence Vence

NAVAL POSTGRADUATE SCHOOL

Monterey, California



THESIS

IMPLEMENTATION AND TESTING OF A
PROPOSED DIFFERENTIAL OMEGA SYSTEM

by

Robert Lawrence Vence, Jr.

Thesis Advisor:

C. E. Menneken

June 1972

Approved for public release; distribution unlimited.

Implementation and Testing of a
Proposed Differential Omega System

by

Robert Lawrence Vence, Jr.
Lieutenant Commander, United States Coast Guard
B.S., United States Coast Guard Academy, 1963

Submitted in partial fulfillment of the
requirements for the degree of

ELECTRICAL ENGINEER

from the
NAVAL POSTGRADUATE SCHOOL
June 1972

ABSTRACT

Omega is a very low frequency (VLF) navigation system which will give world-wide coverage with eight stations when fully implemented. Using published skywave correction tables accuracies of 1 to 2 n.mi. are attainable. Through the use of differential Omega, correction information can be disseminated to users in the vicinity of a monitor site. Differential Omega accuracies are directly proportional to distance from the monitor site and are 0.26-0.5 n.mi. at 200 n.mi. from the monitor site.

A system using U.S. Coast Guard radiobeacons as the differential information transmitter was proposed by Goodman and McKaughan. Their proposals were examined and improvements suggested. Two additional differential Omega systems being proposed by civilian contractors were also examined.

The interface between an Omega receiver and the radiobeacon was built and tested. This device produced a CPE of 25 yds. (0.16 cec) and a 95% circular error of 52 yds. (0.32 cec) at the monitor site for LOPs crossing at 72° which is a marked improvement over accuracies that can be attained using skywave correction tables.

TABLE OF CONTENTS

I.	INTRODUCTION -----	8
A.	LORAN A/C -----	8
B.	RAYDIST "T" -----	9
C.	LORAC -----	9
II.	OMEGA -----	13
A.	SYSTEM DESCRIPTION -----	13
B.	VLF PROPAGATION -----	18
	1. Skywave Correction Tables -----	19
	2. Regular Diurnal Phase Change -----	20
	3. Other Anomalous Variations -----	23
	a. Solar Flares -----	23
	(1) Short Distance Effects -----	23
	(2) Effects at Greater Distances -----	24
	(3) Origin and Energy Spectrum of a Solar Flare -----	24
	(4) Frequency of Flares Versus Disturbance to VLF Transmission -----	25
	(5) Terrestrial Effects of a Solar Flare -----	25
	b. Magnetic Activity -----	25
	c. Meteor Showers -----	27
	d. Atomic Device Explosion -----	28
	(1) Prompt VLF Effects -----	28
	(2) Delayed VLF Effects (1.5 to 5 Minutes) -----	28

(3) Delayed VLF Effects (15 to 40 Minutes) -----	29
(4) Phase Shifts of High Altitude Nuclear Explosions -----	29
e. Ionospheric Variations -----	29
f. Polar Cap Absorption (PCA) -----	31
g. Ground Conductivity -----	32
h. Geomagnetic Path Orientation -----	33
i. Propagation Over Land-Sea Boundary -----	35
4. Model for Phase of Received Signal -----	36
III. DIFFERENTIAL OMEGA -----	42
A. GENERAL CONCEPT -----	42
B. DETERMINATION OF SPATIAL CORRELATION OF OMEGA SIGNALS -----	44
C. PROPOSED DIFFERENTIAL OMEGA SYSTEMS -----	50
1. French System by Sercel Company -----	50
2. Micro-Omega -----	54
IV. DIFFERENTIAL OMEGA SYSTEM USING COAST GUARD RADIOBEACON -----	63
A. GENERAL DESCRIPTION -----	63
B. CHANGES TO GOODMAN'S PROPOSAL -----	67
1. Transmitter -----	67
2. Differential Omega Correction Information -----	70
3. Coding Message Format -----	71
C. IMPLEMENTATION OF RADIOBEACON MODULATOR -----	76
1. Message Format Commutator -----	76
2. LOP Differential Correction Circuit -----	82
a. Voltage Controlled Oscillator (VCO) -----	83

b.	Subtractor Circuit -----	83
c.	Voltage Reference Circuit -----	89
d.	Final Differential Omega Correction Circuit -----	96
V.	TESTING AND ANALYSIS -----	99
A.	RESULTS OF TESTING WITHOUT TRANSMITTER -----	99
B.	RESULTS OF TESTING WITH TRANSMITTER -----	106
C.	ANALYSIS OF RESULTS -----	111
1.	Test Results -----	111
2.	Digitizing Errors -----	112
3.	Receiver Errors -----	113
4.	LOP Errors Caused by Ship Velocity -----	117
D.	ADVANTAGES AND DISADVANTAGES OF USING THE COAST GUARD RADIOBEACON AS A DIFFERENTIAL OMEGA CORRECTION TRANSMITTER -----	118
1.	Advantages -----	118
2.	Disadvantages -----	119
VI.	SUMMARY -----	122
APPENDIX A:	READ ONLY MEMORY TRUTH TABLE -----	127
APPENDIX B:	COMMUTATOR CIRCUIT -----	131
APPENDIX C:	DIFFERENTIAL OMEGA LOP CORRECTOR CIRCUIT -----	134
APPENDIX D:	COMPUTER PROGRAM -----	136
APPENDIX E:	COMPUTER PRINTOUT -----	138
BIBLIOGRAPHY	-----	143
INITIAL DISTRIBUTION LIST	-----	146
FORM DD 1473	-----	147

LIST OF FIGURES

1.	Comparison of Navigation Systems -----	10
2.	Omega Signal Format -----	16
3.	Omega Implementation Schedule -----	18
4.	Typical Diurnal Phase Change -----	22
5.	Idealized Sunrise Transition on a Long East-West Path -----	22
6.	The Terrestrial Effects of a Solar Flare -----	26
7.	Phase Shift of Omega Signals Due to Three High Altitude Nuclear Bursts -----	30
8.	Effect of Ionospheric Disturbance -----	43
9.	A Differential Omega System -----	45
10.	RMS Differential Omega Error -----	47
11.	Relation of Bearing Angle Error to Phase Deviation -----	49
12.	Sercel Differential Omega Transmitting Station -----	52
13.	Sercel Differential Omega Reception Station -----	52
14.	Test Results of Sercel Differential Omega System -----	55
15.	Micro-Omega Transmitting Station -----	57
16.	Micro-Omega Shipboard Receiver -----	57
17.	Micro-Omega System Geometry -----	58
18.	Goodman's Differential Omega Transmission System -----	64
19.	Manual and Automatic Differential Omega Reception System -----	66
20.	Proposed Radiobeacon Differential Omega System -----	69
21.	Goodman's Differential Omega Message -----	72

22.	McKaughan's Differential Omega Message -----	74
23.	Proposed Differential Omega Message Format -----	77
24.	Block Diagram of Commutator Circuit -----	79
25.	Sample from Read Only Memory Truth Table -----	80
26.	Block Diagram of LOP Correction Generator -----	84
27.	Circuit Diagram for VCO -----	84
28.	Frequency Versus Voltage of VCO -----	85
29.	Subtractor Circuit -----	86
30.	Block Diagram of Differential Omega Corrector Using Adder -----	86
31.	Schematic of Voltage Regulator Circuit -----	90
32.	Example of Cyclic Nature of Omega Corrections -----	90
33.	Voltage Comparator Switching Circuit -----	94
34.	Block Diagram of Differential Omega LOP Corrector -----	97
35.	First Differential Omega LOP Corrector Test Layout Without Transmitter -----	100
36.	Effect of Solar Flare on Phase of Omega Signal and Differential Omega LOP Corrector, 2 March 1972 -----	101
37.	Summary of Accuracy of Differential Omega Corrector Using Strip Chart Recorder -----	104
38.	Second Differential Omega LOP Corrector Test Layout Without Transmitter -----	107
39.	Summary of Differential Omega Corrector Accuracy Using Digital Recorder Without Transmitter -----	108
40.	Differential Omega LOP Corrector Test Circuit with Transmitter -----	109
41.	Summary of Accuracy of Differential Omega Corrector with Transmitter -----	110
42.	Difference Between Two Tracor 599R Receivers Tracking the Same Signal (Trinidad-Hawaii) -----	115
43.	Difference Between Two Channels on the Same Tracor 599R Receiver Tracking the Same Signal --	116

I. INTRODUCTION

In mid-ocean, navigational accuracies of from 2 - 5 n.mi. are generally conceded to be adequate. As the coasts and harbor entrances are approached however, more precise navigation is desirable. This close-in region, generally called the coastal confluence region, extends to about 400 n.mi from the coast. Several systems are presently being used for navigation in the coastal confluence region and two of these are also useful for mid-ocean navigation. These systems are generally useful for ship positioning where high accuracy and reproducibility are required. Because mid-range frequencies are generally used, the range and accuracy of these systems will be limited during the evening hours by skywave effects. Lane ambiguity problems (to be described in detail later) are troublesome with phase comparison systems and require that the navigator know his initial checkpoint and keep an accurate track record.

A. LORAN A/C

Pulse time measurement systems are capable of fixing a ship's position by reception and identification of pulses received in a timed sequence from transmitting stations of known position. About 35% of the northern hemisphere is effectively covered by Loran A and 8% by Loran C [24]. Loran C equipment makes use of lower frequencies than Loran A and uses both pulse time and phase matching techniques.

Although the worldwide coverage is not as great for Loran C as it is for Loran A, the system is useful to greater ranges from the transmitter--100 - 2300 n.mi.--and is capable of high accuracy. With good operating conditions Loran C accuracy can approach one foot per mile of range. Loran A has an estimated accuracy of 0.5 to 3.0 n.mi., depending on where the user lies in the hyperbolic net. Neither Loran A or Loran C suffers any ambiguity problems.

B. RAYDIST "T"

Raydist "T" is a hyperbolic phase comparison navigation system which requires four shore stations. Since this system uses phase comparison techniques for establishing ranges from the receiver to each shore station, lane ambiguities are a major problem.

C. LORAC

The Lorac (Long-Range Accuracy) system was developed for oil exploration activities. It uses a CW phase comparison method which requires three shore stations. The lane ambiguity problem can be minimized by doubling the number of transmitters. This system is used by both commercial and Government survey groups for near shore control work. Working ranges are 100 - 150 n.mi. Ranging accuracies of 1:50,000 are readily obtained with this system.

Since Loran A was introduced to the navigator during WW II, the search for longer range, more accurate electronic navigation systems has been pursued. One of the proposed

LORAN A	700 - 900 n.mi.	$\pm 0.5 - 3.0$ n.mi.	1.75 - 2 MHz	Easy to use, insufficient coverage, subject to skywave interference. Less accuracy with sky-wave.
LORAN C	1200 - 1500 n.mi.	$\pm 0.2 - 0.5$ n.mi.	100 kHz	Accurate, easy to use, insufficient coverage, expensive installation. Less accuracy with sky-wave.
LORAC	135 n.mi.	25 - 100 feet	1.7 - 2.5 MHz	Hyperbolic geometry portable survey system; requires three shore sta. Continuous tracking reqd. Night effect reduces range.
Raydist T	25 - 200 n.mi.	25 - 250 feet	3.3 MHz	Hyperbolic geometry system. Night effect reduces range. Continuous tracking required.
Omega	5000 n.mi	$\pm 1.0 - 2.0$ n.mi.	10 - 14 kHz	World-wide coverage. Will use three frequencies to yield both coarse and fine grids.

Figure 1. Comparison of Navigation Systems.

systems, called Radux, used the arrival time of the signal in terms of the phase of the transmitted signal instead of the beginning of the pulse signal as Loran A does. As an outgrowth of Radux experiments and the shortcomings of previous systems, a very-low frequency (VLF) navigation system called Omega was proposed. VLF was chosen because the Radux experiments showed that timing errors did not increase markedly with increasing distance and VLF showed extremely low attenuation rates [24]. The VLF band also shows very stable propagation characteristics that can be readily predicted.

Despite the advantages of VLF transmission, there are several drawbacks, the most serious of which is the diurnal (daily) phase shift of the VLF signal due to changes in the ionosphere. Other effects caused primarily by the sun's emissions produce variations (anomalies) to the predicted diurnal phase values.

These anomalous variations in the phase of the VLF signal are why the concept of differential Omega is of value. If some fixed site, referred to as the monitor site, receives the Omega signals and compares them to what they should be at the monitor site's geographic position, then the difference between the expected and the actual values can be disseminated by some means to Omega users in the immediate vicinity who may be subject to the same error. Upon receipt of this information the navigator may apply the corrections to his received Omega LOPs. The differential or relative Omega concept is

not new but has been referred to before in "A Technical Evaluation of the Omega System" dated 18 December 1962 by NELC, San Diego and in many other reports since then. The use of differential Omega and Omega would allow one system to serve both the mid-ocean and coastal confluence navigator.

Goodman's thesis [7] proposed the already established U.S. Coast Guard radiobeacon net as an inexpensive, readily available means of transmitting differential information along the United States' coastlines. Goodman's and McKaughan's [13] coding message formats have been examined in this thesis and improvements suggested. The design of a commutation circuit to implement the coding format for the differential Omega message was completed. A single line of position differential Omega correction device was built and tested first by itself and then using the CG radiobeacon as a transmission vehicle in a closed loop transmission system. The reasons for the anomalous phase variations were also examined. In addition other differential Omega systems currently being considered for implementation in the United States and France were investigated.

II. OMEGA

A. SYSTEM DESCRIPTION

Omega like Loran measures the difference in time of arrival of two synchronized transmissions and thereby arrives at a hyperbolic line of position representing an equal time difference. As mentioned previously Omega measures the time difference by comparing the phase of the arriving signal. Since the baseline--a great circle connecting two Omega stations--is approximately 5000 - 6000 n.mi. long and the wavelength of 10.2 kHz radio waves is approximately 16 n.mi., it is apparent that there are many wavelengths of Omega signals and therefore many points of equal phase between the two stations. Line of position (LOP) ambiguities result because phase can only be electronically resolved into 360° segments within the receiver. The segments are reduced from 16 to 8 n.mi. when navigating using the hyperbolic mode because, as a ship travels one-half a wavelength along the baseline between two stations, the phase of the received signal of the station toward which the ship is moving, compared to the receiver internal oscillator, will decrease 180° . At the same time the received phase comparison for the other station will increase 180° since the ship has moved one-half wavelength away from that station. The resultant phase-difference between the two stations is 360° --this corresponds to an effective lane width for 10.2 kHz

on the baseline of 8 n.mi. Without additional information, the navigator cannot tell in which one of hundreds of 8 n.mi. lanes he lies. This problem is effectively eliminated by the transmission of multiple frequencies as will be explained later.

The extremely long baseline of VLF systems are especially effective on a spherical earth. For example, with a baseline subtending 60° of arc (approximately 4000 n.mi) the divergence between the hyperbolic LOPs is limited to a factor of two as one moves from the baseline instead of increasing infinitely as it does with a baseline negligibly long in comparison with the curvature of the Earth [24]. In addition to the decrease in divergence there is another important geometric factor which favors long baseline systems. Long baseline systems with optimum station placement insure that the crossing angles between LOPs will be large.

The use of VLF transmissions allows more than the necessary three stations needed for hyperbolic navigation to be observed at any point. Because each of the eight Omega stations will serve about $\frac{3}{4}$ of the surface of the Earth, there will usually be five or six stations providing useful signals [24]. Since any station can be measured with respect to any other, there will be either 10 or 15 LOPs available. The navigator is free to choose the three LOPs that give him the best signal or fix geometry.

Unlike the Loran A system which requires the receipt of the master pulse at the slave station before the slave transmits, Omega transmissions are synchronized to a common

precise time standard, universal time. This change was made possible by the introduction in 1953 of atomic time standards accurate to one part in 10^{10} . Each Omega station has a bank of four cesium atomic standards which when intercompared result in frequency accuracies better than one part in 10^{12} [21]. The standards are used both for carrier frequency synthesis and timing transmissions.

The various Omega stations transmit in accordance with the format shown in Figure 2. The length of the transmissions can be seen to vary between 0.9 and 1.2 seconds. This transmission sequence is designed to enable the user to identify each individual station since the pattern surrounding each station's transmission is unique. For example, to identify station D, the navigator would locate the 1.2 second pulse preceeded and followed by a 1.1 sec pulse. Station D can thus be distinguished from station G which also transmits a 1.2 sec pulse. The beginning of station A's transmission is synchronized so that A transmits at 0000 GMT each day and every ten seconds after that. Therefore a user with a WWV or WWVL receiver could manually synchronize his receiver commutator to match the transmission sequence. Modern Omega receivers perform this synchronization automatically by measuring the length of the transmission pulses and comparing them to the known transmission pattern until station identification has been completed.

Omega, as stated previously, differs from other hyperbolic systems in the use of very-low frequencies (10-14 kHz)

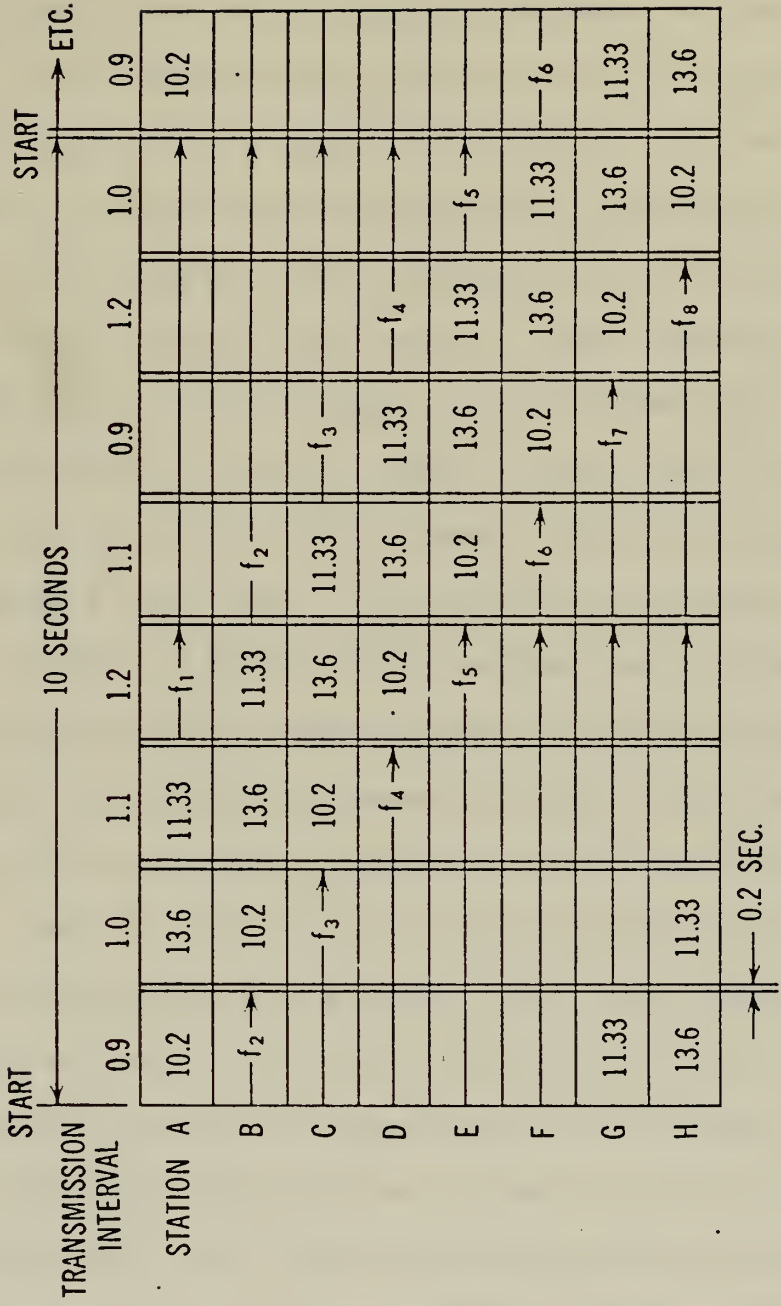


Figure 2. Omega Signal Format.

characterized by relatively stable propagation to very long distances (5000 to 8000 n.mi.). The 10.2 kHz signal provides the ship navigator with general navigation of the order of 1 mile accuracy using the published skywave correction tables, but with 8 n.mi. ambiguities. This is not a limitation when tracking the 10.2 kHz signal continuously. If there is an interruption to the reception owing to a station failure, or failure of the receiver, the navigator can re-establish the correct 8 mile lane by other means. Dead reckoning would suffice during the Omega outage if the accumulated error remained less than 4 miles. Weather permitting, celestial fixes to this same order of accuracy would also define the correct Omega 8 mile lane. Failure of one station in the proposed 8 station network would enable the navigator to select another station without loss of lane identity.

In order to reduce the dependency upon other navigation information to avoid lane ambiguity, additional frequencies are used. Use of 10.2 and 13.6 kHz provides a virtual difference frequency of 3.4 kHz. This lower frequency establishes a coarse lane with ambiguities spaced 24 n.mi. Although the precision of measurement at 3.4 kHz is reduced, it will suffice to identify the correct 8 mile lane within the 24 mile lane. For those navigators who know their position only to within \pm 36 miles, a third frequency, 11.33 kHz has been proposed. This would provide an unambiguous lane 72 n.mi. wide when used in conjunction with the 10.2 kHz signal.

At the present time there are four Omega stations transmitting at reduced power. These are located in Norway, Trinidad, Hawaii and New York. The New York station will be replaced by one at La Moure, North Dakota before the summer of 1972. The following figure shows the anticipated goal for placing the present stations on the air at full power--10 kW--and the construction dates of the remaining four stations.

10.2 kHz Transmission Segment	Station	On Air Date with 10 kW
A	Norway	Late 1973
B	Trinidad	Late 1973
C	Hawaii	Late 1972
D	North Dakota	Summer 1972
E	Reunion Is.	Late 1973
F	Argentina	Early 1974
G	Australia	Early 1974
H	Japan	Late 1972

Figure 3. Omega Implementation Schedule [2].

B. VLF PROPAGATION

Omega is a propagation limited system [28]. VLF propagation can best be regarded as being composed of various modes within the spherical waveguide formed between the earth and ionosphere. If several modes are present, modal interference may occur resulting in phase irregularities.

However, the principal mode may be expected to have the lowest attenuation rate and hence dominate at sufficiently large distances [23]. Because of this, Omega is considered a long range system and it is not recommended that any station closer than 600 n.mi. be used. The severity of modal interference will depend not only on separation from the transmitter but also propagation details such as the path, geomagnetic latitude, bearing and diurnal period.

Since waves are propagated within the guide formed between the earth and the ionosphere, variation of modal parameters such as phase velocity may be expected as a result of changes in the ionosphere or ground. The obvious navigationally undesirable variation is diurnal phase change. An uncorrected Omega LOP may vary as much as one complete lane from day to night. Ground-conductivity, latitude, Earth's magnetic field, path bearing, season and solar activity have also been demonstrated to have an effect on VLF phase.

1. Skywave Correction Tables

Diurnal and undesirable spatial variations are incorporated in skywave correction tables published by the Naval Oceanographic Office. All skywave correction tables published previous to 1970 were based on a global theory of Omega propagation incorporating theoretical and empirical physical principles where the relative contributions of the various effects are determined by regression analysis on millions of hours of data. The physical model has undergone

continual refinement at the Naval Electronics Laboratory Center for ten years [28]. Since the fall of 1970 skywave corrections, limited areas have been receiving the benefit of a force fit wherein local prediction errors are determined by monitoring and then removed over whatever spatial extent may be justified by the statistics [10].

2. Regular Diurnal Phase Change

When dealing with changes of phase it is important to understand what is meant by phase decrease or phase increase. In all cases in this thesis, the term phase decrease will mean that the number of centicycles (cec) decreases.¹ The term phase increase means the number of centicycles has increased. If one associates phase changes with changes of phase velocity brought about by changes in effective ionospheric reflecting height, a phase decrease corresponds to an increase in the phase velocity as a result of a decrease in height.

The apparent height of the reflection layer during the day varies with the zenith angle of the sun. The formula is

$$h_x = h(x=0) + h_s \log \sec x \quad (1)$$

provided $x < 85^\circ$. Here $h(x=0)$ is the height for an overhead sun and h_s is the change in height of the ionosphere

¹A centicycle is a term which is used frequently in connection with Omega navigation signals. It is defined as one-hundredth of a full cycle of phase change at the frequency under consideration. Therefore one cec at 10.2 kHz equals a LOP displacement of approximately 480 feet on the hyperbolic system baseline.

at the region of reflection. h_s has a mean value of 5.5 km but rises to about 7 km in October and April and falls to about 4 km in June and January. The value of $h(X=0)$ is 69 km [27].

The phase behavior of VLF signals propagated over long paths shows that the diurnal phase variation is trapezoidal with almost constant values during periods of nighttime or daytime propagation. A more or less steep phase increase and phase lag occurs at sunset and sunrise respectively.

Diurnal phase change of VLF signals is commonly expressed in microseconds as

$$\Delta t = D \left(\frac{1}{V_n} - \frac{1}{V_d} \right) 10^6 \quad (2)$$

where D is the path distance and V_n and V_d represent the night and day phase velocities of the first-order mode. This linear relationship is true only if no higher-order modes exist in the day or night earth-ionosphere waveguide at the receiver location [33]. Owing to the strong attenuation of the higher order modes, the model of the single-mode propagation applies approximately to the propagation over long distances.

Another expression used shows that the diurnal phase shift is almost directly proportional to the length of the path which is in daylight. This expression is

$$\Delta t = \frac{t \Delta h}{103 h} \quad (3)$$

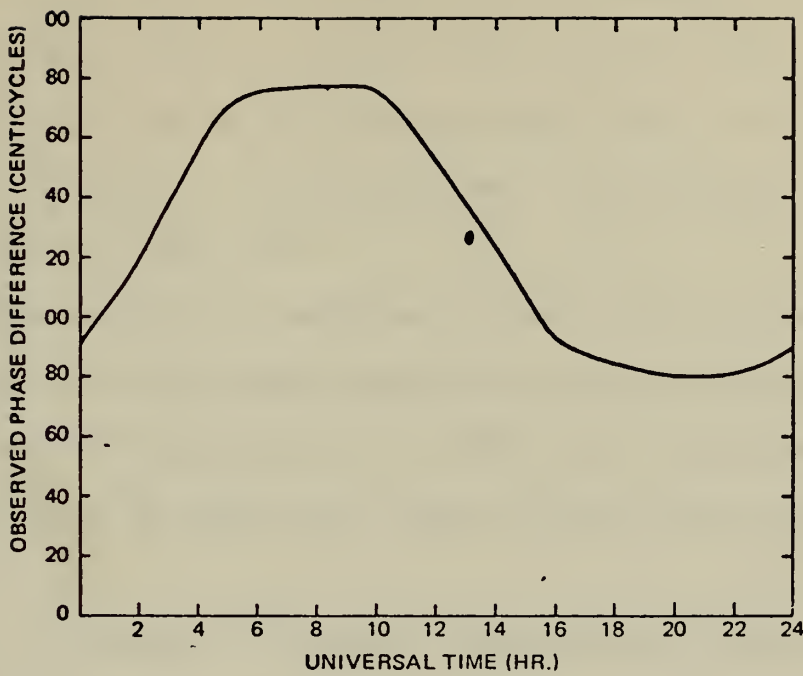


Figure 4. Typical Diurnal Phase Change (Haiku to Forestport, September 1968) [18].

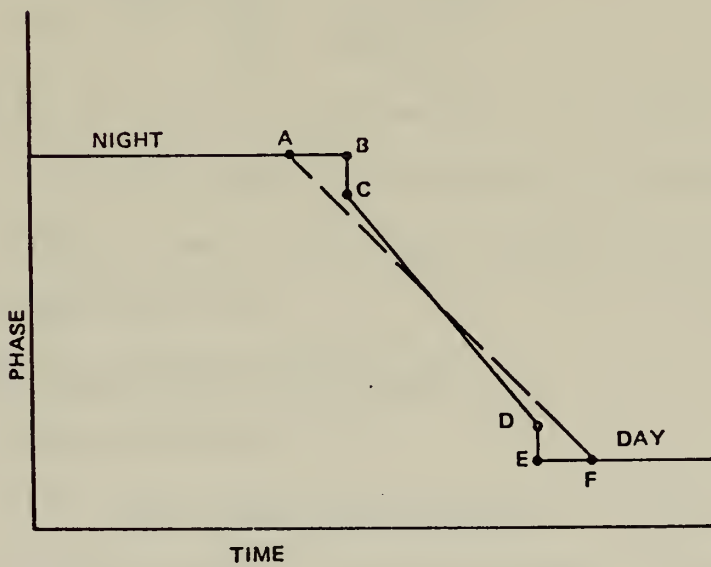


Figure 5. Idealized Sunrise Transition on a Long East-West Path. Sunrise occurs at the transmitter at Point A. The interval AB is approximately one-half hour. Phase shifts BC and DE are due to sudden changes in excitation factor. Point F shows sunrise at the receiver [18].

where $h = 80$ km, is taken to be the mean height between day and night, Δh = change in height from day to night, Δt = change in time of arrival of signal and $t = s/c$ where s = length of path in daylight under consideration and c = velocity of light [9].

This expression applies to the principal mode of propagation in a perfectly-conducting wave guide, and solutions using this expression are valid for distances greater than about 3000 km where the higher order modes may be neglected.

a. Variation of Diurnal Phase Shift with Distance

A final expression that expresses the change of phase of a received signal due to distance and the height changes in the ionosphere is

$$\Delta\phi = \frac{-2\pi d}{\lambda} \left[\frac{h}{2a} + \frac{\lambda^2}{16h^2} \right] \frac{\Delta h}{h} \quad (4)$$

where λ is the free space wavelength, h is the height of reflection, a is the radius of the earth, Δh the height of reflection changes, and d is the distance of the observer from the transmitter [5].

3. Other Anomalous Variations

a. Solar Flares

(1) Short Distance Effects. At short distances, up to 1000 km, the effects of solar flares on the phase of VLF signals are clearly visible. A flare effect is observed only during daylight hours and is associated with sudden ionospheric disturbances. These disturbances have a rapid

onset and slower recovery and last for times that vary from a few minutes up to a few hours. A phase decrease is observed at the same time as an HF radio fadeout and the optical sighting of the solar flare. It is found that the amplitude of the VLF signal does not change appreciably during the disturbance but the phase of the skywave decreases; hence the effect has been termed the "sudden phase anomaly" (SPA).

(2) Effects at Greater Distances. At oblique incidence, SPA's have been reported during the optical sighting of solar flares. The phase advance has an onset time of about 1 to 3 minutes, and recovery requires 30 minutes to 2 or 3 hours [4]. The magnitude of the phase shift is apparently related to the increase in solar radiation, its angle of incidence at the ionosphere and to the length of the path over which a lowering of the apparent reflection height occurs.

Sometimes solar flares occur which produce cosmic ray particles (solar protons). The sudden phase anomalies observed during these events are unusually large. Such events are quite rare however. The rapid ionization of the lower region of the ionosphere as a result of and coincident with the arrival of the cosmic-ray particles causes the phase of a VLF transmission to decrease at a rate apparently proportional to the increase in intensity of the solar cosmic radiation.

(3) Origin and Energy Spectrum of a Solar Flare.

During quiet conditions, the radiation of the quiet corona

and the transition region to the chromosphere exist permanently, whereas the emission of the hot regions occurs only during disturbed conditions. There is considerable evidence that when certain solar flares occur, the flux of energy arriving at the earth's atmosphere contains x-rays. These x-rays were produced in the coronal region at temperatures on the order of 10^8 degrees Kelvin. This is two orders of magnitude hotter than quiet sun conditions [4].

(4) Frequency of Flares Versus Disturbance to VLF Transmission. Just because a solar flare occurs, there is no direct probability that it will cause an SPA. For example from Ref. 1 it was shown that between late 1961 and mid 1964, 1846 optically detected solar flares were observed. Of these, 66 produced phase anomalies. The probability of occurrence increased approximately with flare area, but was less than probabilities for sudden ionospheric disturbances (SID) determined by other means. This indicates that VLF phase is not as sensitive as other SID indicators.

The number of flares accompanied by SPA's varies from about 7 percent of all the observable flares in one month to none in another. For example, 104 flares were reported in June 1962; of these flares, 22 were of class 1 or greater, but no VLF phase anomalies were observed [1].

(5) Terrestrial Effects of a Solar Flare. See Figure 6.

b. Magnetic Activity

Magnetic storms caused by solar flares also affect the phase of the downcoming skywave. The major

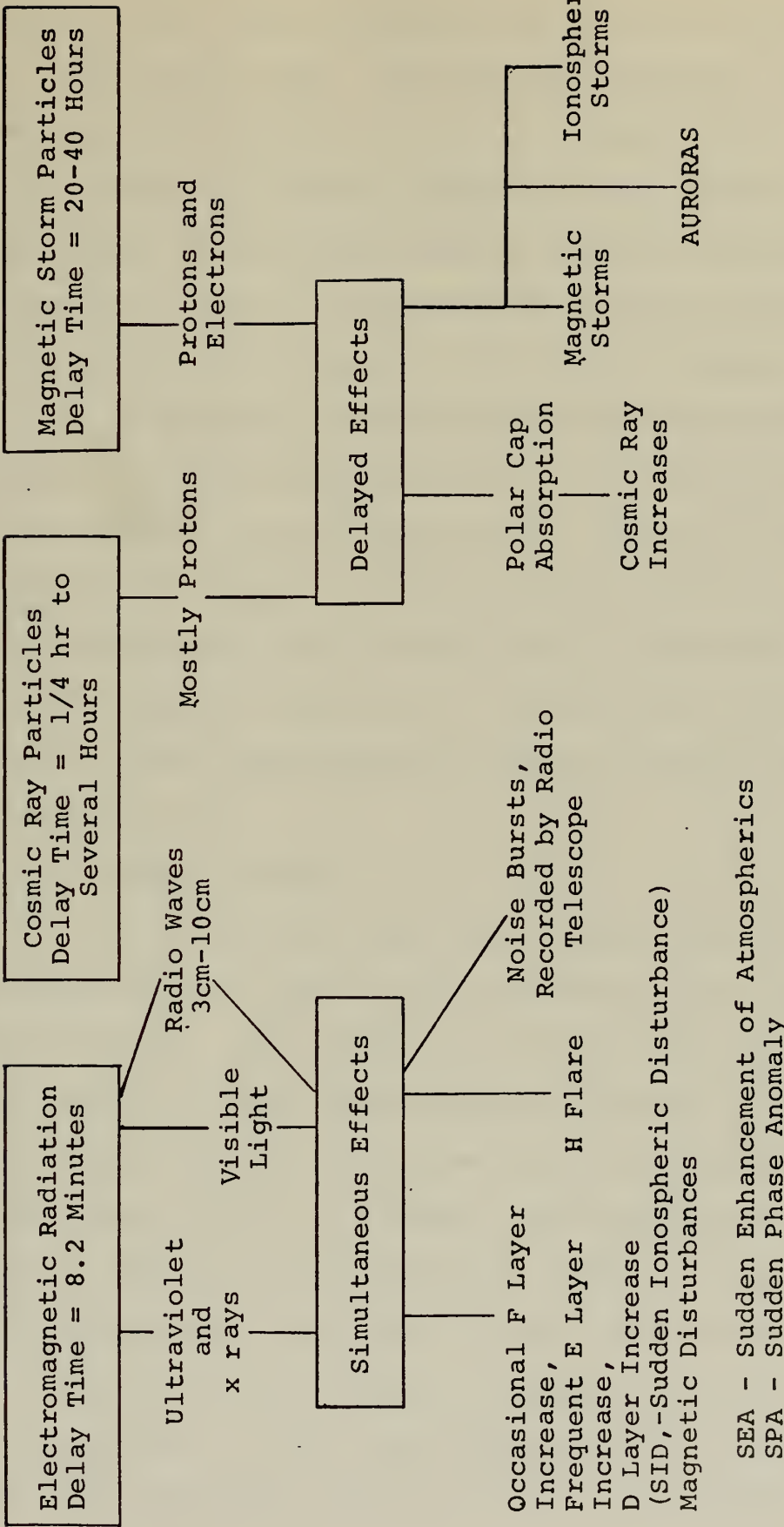


Figure 6. The Terrestrial Effects of a Solar Flare [15].

difference is that these anomalies may occur by day or night and may last several days. These disturbances are associated with magnetic disturbances but not in a very definite way. The long distance VLF effects associated with magnetic activity appear to accompany isolated magnetic bays and great magnetic storms. During extreme magnetic storms the phase may change as much as 150° (42 cec) per minute.

In addition to the above mentioned anomalies associated with great magnetic storms, smaller phase anomalies are observed, during both day and night, which appeared to correlate with magnetic storms of less intensity. Some of these effects are found to occur about 3 days after the onset of the magnetic storm [27]. The magnetic variations generally occurred approximately 30 minutes earlier than the phase variations [4].

c. Meteor Showers

In addition to solar and magnetic activity causing phase anomalies, there is some evidence of an effect due to meteor showers. The anomalous effect in the diurnal phase pattern associated with meteor showers is shown in Ref. 4. The effect was observed during the hours of sunrise along a path from Great Britain to Boulder, Colorado when the phase is steadily decreasing (approximately 240° in 8 hours). At the time of passage of the meteor shower, the steady phase decrease associated with sunrise is delayed until the meteor shower has passed, or until the entire path is in daylight, at which time the phase returns to the normal daytime value.

d. Atomic Device Explosion

In order to understand what occurs to the phase of VLF signals during a high altitude nuclear explosion it is necessary to know how the D region is modified by high altitude nuclear bursts. There are several nuclear-burst processes which can greatly modify the D region of the ionosphere, including prompt-gamma-ray and thermal x-ray ionization, prompt-neutron decay, fission-beta decay and beta decay of the debris material [1].

(1) Prompt VLF Effects. The prompt VLF effects observed during nuclear testing occurred within seconds after the detonations. Since some of the paths considered are shielded by the earth from direct ionization radiation such as x-rays and γ -rays created in the detonation, it is asserted that prompt neutrons from the burst decay into protons and beta particles, with a half-life of about 13 min; the betas then spiral down the geomagnetic field lines into the D region of the ionosphere where they enhance the ionization and cause increased absorption and decreased propagation times of VLF radio waves propagating in the earth-ionosphere wave guide. The geometry of the detonation point and VLF propagation path must be such that the geomagnetic field lines which intersect the propagation path are within line of sight of the burst [15].

(2) Delayed VLF Effects (1.5 to 5 minutes).

The VLF anomalies on paths where the geomagnetic lines are below the shadow cone which is tangent to the earth's

surface and whose apex is at the detonation point can be explained in terms of the eastward drift and energy spectrum of the electrons comprising the bomb-induced radiation belts which form in the geomagnetic meridian through the burst point. Those that are trapped will precess eastward at a rate proportional to their energy. A 1 MeV electron drifts at a rate of about 6-10 degrees of longitude per minute [1].

(3) Delayed VLF Effects (15 to 40 minutes):

VLF anomalies delayed by tens of minutes are believed to be caused by the eastward drift and energy spectrum of trapped radiation composed largely of neutron-decay electrons. It is possible that some of the field intensity anomalies observed may be attributed to trapped neutron decay electrons which drifted several times around the world [15].

(4) Phase Shifts of High Altitude Nuclear Explosions. High altitude nuclear explosions produce clearly identifiable phase shifts if the VLF path is located sufficiently close to the burst. The prompt neutron precipitation forms the burst signature--a sudden fast phase decrease, a slower decrease which lasts a minute or two, then a return to normal lasting tens of minutes, quite like that of a solar flare SPA. Figure 7 shows the magnitude of the phase shifts.

e. Ionospheric Variations

It has been shown earlier that changes in the height of the ionosphere alter the phase velocity of the signal in the earth-ionosphere waveguide. Therefore anything

Transmission Path	Length of Path (km)	Approximate Distance from Detonation to Nearest Point of Path (km)	Maximum Phase Change Recorded (micro-seconds)
Balboa to NEL	4666	5526	39
Balboa to Pt. Barrow	8598	5893	55
Balboa to Forestport	3836	9118	39
Balboa to Thule	7631	9896	40
Balboa to Opana	8452	1357	8
Haiku to NEL	4188	1357	26
Balboa to Opana	8452	1357	12
Haiku to Rome, N.Y.	7813	1357	18
Haiku to NEL	4188	1357	20

Figure 7. Phase Shift of Omega Signals Due to Three High Altitude Nuclear Bursts [16].

that affects the height of the D region, which acts as the upper surface of the earth-ionosphere waveguide, will greatly affect the phase of the VLF signal. Since the occurrence of SID's follows the same 11 year occurrence cycle as do flares and sunspots, then their effect on propagation would be expected to follow the solar cycle. The season of the year, latitude of the observer and the position of the moon also have a direct effect on the phase variation of VLF signals [32].

There is an appreciable change in nighttime phase velocity with latitude. This change appears as an increase in the nighttime phase velocity with latitude for paths within the temperate zone. An apparent semidiurnal height variation of about 0.1 km appears to be related to the moon. The maximum height which occurs about two hours before lunar transit may be caused by a maximum rate of change in particle height which would be expected three hours before tidal maximum [32].

f. Polar Cap Absorption (PCA)

Polar Cap Absorption is believed to be due to high energy solar protons in the 10 MeV range which penetrate deeply into the atmosphere over the polar cap and greatly enhance the ionization in the 50 to 80 km range [15]. The start of a PCA is from a fraction of an hour to several hours after a solar flare is observed. They usually last from 1 to 10 days with most lasting three days. Since the region of excitation is somewhat lower for these particles,

the general effect is not only a lowering of the ionosphere but also an increase in the gradient of the reflection layer which usually results in an increase in attenuation rate [32]. Unusually large phase changes at VLF are observed during PCA so therefore it is fortunate that their occurrence is rare. From October 1961 to October 1963 only seven PCA were observed on the polar path from Great Britain to College, Alaska [1]. Since these are polar path events, they are of little concern to those who are using temperate latitude propagation paths.

g. Ground Conductivity

As the conductivity of the Earth's surface decreases, the phase of the reflection coefficient decreases, i.e., becomes a larger negative value. Watt has shown the manner in which the phase velocity changes with ground conductivities for day and night paths. His conclusions were that the change in velocity is appreciably greater for the lower frequencies and also that the nighttime changes in relative phase velocity are appreciably less than those that occur during the day [32].

Swanson compared the variation of phase velocity with electrical ground conductivity for the daytime ionosphere and also the velocity variation of 10.2 and 13.6 kHz signals with ground conductivity [17]. He concluded that the variation of velocity at 10.2 kHz was relatively minor until conductivities become quite low at which point variations become more significant. In the case of 10.2 kHz the phase

velocity decreased monotonically as the conductivity decreased. In the case of 13.6 kHz, however it appeared that a rounding or change may be occurring in the region 0.006 to 0.1 millimhos per meter. The large anomaly centered near 20 kHz apparently shifts toward lower frequencies as conductivity is decreased. The effects are therefore significant and cannot be anticipated with any certainty without direct calculations for the conductivity range involved [17]. Since skywave corrections are now being force fit to meet local conditions, the effect of ground conductivity changes will become minimal.

h. Geomagnetic Path Orientation

The Earth's magnetic field has an appreciable effect upon the motion of the electrons in the lower ionosphere and this change in motion can affect the relative reflection characteristics for VLF waves. There is not only a significant change in the amplitude of the reflection coefficient with direction of propagation, but there is also an appreciable change in the phase of the ionospheric reflection coefficient as the direction of propagation changes from east to west. The general tendency is for the phase to decrease as the direction of propagation changes from west-east to east-west, i.e., to the west propagation has less phase lag than to the east [32]. This can be explained by the radio wave interacting with the Earth's magnetic field resulting in an aiding effect east to west and hindering effect west to east. The attenuation rates are also

different for west-east and east-west transmissions at VLF with to the west being less. Since the characteristics of the ionospheric reflection coefficients are a function of the sharpness of the ionospheric boundary as well as frequency, the directional properties are different for day and night conditions. Nonreciprocal effects also change throughout the frequency range of the VLF band. Since the characteristics of the ionosphere can change throughout the solar cycle, directional effects also change throughout the solar cycle. The two primary influences which are important in this regard are the change in collisional frequency with solar activity and the change in galactic cosmic ray intensity [32].

The NELC computer program used for obtaining the skywave corrections and curves which approximate the complete wave solution, uses an expression of the form:

$$b_1 \sin \theta + B \cos 2\theta + K_1 = b \sin \theta - 2B \sin^2 \theta + K_2 \quad (5)$$

where θ = bearing angle with respect to magnetic field.

b_1 , B , K_1 and K_2 = constants.

Swanson also compares the experimental curve with that obtained from the NELC program. There is quite good agreement between them. However, the NELC computer results of the complete wave solution are applicable only for conditions similar to those between Hawaii and San Diego. The experimental results are based on the synthesis of data involving not only a wide range of bearing angle, but also various values of the total field and various dip angles [17].

i. Propagation Over Land-Sea Boundary

When the propagation path is mixed, i.e., contains areas of appreciably different conductivity, determining the phase and amplitude of a signal across the boundary becomes more difficult. When the distance separating the transmitter and the boundary discontinuity is relatively small, it can be shown that the transition from the form of variation with distance characteristic of the first medium to that of the second medium is quite rapid. On the other hand, when the distance from a transmitter is large, the transition takes place over a much longer distance. At VLF the phase is very sensitive to the difference in conductivities between land ($\sigma = 10^{-2}$ mho/m) and sea ($\sigma = 4$ mho/m). For example at 1000 km an all land path experiences an angular shift of -82° whereas an all sea path has only a -33° angular shift [32].

j. Fluctuations Due to Whistler Mode Signals.

Whistler mode signals are signals radiated into the ionosphere near the transmitter and guided along the Earth's magnetic field lines back to the Earth in the vicinity of the magnetic conjugate of the transmitter. The magnetic conjugate is the point where the magnetic field line reenters the Earth's crust. A receiver near the conjugate point may thus receive the normally propagated signal together with the whistler mode signal. Since the whistler mode signal varies with time, the resultant signal will exhibit, in general, both phase and amplitude variations.

Some observations have been made in New Zealand of the phase stability of whistler mode signals at VLF from NPG, Seattle. The magnetic conjugate of NPG lies about 3000 km SE of Lower Hutt, New Zealand and its direction is nearly perpendicular to the great circle path from NPG. Thus a pair of perpendicular loops were used to receive the direct and whistler signals separately. The observations indicated that the whistler signals tend to be shifted in frequency by several cycles per minute, the frequency shift being greatest (10 Hz/min) near midnight. The signals were observed when the source and conjugate were dark, but not when both were in daylight. The amplitude of the whistler mode signals was about 10 percent of the direct signals [4].

It is thus apparent that phase observations on NPG at Lower Hutt using an omnidirectional antenna would be characterized by phase fluctuations of the order of $\pm 6^\circ$ occurring several times per minute. Such variations might be important in a phase recording system having a fast response, but would be removed with phase recording systems with longer time constants such as the Tracor 599R with a time constant of 70 seconds.

4. Model for Phase of Received Signal

As delineated earlier in this paper, the phase velocity at VLF and hence 10.2 kHz is dependent upon numerous parameters. The parameters are again:

- a. Propagation over sea (distance)
- b. Propagation over land (distance)

- c. Ionospheric height caused by
 - (1) Day or night
 - (2) Sun's zenith angle
 - (3) Solar activity
- d. Magnetic abnormalities
- e. Earth's magnetic field
- f. Earth conductivity
- g. Latitude effects
- h. Excitation factors
- i. Season of the year

E. R. Swanson of NELC has developed a prediction model and a computer program to determine the parameter coefficients for that model [15].

In general, four regions in the electromagnetic field may be considered at 10.2 kHz: near field--0 to 30 km; medium field--30 to 1000 km; far field--1000 km to the boundary of the antipode region; and the antipodal region approximately 1000 km wide. The antipode is the point on the surface of the Earth diametrically opposite the transmitter. The near and medium fields are contaminated by high-order modes, skywaves, ground-wave interference, and the induction field of the transmitting antenna. The antipodal region will be excluded because of interference between the same signal coming from several directions simultaneously. This leaves only the far field which can be considered on a linear basis, permitting simple summation of propagation effects. Thus, the propagation can be a function of several

parameters such as time, distance, and others mentioned above. Therefore the equation for a plane wave would be

$$E = |E_a(d)| e^{2\pi i (ft - k_c(d,t)D)} \quad (6)$$

and the phase of a signal in cycles at some point is:

$$\phi = ft - k_c(d,t)D \quad (7)$$

However, k_c is generally independent or, at least, nearly independent, of time so

$$k_c(d,t) \doteq k_c(d)$$

and

$$\frac{v}{c} = \frac{1}{\frac{\partial k_c(d)D}{\partial D}} \quad (8)$$

Since, in the far field, the parameter coefficients were assumed to be linear the coefficient $k_c(d)$ can be considered to be the sum of several terms and a correction factor:

$$k_c(d) = K_1 D + K_o + \phi_c(d) \quad (9)$$

K_1 and K_o may be determined by linear regression and $\phi_c(d)$ is a constant and lost upon differentiation of equation (9). Furthermore, a phase designation also independent of time can be substituted for $k_c(d)$ in equation (9), resulting in

$$P = K_1 D + K_o, \text{ cycles} \quad (10)$$

K_o is an excitation factor which merely indicates the phase lead or lag of the field relative to the antenna. Equation

(10) permits the calculation of phase at any point but assumes like conditions for the entire path. However, it is very unlikely that a uniform path will ever be encountered in actuality. So, equation (10) must be expanded. Since the far field only is considered in Omega navigation, linear propagation paths are assumed and K_1 of equation (10) becomes:

$$K_1 = \sum_{i=1}^n K_i \quad (11)$$

and for a land-sea path:

$$P = K_s D_s + K_1 D_1 + K_o \quad (12)$$

where

K_s = Parameter coefficient over sea water

K_1 = Parameter coefficient over land

D_s = Normalized distance over sea, referenced to 10.2 kHz

D_1 = Normalized distance over land, referenced to 10.2 kHz

K_o = Excitation factor

Equation (12) requires expansion to be really useful, since it includes only expression for land and sea propagation and excitation. It neglects important parameters such as ground conductivity, sun's zenith angle, Earth's magnetic field and others. However it can be expanded to become generally applicable:

$$P = K_o + K_1 B_1 + K_2 B_2 + \dots + K_n B_n \quad (13)$$

where $K_n B_n$ defines respectively the parameter coefficients

and the parameters. When the individual parameter's expressions and their coefficients are determined, equation (13) can accomodate them and will result in increased accuracy of position.

NELC, San Diego has determined a number of the coefficients experimentally and is using these for tabulation of skywave corrections.

The form of equation (13) presently used is

$$P = K_1 D_1 + K_s D_s + K_o + K_5 B_5 + K'_5 B'_5 + K_6 B_6 \quad (14)$$

where K_1 , D_1 , K_s , and K_o were previously defined and:

K_5 = Coefficient of magnetic orientation

B_5 = Parameter of magnetic orientation $\int \cos\phi \sin\theta dD$

K'_5 = Additional coefficient of magnetic orientation

B'_5 = Additional parameter of magnetic orientation,
 $\int \cos\phi \sin^2 \theta dD$

K_6 = Coefficient of Latitude

B_6 = Parameter of latitude, $\int \cos\phi \cos(\text{dip}) dD$

where θ = magnetic bearing and ϕ = geomagnetic latitude in degrees.

The values of the coefficients can be found in table 3.1 of Ref. 15.

Equation (14) has been derived in such a manner that it can readily include any additional parameters defined at some future date. Accuracy of the phase model, and consequently the fix position, will improve as pertinent parameters are defined and included. Omega system operation will

furnish the data from which these additional parameters can be determined.

III. DIFFERENTIAL OMEGA

A. GENERAL CONCEPT

The effectiveness of Omega is predicated on the predictability of a VLF phase measurement made at any time and place. Environmental influences active over given areas for various periods of time contribute to anomalous phase variations. Use of published skywave corrections [31], which are based on a time and location dependent propagation model, eliminate a large portion of the anomalous variations. However, certain residual phase errors remain and result in Omega position inaccuracies on the order of one n.mi.

Because of the space and time characteristics of both Omega propagation and the skywave correction model, it is natural to expect that any remaining phase errors will to some extent be correlated in distance and time rather than simply being a random process. It is seen from Figure 8 that a random, unpredicted ionospheric disturbance in area A will cause similar or correlated phase variations at points P1 and P2 because the paths are effectively parallel and closely spaced. Since the distances involved with Omega are quite large (propagation paths in excess of five thousand miles are possible), the separation between P1 and P2 could be appreciable while remaining errors would still be correlated.

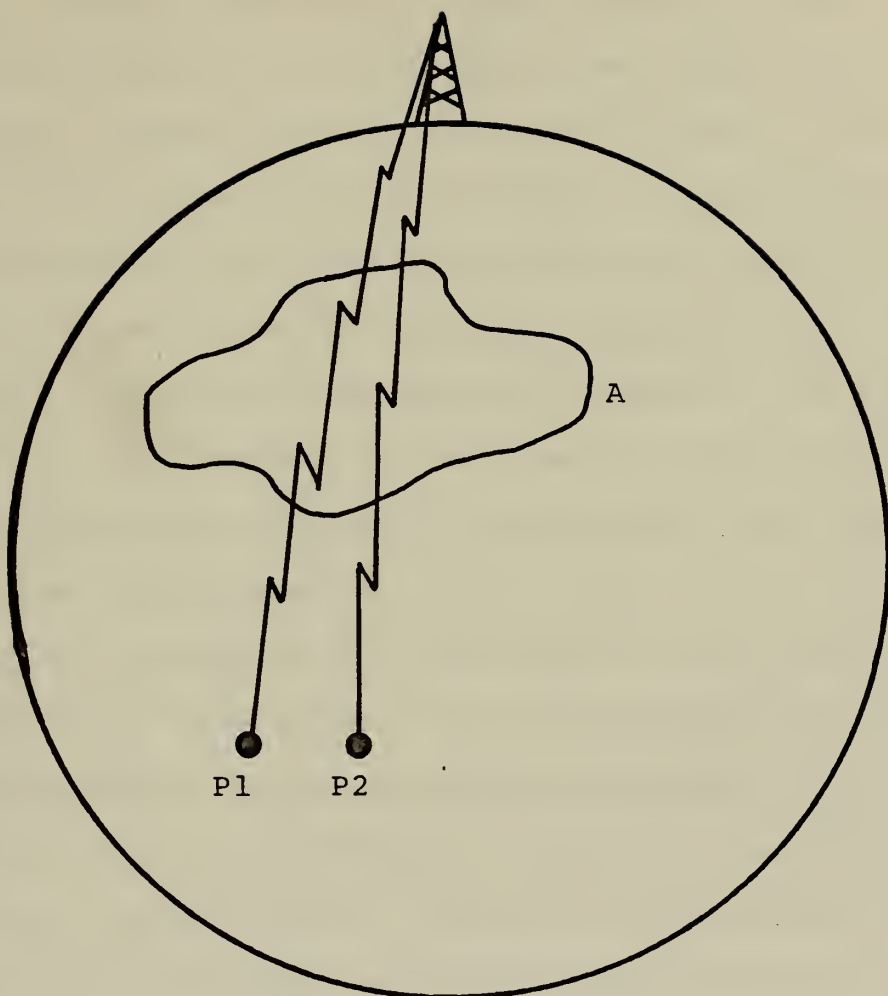


Figure 8. Effect of Ionospheric Disturbance.

If P1 is a fixed geographic site whose Omega coordinates are accurately determined, then this site--called the monitor site--can compare the received Omega signal to the correct value associated with an undisturbed path and obtain a "difference" between actual and correct values. This is the meaning of the term differential Omega. If the monitor site has the capability of transmitting this differential information to a user in the differential operating area, then a complete differential Omega system is formed (see Figure 9). The size of the differential area has not yet been experimentally determined--however it can be said that the area would be no larger than the area in which the use of the differential correction as transmitted by the monitor site provided better results than the use of Omega and skywave correction tables. Once the skywave correction results were equal or better than differential Omega then only skywave corrections would be used. Different investigators have proposed various maximum separation distances for P1 and P2 but it is generally agreed that 250 n.mi. is a good approximate value [19,20,25,30].

B. DETERMINATION OF SPATIAL CORRELATION OF OMEGA SIGNALS

From the intuitive notion of differential Omega investigators were led to an examination of Omega phase error data to determine an approximate model for the spatial correlation. Separations between locations where extended data was available were too large to adequately analyze differential Omega in a straightforward line-for-line approach. Instead

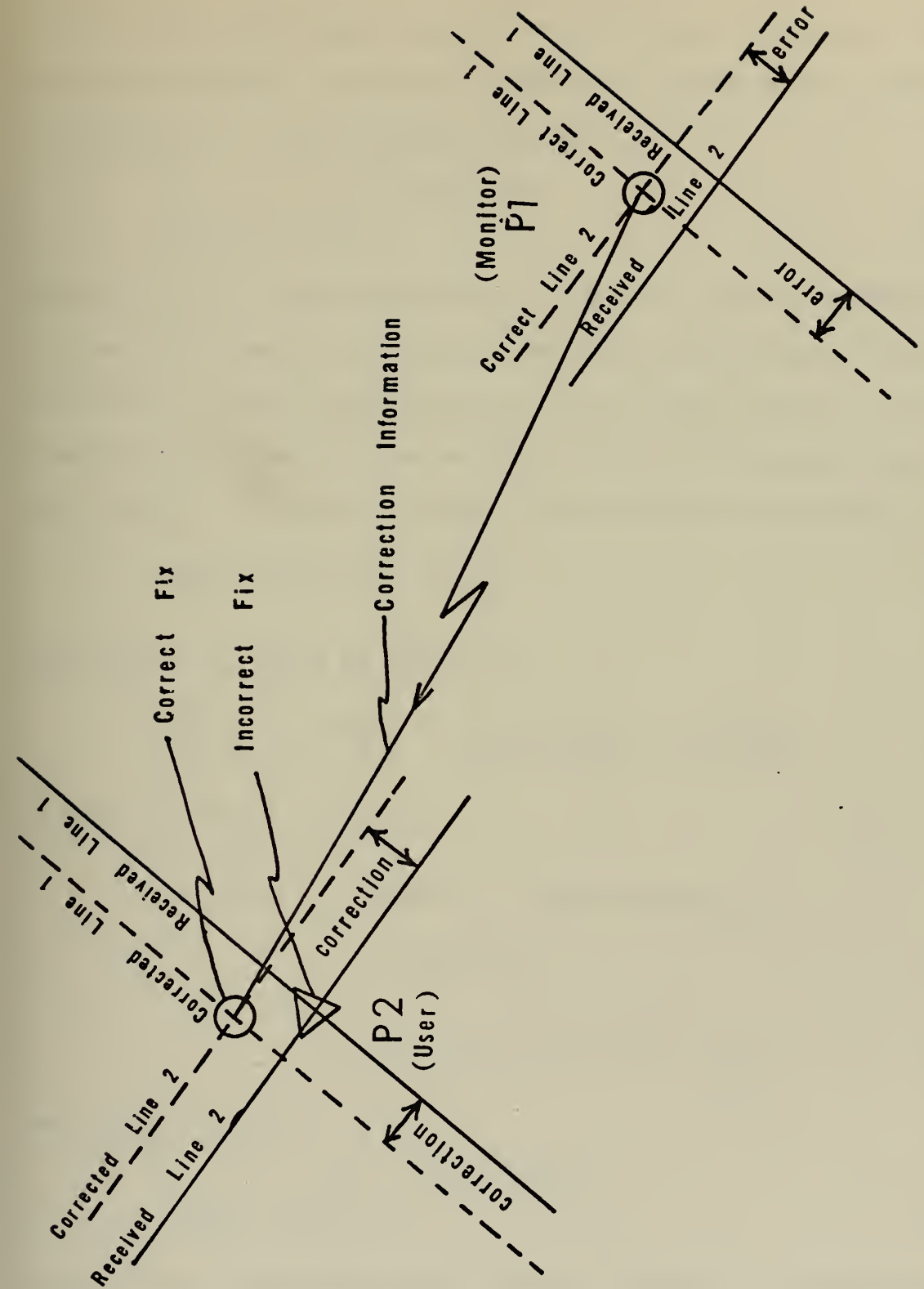


Figure 9. A Differential Omega System.

Kasper [6,11,12] used statistical analysis techniques and autocorrelation functions to describe Omega error spatial correlation. The function used was:

$$R_{\Omega}(\Delta x) = \sigma_{\Omega}^2 e^{-|\Delta x|/1500} \quad (15)$$

where $R_{\Omega}(\Delta x) = E[\delta\phi(x)\delta\phi(x+\Delta x)]$ and $E(\cdot)$ denotes expected value. The users' location is defined as x and the monitor site as x_0 . The uncorrected error at x is $\delta\phi(x)$; the correction broadcast by the monitor site is the phase error at x_0 , $\delta\phi(x_0)$. Thus the residual error after correction is

$$\Delta\phi(x) = \delta\phi(x) - \delta\phi(x_0) \quad (16)$$

RMS error is found by squaring

$$\Delta\phi^2(x) = \delta\phi^2(x) - 2\delta\phi(x)\delta\phi(x_0) + \delta\phi^2(x_0) \quad (17)$$

taking expected values,

$$\begin{aligned} E[\Delta\phi^2(x)] &= E[\delta\phi^2(x)] - 2E[\delta\phi(x)\delta\phi(x_0)] \\ &\quad + E[\delta\phi^2(x_0)] \end{aligned} \quad (18)$$

$$= \sigma_{\Omega}^2 - 2\sigma_{\Omega}^2 e^{-|\Delta x|/1500} + \sigma_{\Omega}^2 \quad (19)$$

and square roots

$$\Delta\phi_{RMS} = \sigma_{\Omega} \left(2 - 2e^{-|\Delta x|/1500} \right)^{\frac{1}{2}} \quad (20)$$

where Δx is the separation distance between the monitor and the user in n.mi. RMS differential Omega error is shown as a function of Δx in Figure 10 (upper curve). A value for σ_{Ω} of 1 n.mi. is used. Within 200 n.mi. of the monitor

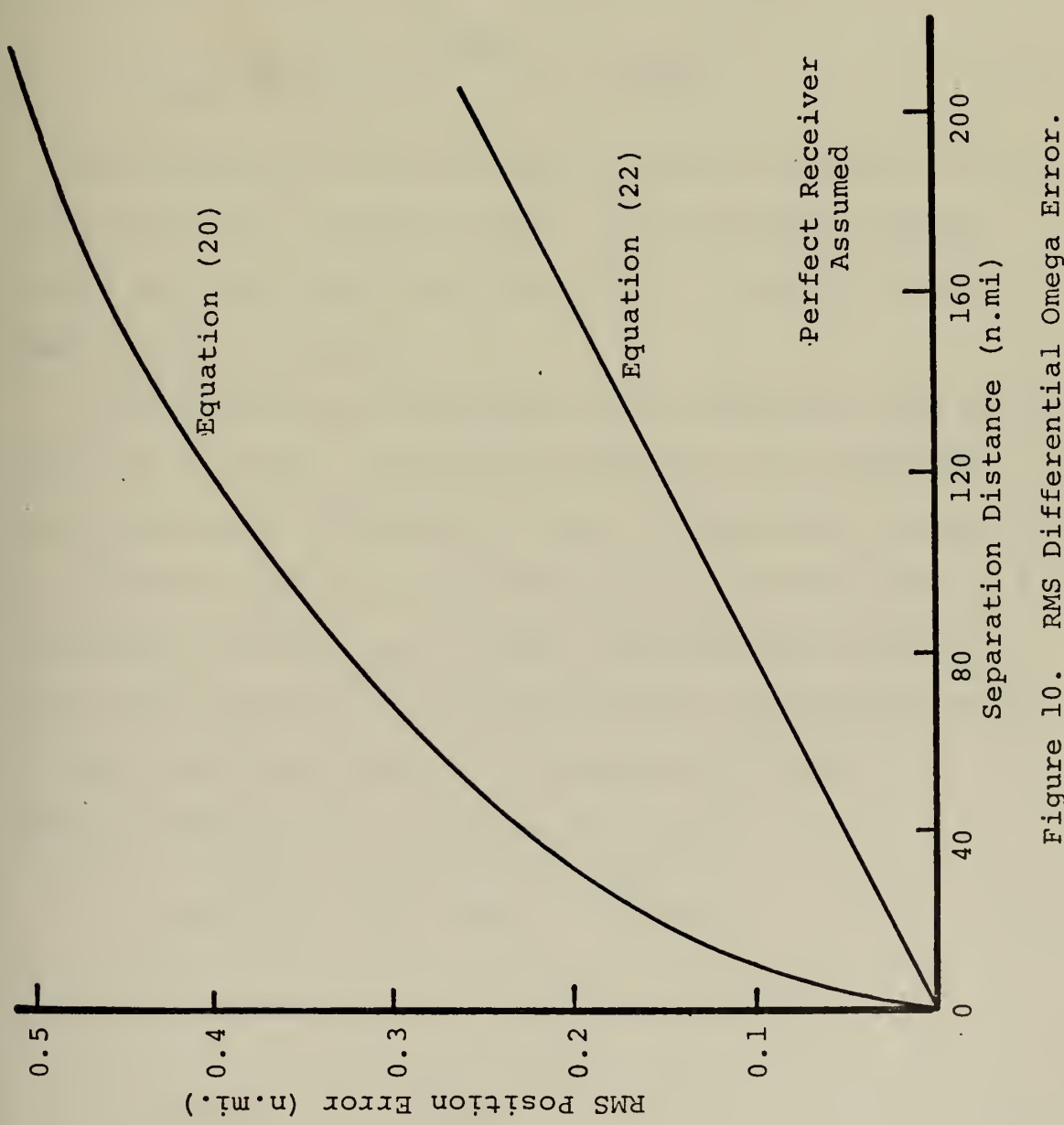


Figure 10. RMS Differential Omega Error.

site, RMS errors are less than 0.5 n.mi. Receiver errors are not included in the above analysis.

Another statistical model for Omega error has been considered [12]; its autocorrelation function is

$$R(\Delta x) = \sigma_{\Omega}^2 e^{-|\Delta x|/698} \left\{ 1 + \frac{|\Delta x|}{698} \right\} \quad (21)$$

RMS differential Omega error for this model is obtained the same way as before resulting in equation (22)

$$\Delta\phi_{RMS} = \sigma_{\Omega} \left[2 - 2e^{-\frac{|\Delta x|}{698}} \left(1 + \frac{|\Delta x|}{698} \right) \right]^{\frac{1}{2}} \quad (22)$$

This function is also shown in Figure 10 (lower curve). Within 200 n.mi. of the monitor, RMS differential Omega errors are less than 0.26 n.mi. if a 1 n.mi. RMS unaided Omega error is assumed.

It is likely that the actual error behavior lies between these two results. Gossard and Norgard [19] stated that the accuracy of differential Omega is inversely proportional to receiver separation and will be 0.2 statute miles at a separation of 100 miles. These investigators arrived at their conclusion in the following way. The bearing error, $\Delta\theta$, can easily be related to the phase deviation, $\Delta\phi$, as shown in Figure 11. It can be seen that

$$\Delta\phi = \frac{2\pi}{\lambda} \delta = \frac{2\pi}{\lambda} d \sin \Delta\theta \doteq \frac{2\pi}{\lambda} d \Delta\theta \quad (23)$$

for small bearing errors. It follows that

$$\sqrt{\frac{\Delta\theta^2}{\Delta\phi^2}} = \frac{\lambda}{2\pi} \frac{\sqrt{\Delta\phi^2}}{d} \quad (24)$$

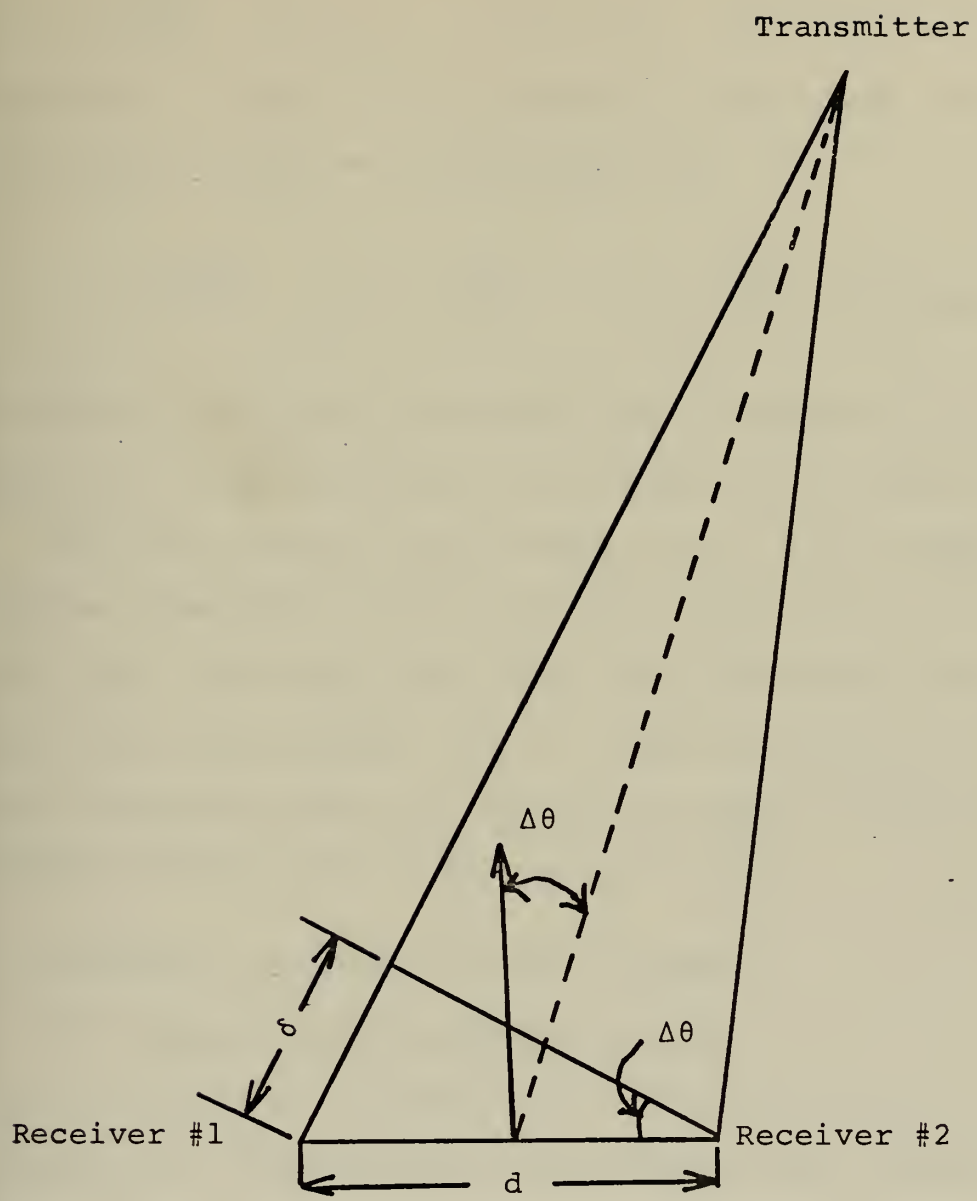


Figure 11. Relation of Bearing Angle Error to Phase Deviation.

For small fluctuations $\Delta\phi$ is proportional to d so the slope $\frac{\sqrt{\Delta\phi^2}}{d} = \text{constant}$. Eventually, the separation of receivers (1) and (2) will become so great that the phase fluctuations will be uncorrelated and

$$\sqrt{\Delta\phi^2} = \sqrt{2} \sqrt{\phi_1^2} = \sqrt{2} \sqrt{\phi_2^2} = \text{constant} \quad (25)$$

By taking the slope of the RMS phase difference vs. receiver separation they determined the differential omega fix error.

The above results are dependent only on the angle between the two receivers and the distance between them. It appears that this result will give the phase difference due to distance and angle between the two locations but will not give any information about the effects on phase of SIDs, PCAs or magnetic storms along the propagation path.

C. PROPOSED DIFFERENTIAL OMEGA SYSTEMS

1. French System by Sercel Company

The Sercel Company has been experimenting with a differential Omega system which showed great promise in tests made in late 1971 over distances of from 5 to 300 km from the monitor station. The results will be discussed later. The Sercel system requires a fixed monitor site from which to obtain and transmit the variations in the signals received from each Omega transmitter. There are as many correction values to be transmitted to the mobile receivers as there are useable Omega signals in the area. The phase determined

by the receiver at the monitor site for each signal is with respect to the phase of its local oscillator. The local oscillator in the monitor and mobile receivers must be very stable so that its frequency doesn't change appreciably from the time that one signal is received until the second signal is received (as much as five seconds). If it did change then the phase reference would be different for the two signals and some LOP error would result. Since at the mobile receiver all the received Omega signals are with respect to the same local oscillator, when two stations' phase signals are subtracted from each other to generate a hyperbolic LOP, the common local oscillator reference signal is eliminated. Phase correction signals at the monitor site for the respective stations are continuous 1 kHz sine waves. The value of the phase correction to be transmitted is in the form of a phase difference with respect to the 1 kHz internal reference, the latter in turn being phase coherent with the local oscillator. In effect, the analog transmission contains a total of five signals: four phase signals plus the reference signal. In order to minimize the transmission bandwidth all the signals are first reduced to a conveniently low (20 Hz) frequency, which constitutes a satisfactory compromise between the full transmission width and the effect of transmission defects likely to result from transmission speed and signal fading [14]. All five signals are then time multiplexed so as to correspond with the basic Omega format. This multiplexed information

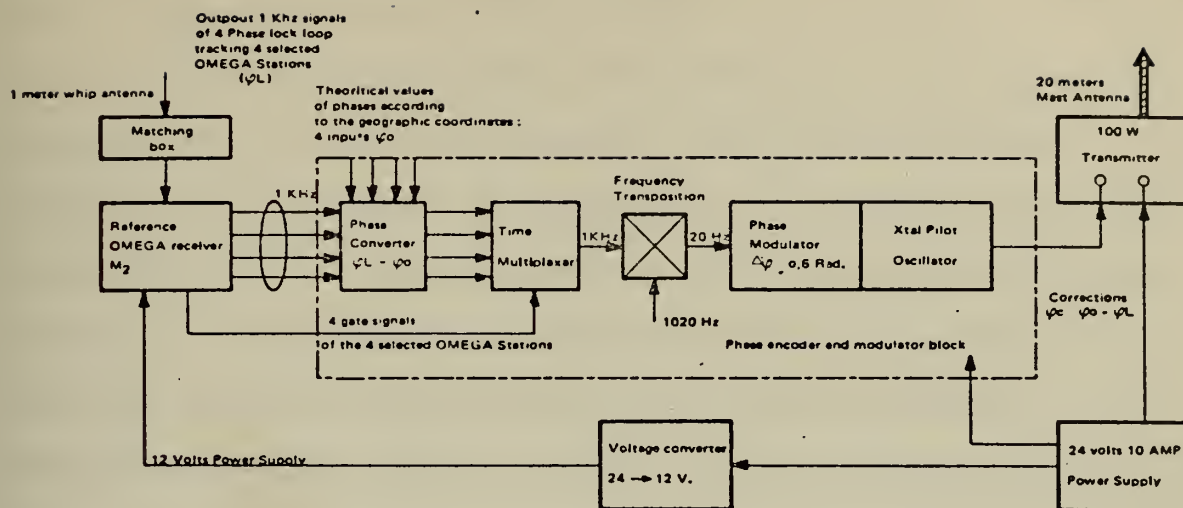


Figure 12. Sercel Differential Omega Transmitting Station.

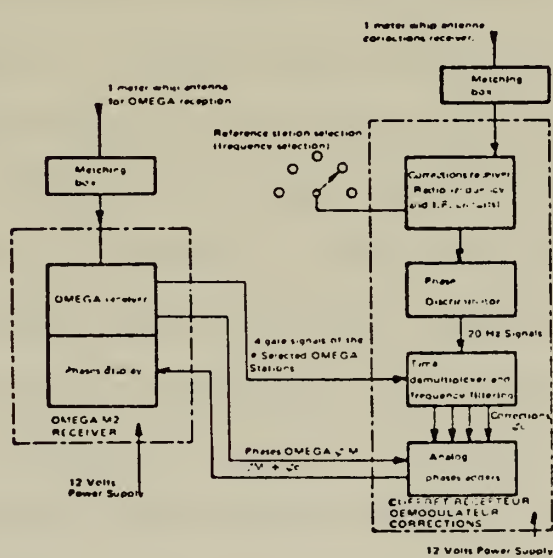


Figure 13. Sercel Differential Omega Receiver Station.

is then routed to a 100-watt transmitter in the 2 MHz range where it phase modulates the carrier.

The shipboard installation includes a correction receiver which accepts and handles the phase correction signals. This receiver is connected via a single cable with the standard Sercel Omega receiver. The correction receiver contains a double superheterodyne section, the second frequency converter being driven by a small frequency synthesizer. This offers a choice of four frequencies above and four below the reception frequency, the interval between any two frequencies being 160 Hz. The second channel has a bandwidth of 50 Hz adapted to the frequency spectrum of one transmitter. The receiving system is thus capable of receiving the signals from eight correction transmitters which may be installed in a chain up and down the coast.

Selection of a station may be achieved by simply selecting the frequency of the second local oscillator in the receiver. A discriminator and a filter placed after the second frequency converter is used to separate the 20 Hz signals. The timing signals obtained from the ship's Omega receiver are used by the correction receiver as demultiplexing commands for the 20 Hz signals. The four 20 Hz signals are demultiplexed and demodulated according to two quadrantal components by a 20 Hz signal generated locally in the correction receiver. The demodulated signals are routed through narrow-band filters and the resulting voltages appear across four pairs of leads (one pair per station). These voltages

are equal to the sines and cosines of the angles corresponding to the corrections.

In conventional Omega operation received signals are applied to the receiver's meters which show the phase differences between the selected stations. In differential Omega navigation the four signals which carry the phase information of the Omega station being received are taken from the Omega receiver and routed over a cable to the correction receiver which contains four electronic phase shifters. Each of these is driven by voltages obtained from the correction receiver equal to the sines and cosines of the correction angle. Each of the signals taken from the Omega receiver goes through the corresponding phase shifter where it is subjected to a phase shift equal to the correction angle prior to being returned to the Omega receiver meter input. By this method corrections are received and decoded by the correction receiver and automatically applied to the ship's Omega receiver. Figure 14 shows the results obtained from the tests held in late 1971 for two hyperbolic LOPs, Norway-New York (A-D) and Trinidad-New York (B-D). $\sigma_{\text{A-D}}$ and $\sigma_{\text{B-D}}$ are the standard deviation of the LOPs from the correct values. σ_d is the standard deviation of the fix errors from the known fix position.

2. Micro-Omega

Micro-Omega is the name of a differential Omega system developed by Teledyne Hastings-Raydist, Hampton, Va. The operation of the Micro-Omega system is quite similar to

DISTANCE FROM CORRECT. XMTR	TIME GMT	σ		σ		σd , meters with 1 lane A-D = 23 km 1 lane B-D = 44 km crossing angle 60°	σd , meters with 1 lane A-D = 23 km 1 lane B-D = 44 km crossing angle 80°
		A-D CEC	B-D CEC	B-D CEC	C-E		
11 km	1500-2300	3.2	2.3			1450	1050
	2300-1100	1.0	0.8			420	300
	1100-1900	2.3	2.0			1050	650
50 km	Round the Clock	2.2	1.5			850	580
	Round the Clock	3.5	2.8			1700	1050
95 km	0600-2200	2.6	2.4			1500	900
	2200-0600	5.8	3.5			2200	1450
260 km	Round the Clock	2.8	2.15			1340	700
	Round the Clock						
200-300 km	Round the Clock						
	Round the Clock						

Figure 14. Test Results of Sercel Diff. Omega System [14].

the Sercel system although it is not as adaptable as the Sercel system and uses a different modulation frequency and technique. In the Micro-Omega system, Omega signals received at the monitor station are converted to low frequency (300 Hz) audio tones, phase locked to one of the incoming signals. Each of the audio tones is phase shifted a fixed predetermined amount, which has the effect of subtracting out the known Omega readings. The audio tones are then retransmitted as single sidebands on an HF carrier. Omega signals received on the vessel are processed similarly to obtain a sequence of audio tones of the same frequency.

A vessel using Micro-Omega receives the single side band transmissions. The latter are processed to recover the audio tones. Thus, a pair of simultaneous audio tones at a single frequency is obtained on the vessel for each Omega transmission. The audio tones resulting from a single transmission are applied to a phasemeter. Unique phase angles are thereby derived for each station. The phase angles with respect to the local oscillator for two stations are then fed to a subtractor circuit which gives the phase difference and generates the hyperbolic LOP on which the vessel lies.

The analysis below from Reference 8 derives the phase relationships which exist within the Micro-Omega system. The formulas derived only apply to one line-of-position but are equally applicable for as many Omega stations received at the monitor and user locations.

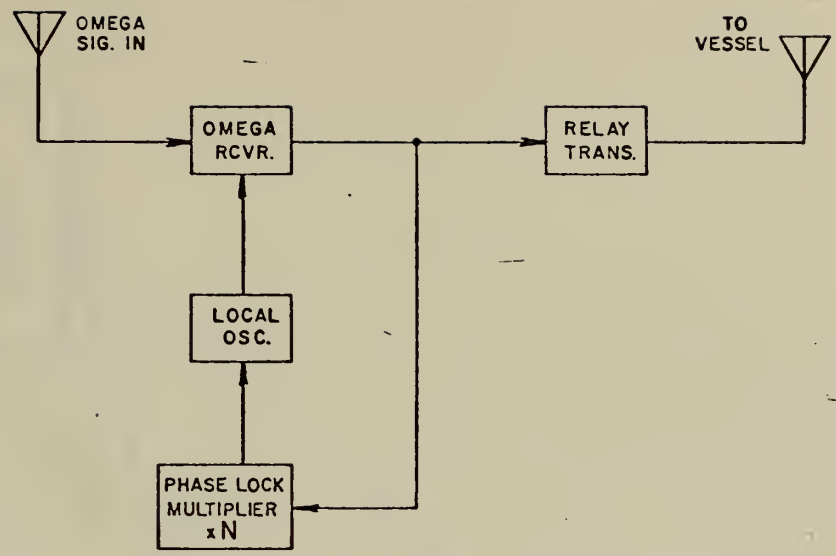


Figure 15. Micro-Omega Transmitting Station.

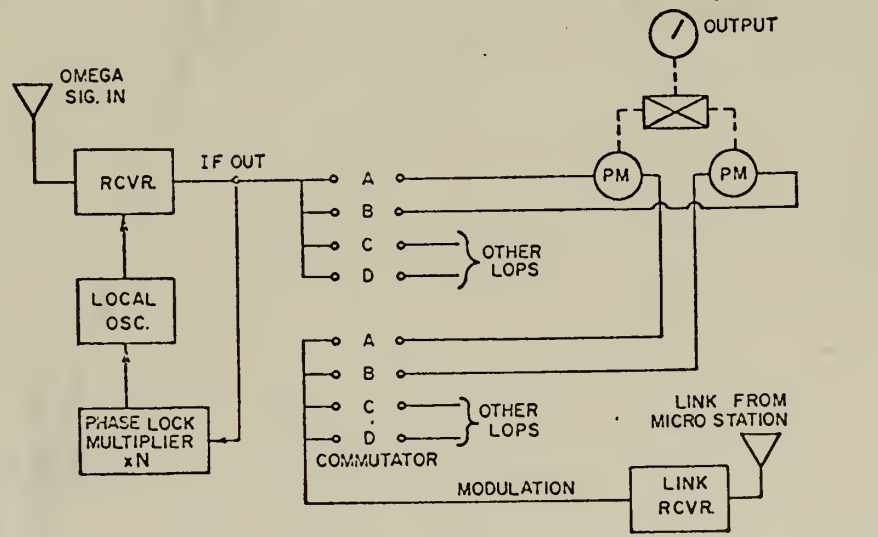


Figure 16. Micro-Omega Shipboard Receiver.

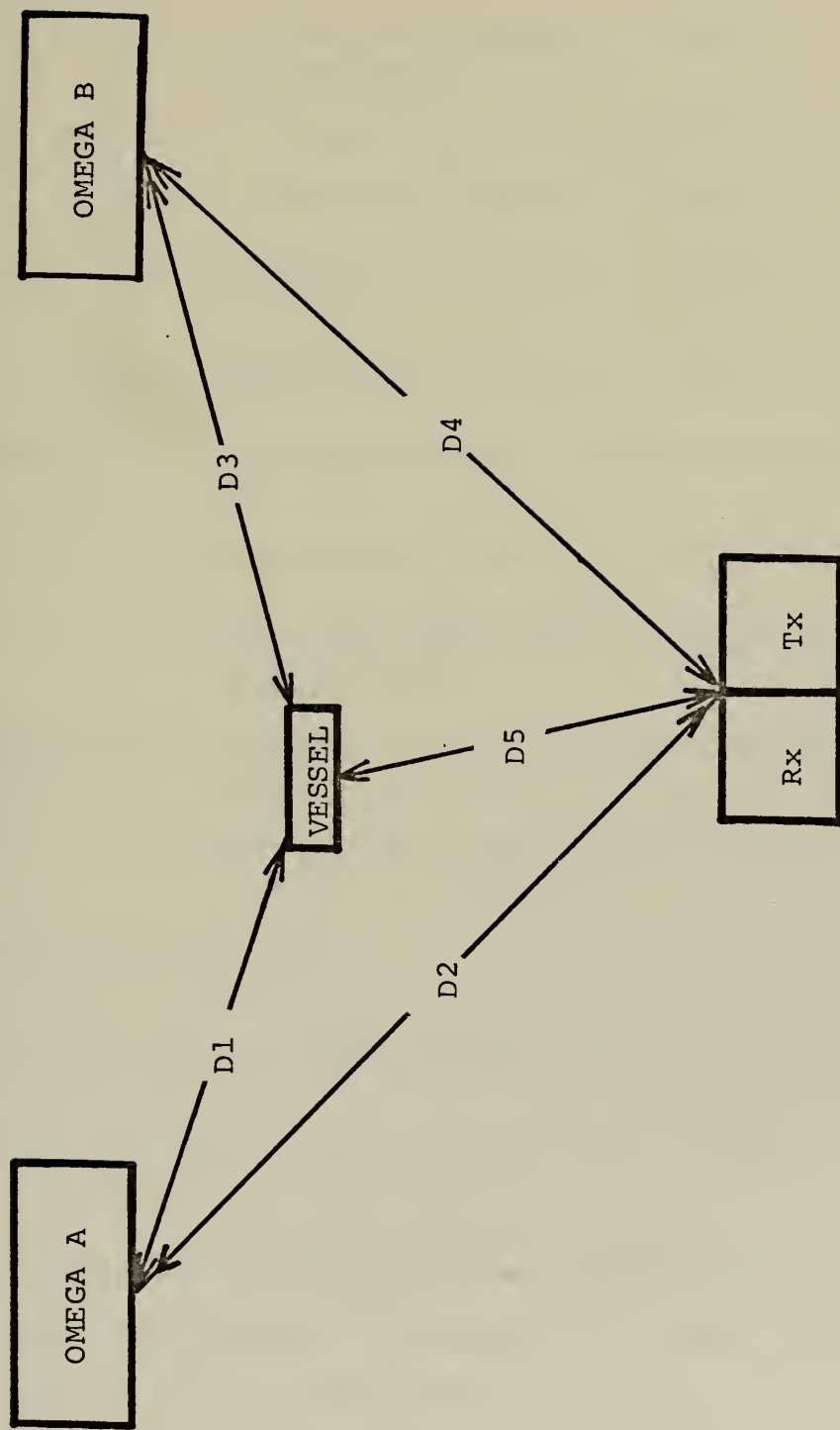


Figure 17. Micro-Omega System Geometry.

The following definitions are used:

θT_a = Instantaneous phase of signal A at transmitter A

θT_b = Instantaneous phase of signal B at transmitter B

θT_{aV} = Instantaneous phase of signal A at vessel

θT_{bV} = Instantaneous phase of signal B at vessel

θT_{aM} = Instantaneous phase of signal A at Micro-Omega Sta.

θT_{bM} = Instantaneous phase of signal B at Micro-Omega Sta.

D_1, D_2, D_3, D_4, D_5 = Distances between stations shown in Fig. 17

c = Propagation velocity of radio waves in air

t = Time from some arbitrary initial time.
t is eliminated later in the algebraic manipulations

e_1, e_2, e_3, e_4 = Distance error equivalent of skywave along paths 1, 2, 3, and 4

N = Multiplying factor in the phase locked loop local oscillator

We have $\theta T_a = \theta T_b = 2\pi ft$

$$\theta T_{aV} = 2\pi ft - \frac{2\pi f D_1}{c} - \frac{2\pi f e_1}{c} = 2\pi ft - \frac{2\pi f}{c} (D_1 + e_1) \quad (26)$$

$$\theta T_{aM} = 2\pi ft - \frac{2\pi f}{c} (D_2 + e_2) \quad (27)$$

At the vessel the local oscillator is synchronized to the A Omega signal and assumes a frequency and phase relationship as follows due to the multiplier N.

$$\text{Local oscillator phase on vessel} = \frac{N}{N-1} \left(2\pi ft - \frac{2\pi f}{c} (D_1 + e_1) \right) \quad (28)$$

At the Micro-Omega Station the same synchronization on the A Omega station is accomplished (see Fig. 15).

$$\text{Local oscillator phase at Micro-Omega Station} = \frac{N}{N-1} (2\pi ft - \frac{2\pi f}{c} (D2+e2)) \quad (29)$$

and the following signal is fed to the transmitter

$$\frac{1}{N-1} (2\pi ft - \frac{2\pi f}{c} (D2+e2)) \quad (30)$$

Both oscillators remain stable through B transmission when Omega B transmits. For the B transmission,

$$\theta T_b R_v = 2\pi ft - \frac{2\pi f}{c} (D3+e3) \quad (31)$$

$$\theta T_b R_m = 2\pi ft - \frac{2\pi f}{c} (D4+e4) \quad (32)$$

When $\theta T_b R_v$ is received by the ship and $\theta T_b R_m$ is received by the monitor site, they are heterodyned with their local oscillators. The difference signal between the received signal and the local oscillator is fed through the commutator (see Fig. 16) to the phasemeter on the vessel. The corresponding signal at the Micro-Omega station modulates the Micro-Omega carrier.

The IF output = Local oscillator - Incoming signal
On the vessel direct from B

$$\begin{aligned} \text{IF output} &= \frac{N}{N-1} (2\pi ft - \frac{2\pi f}{c} (D1+e1)) - 2\pi ft \\ &\quad + \frac{2\pi f}{c} (D3+e3) \end{aligned} \quad (33)$$

$$\begin{aligned} \text{IF output} = & \frac{1}{N-1} 2\pi ft - \frac{N}{N-1} \left(\frac{2\pi f}{c} (D_1+e_1) \right) \\ & + \frac{2\pi f}{c} (D_3+e_3) \end{aligned} \quad (34)$$

On Micro-Omega Station direct from B

$$\begin{aligned} \text{IF output} = & \frac{N}{N-1} \left(2\pi ft - \frac{2\pi f}{c} (D_2+e_2) \right) \\ & - 2\pi ft + \frac{2\pi f}{c} (D_4+e_4) \end{aligned} \quad (35)$$

$$\begin{aligned} \text{IF output} = & \frac{1}{N-1} (2\pi ft) - \frac{N}{N-1} \left(\frac{2\pi f}{c} (D_2+e_2) \right) \\ & + \frac{2\pi f}{c} (D_4+e_4) \end{aligned} \quad (36)$$

The latter signal, equation (36), is transmitted to the vessel as modulation from the Micro-Omega Station. The vessel receives a slightly delayed signal at the lower frequency

$$\left(\frac{1}{N-1} (2\pi ft) \right) \quad (37)$$

When B is "ON" the vessel receives from the Micro-Omega station

$$\begin{aligned} \frac{1}{N-1} (2\pi ft) - & \frac{1}{N-1} \left(\frac{2\pi f D_5}{c} \right) - \frac{N}{N-1} \left(\frac{2\pi f}{c} (D_2+e_2) \right) \\ & + \frac{2\pi f}{c} (D_4+e_4) \end{aligned} \quad (38)$$

When A is "ON" the vessel receives from the Micro-Omega station

$$\frac{1}{N-1} \left(2\pi ft - \frac{2\pi f}{c} (D_2+e_2) \right) - \frac{1}{N-1} \left(\frac{2\pi f D_5}{c} \right) \quad (39)$$

Comparing both A signals (equations (26) and (39)) in a phasemeter gives

$$\frac{1}{N-1} \left(\frac{2\pi f}{c} (D_1 + e_1 - D_2 - e_2 - D_5) \right) \quad (40)$$

Comparing both B signals (equations (31) and (38)) in a phasemeter gives

$$\begin{aligned} \frac{N}{N-1} \left(\frac{2\pi f}{c} (D_1 + e_1 - D_2 - e_2) \right) &+ \frac{2\pi f}{c} (D_4 + e_4 - D_3 - e_3) \\ &- \frac{1}{N-1} \left(\frac{2\pi f D_5}{c} \right) \end{aligned} \quad (41)$$

Subtracting A phasemeter from B we have

$$\frac{2\pi f}{c} (D_4 + e_4 - D_3 - e_3) + \frac{2\pi f}{c} (D_1 + e_1 - D_2 - e_2) \quad (42)$$

Now since $e_4 = e_3$ and $e_1 = e_2$ and D_4 and D_2 are constants

$$\text{Phasemeter} = \frac{2\pi f}{c} (D_1 - D_3) \quad (43)$$

This phasemeter output is equal to the correct hyperbolic line of position with no skywave error included.

Published test results of the Micro-Omega system are quite limited. The data obtained during an eighteen month evaluation program yielded an RMS system error of less than one centicycle (480 ft on Omega baseline) under favorable signal-to noise conditions. Reference 8 stated that these conditions prevailed more than ninety-five percent of the time for one line (Trinidad-New York) and only twenty percent of the time for the other available line (Hawaii-New York). There was no data presented as to position errors versus distance from the monitor site.

IV. DIFFERENTIAL OMEGA SYSTEM USING COAST GUARD RADIOBEACON

A. GENERAL DESCRIPTION

Goodman [7] first proposed using the present system of U.S. Coast Guard radiobeacons, Type T-747A/FRN, as the transmission vehicle for the differential correction message along the coasts and harbors of the United States (see Fig. 18). The correction information would be in the form of audio tones that are directly related to the Omega corrections for specific hyperbolic LOPs. A total of four LOP corrections and five calibration tones would be transmitted in a one minute interval once every five minutes. The message format will be described in detail later but in general a 600 Hz tone would be equivalent to no LOP correction and 500 Hz excursions above and below this value would correspond to ± 50 cec LOP corrections. This audio tone would be used to AM modulate the radiobeacon carrier (285-325 kHz).

Instead of using the standard AM modulation technique where the carrier's amplitude is modulated with the signal of varying frequency, Goodman proposed using the dual carrier technique presently being used on many Coast Guard radio-beacons. This modulation method uses two RF carriers separated in frequency by the audio frequency corresponding to the audio tone desired. When received these two carriers produce the same effect in the receiver as conventional AM but require only half the bandwidth--thus conserving frequency spectrum.

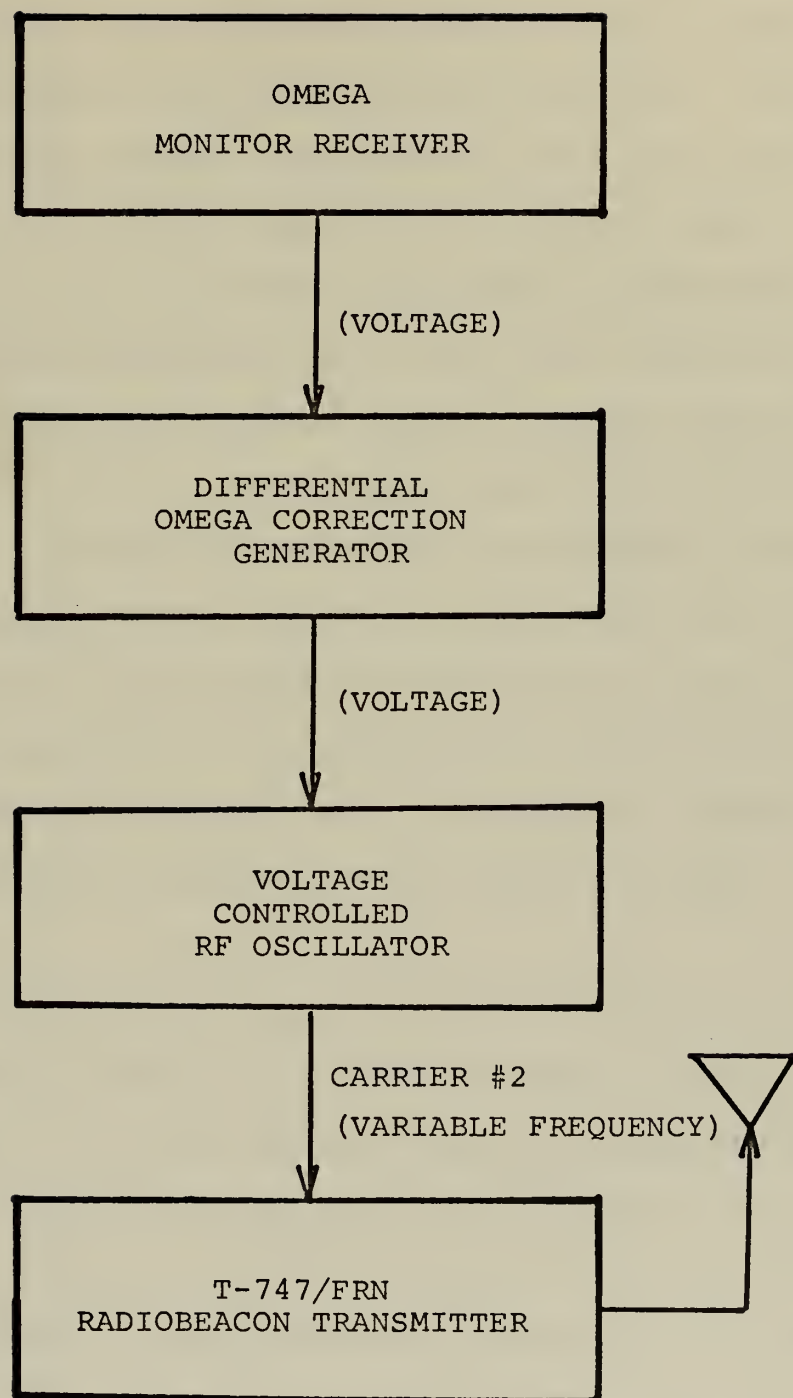


Figure 18. Goodman's Differential Omega Transmission System.

The use of the radiobeacon and the differential Omega message proposed by Goodman were predicated on the assumption that a small vessel could use the system as well as the large vessel having computer oriented navigation systems. In order to use the proposed system, the shipboard user must have a low frequency (LF) receiver aboard as well as an Omega receiver (see Fig. 19). For the small users (commercial fishermen, coastal freighters, etc.) the audio output of the LF receiver is fed into a simple frequency meter that has a range of 100 to 1100 Hz. The frequent calibration tones used by Goodman were intended primarily for the navigator using an analog frequency meter. The face of the meter could be calibrated directly into corrections according to the conversion scale described below without having the navigator manually convert the frequency into corrections. These corrections can then be applied to the received Omega readings.

As the sophistication of the shipboard navigation system increases, a digital meter can be used instead of the analog meter used above. The digital meter would be preferred because of its higher accuracy and ease of reading in a shipboard environment. A standard digital frequency meter is easily modified to read directly in centicycles instead of frequency. For Goodman's proposal all this would entail is subtracting 600 from the frequency received and dividing the result by ten.

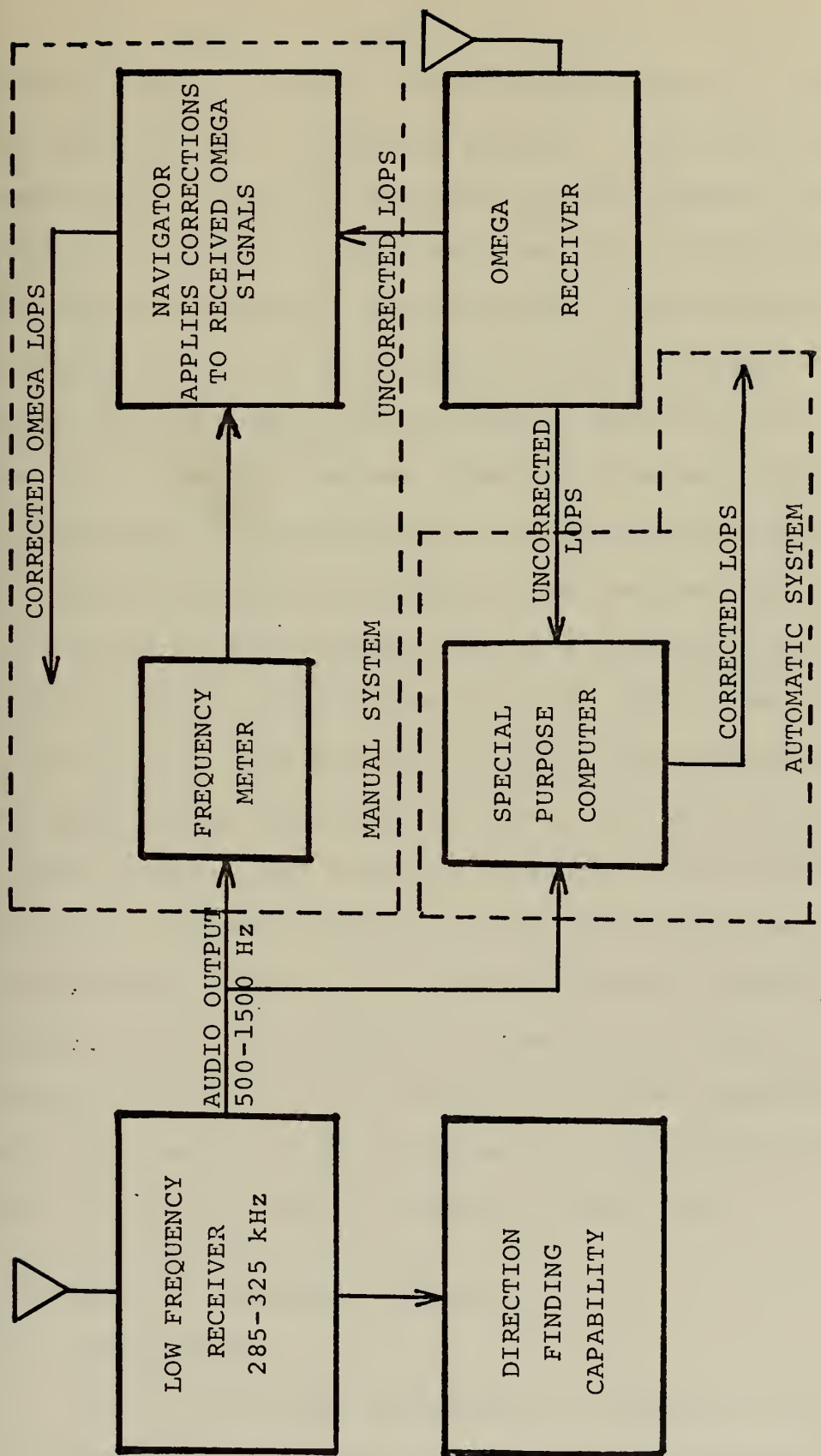


Figure 19. Manual and Automatic Differential Omega Reception System.

For automatic operation, the output of the LF receiver could be fed to a small special purpose computer which may include a frequency counter. The output of the Omega receiver can also be routed to the computer and the corrections applied to the Omega readings and displayed on the computer console or rerouted back to the Omega receiver and displayed on it. The special purpose computer would have to have an input register which identified the LOPs to which the correction message (described below) applied and what LOPs were being fed into it from the Omega receiver. The initial calibration tone could be used as an indication of the start of the message and the LOP identifiers as an indication to the computer as to which LOP it was to apply the correction. The correction could be determined by the same method described above in connection with the digital frequency meter. The computer operations can also be handled by a sub-routine in a large, multi-purpose computer already aboard instead of a special purpose computer. The important point that should be reemphasized however is the automatic system can use the same correction message as the manual user and thus the proposed system does not discriminate against the small, unsophisticated user.

B. CHANGES TO GOODMAN'S PROPOSAL

1. Transmitter

- The T-747-A/FRN radiobeacon transmitter can be used in a variety of ways without additional circuitry:
- a. Keyed carrier, no modulation
 - b. Keyed carrier and tone modulation

- c. Continuous carrier with keyed tone modulation
- d. Dual carrier, both keyed simultaneously
- e. Dual carrier, either keyed separately

Goodman also investigated the following ways of modulating the radiobeacon--all of which would require transmitter modifications:

- a. PAM--Pulse Amplitude Modulation
- b. PWM--Pulse Width Modulation
- c. PPM--Pulse Position Modulation
- d. FM--Frequency modulation
- e. Amplitude modulation with a modulation signal of varying frequency
- f. Carrier separation Modulation (similar to dual carrier modulation above except that one of the carrier's frequencies varies).

Goodman decided that the carrier separation modulation technique was best since it only required changing the second RF carrier oscillator in the transmitter to a voltage controlled oscillator (VCO) and secondly used only half the frequency spectrum of conventional AM modulation.

One of Goodman's major goals was the reduction of the number of modifications required to the radiobeacon transmitter. In this thesis amplitude modulation with the modulating signal of varying frequency is suggested since there are no wiring changes required to the transmitter under the arrangement described below.

To implement the system proposed in this thesis all that is required is the removal of the temporary jumper connection between J101 and J102 or J102 and J103 on the

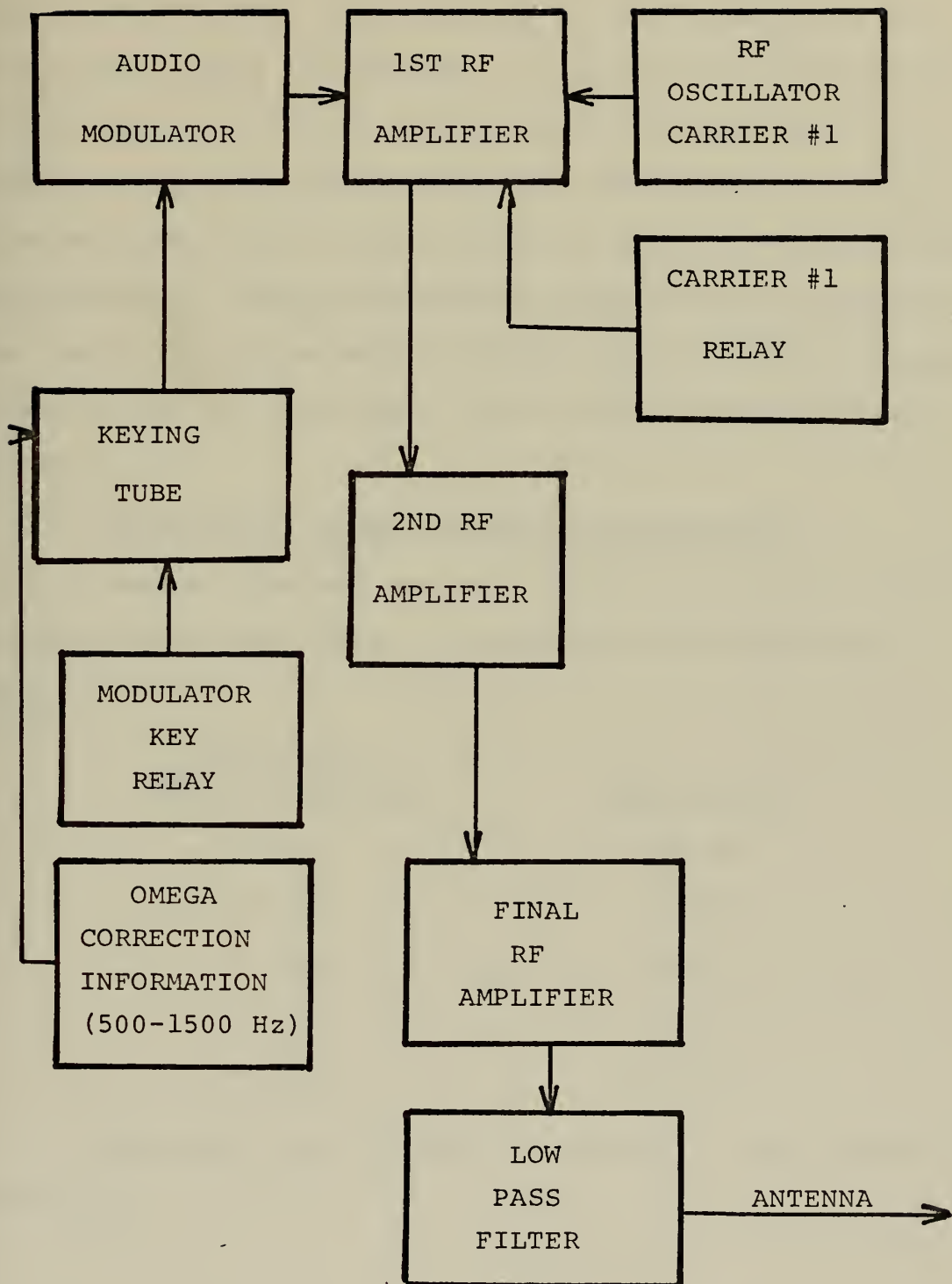


Figure 20. Proposed Radiobeacon Differential Omega System.

transmitter oscillator chassis. The connection of the Omega correction device (described below) to J102 is the only other step necessary for operation of the transmitter as a differential Omega transmitter. It should be noted that the radiobeacon can still be used by the non-Omega user for direction finding purposes since the radiobeacon normally is AM modulated with a 500 or 1020 Hz signal. The addition of differential Omega information merely makes the modulation frequency vary anywhere between 500 and 1500 Hz instead of one of the two previously used fixed frequencies (see Fig. 20).

2. Differential Omega Correction Information

Goodman proposed use of an audio tone which varied in proportion to the Omega correction in the following manner:

<u>Differential Omega Correction</u>	<u>Audio Tone</u>
+50 cec	100 Hz
+25 cec	350 Hz
0 cec	600 Hz
-25 cec	850 Hz
-50 cec	1100 Hz

The audio tone variation proposed in this thesis is as follows:

<u>Differential Omega Correction</u>	<u>Audio Tone</u>
+50 cec	1500 Hz
+25 cec	1250 Hz
0 cec	1000 Hz
-25 cec	750 Hz
-50 cec	500 Hz

The reasons for the changes are:

a. Since there is an extremely stable 1000 Hz source available--an output at the back of the Tracor 599R Omega receiver--this can provide an extremely accurate source for a mid-scale calibration tone whose use will be described later.

b. A minor change, but one that would be significant to a user, is to reverse the meaning of the high and low frequencies. It is natural for a user to think of a pointer deflection to the right of center as positive and to the left of center as negative. If Goodman's frequency schedule were fed into a frequency meter, mid-scale would correspond to zero correction, as in the newly proposed system, but high scale would correspond to a negative correction; the reverse of the natural tendency of most users.

3. Coding Message Format

Since the vehicle and modulation technique for transmitting the differential Omega information had been selected, it was necessary to decide in what format the information was to be transmitted. Both Goodman [7] and

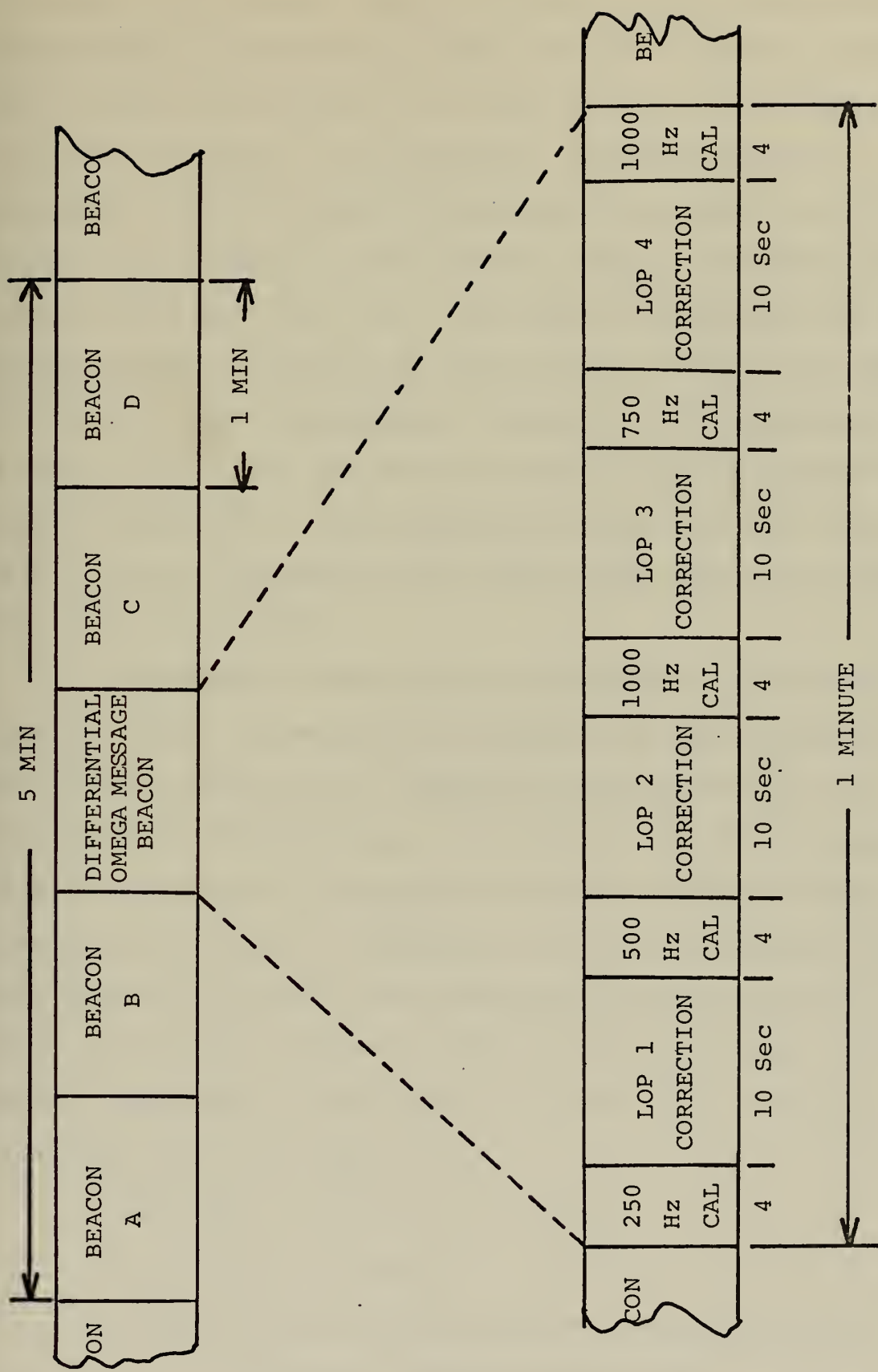


Figure 21. Goodman's Differential Omega Message.

McKaughan [13] decided that the simplest, most easily decoded message was a correction for each of the four best hyperbolic LOPs through the monitor site (best as far as fix geometry and signal strength are concerned). Goodman decided to transmit four differential Omega correction signals and five calibration signals in a one minute segment, repeating every five minutes (see Fig. 21). The reason for choosing the one minute segment length was in order not to disrupt the normal radiobeacon chain transmission sequence. One radiobeacon in a net of five along the coast normally transmits during one minute out of five. The calibration tones were for users with an analog frequency meter which might require calibration every 30 minutes.

McKaughan's coding message was slightly different (see Fig. 22). He decided to transmit the differential corrections continuously, repeating every minute for 29 minutes, then transmitting a calibration tone for one minute. This would allow the alignment of analog frequency meters once every half-hour. McKaughan's reason for changing from once every five minutes to continuous transmissions was given as the rapid change in Omega readings possible if a solar flare occurs at the end of the once per five minute transmission. For example [13]

$$160^\circ \text{ phase shift}/40 \text{ min.} = 4^\circ/\text{min.}$$

$$4^\circ = 1.1 \text{ cec}$$

$$1 \text{ cec} = 160 \text{ yds} \text{ thus } 1.1 \text{ cec} = 176 \text{ yds error/min.}$$

$$5.5 \text{ cec} = 880 \text{ yds error/5 min.}$$

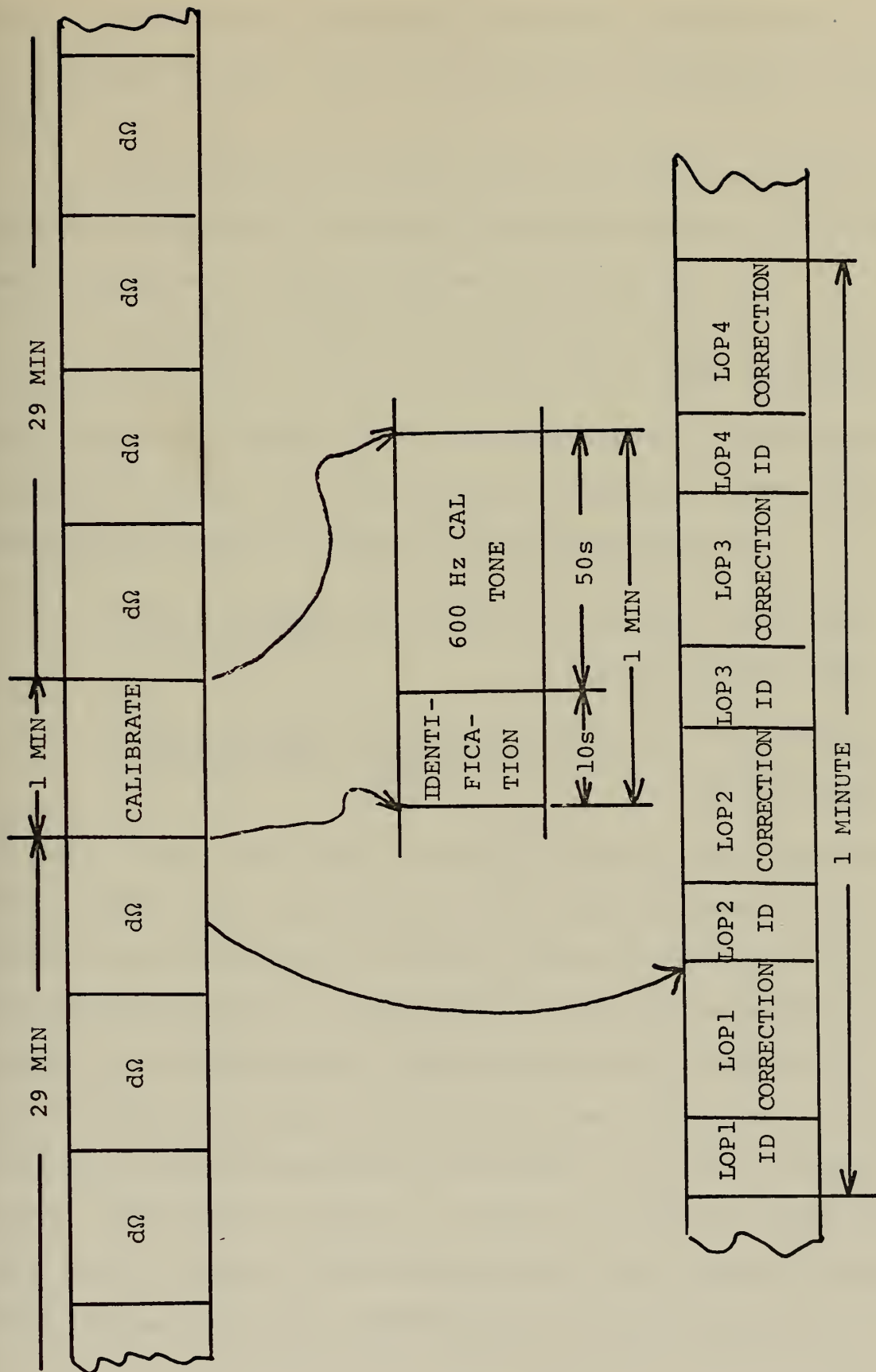


Figure 22. McKaughan's Differential Omega Message.

Using a five minute old set of corrections could result in an error of 880 yds. This is clearly an unacceptable system error.

Rapid changes of phase occur normally twice a day during the day-night, night-day transition period as can be seen in Figure 4. These changes can be as much as

$$20 \text{ cec/hr} = 1.66 \text{ cec error/5 min} = 266 \text{ yds error/5 min}$$

(from Figure 4)

Data taken for a typical LOP (Trinidad-Hawaii) from skywave correction tables for the geographic position of the Naval Postgraduate School yielded the following results:

$$\begin{aligned} 24 \text{ hour average } \Delta \text{cec}/5 \text{ min} &= 0.73 \text{ cec error/5 min} \\ 1-15 \text{ April 1972} &= 117 \text{ yds error/5 min} \end{aligned}$$

$$\begin{aligned} \text{largest } \Delta \text{cec}/5 \text{ min out of 24 hours} &= 2.3 \text{ cec error/5 min} \\ 10-1100 \text{ GMT (sunrise at Trin.)} &= 368 \text{ yds error/5 min} \end{aligned}$$

It can be seen that there is almost half as much incremental phase shift occurring during a five minute segment of the night to day transition period as can occur during a solar flare during the day. Therefore it was found necessary to transmit the differential Omega correction information on a once a minute schedule, as McKaughan had concluded, in order to derive the maximum benefit from its use during periods of normal, rapid phase change. In fact a navigator would probably want correction information more often than once every five minutes if he were approaching a harbor entrance.

The differential Omega correction format proposed in this thesis can be seen in Figure 23. The only differences between this format and McKaughan's was the inclusion of a calibration tone every minute vice every thirty minutes and the method of identification of the correction lines. The inclusion of a calibration tone was deemed necessary since it is possible that a user might first decide to use the differential correction information immediately after the calibration segment was transmitted and would have to wait thirty minutes before he could be sure his frequency meter were properly calibrated. The identification as to which LOP the particular corrections applied would be published on the charts along with the symbol for the radiobeacon station and its operating frequency. For example:

Radiobeacon
Symbol 

310 kHz
LOP 1 B-D
LOP 2 A-D
LOP 3 B-C
LOP 4 A-C

C. IMPLEMENTATION OF RADIOBEACON MODULATOR

1. Message Format Commutator

The differential Omega message format described above requires a device that can shift any one of six different audio tones to the transmitter input J102 (see Fig. 24). These tones are the 1000 Hz calibration and identification tone, LOPs one through four (audio tones of 500-1500 Hz) and no tone for the pause. A 100 Hz signal from the back of the Tracor 599R Omega receiver is put through

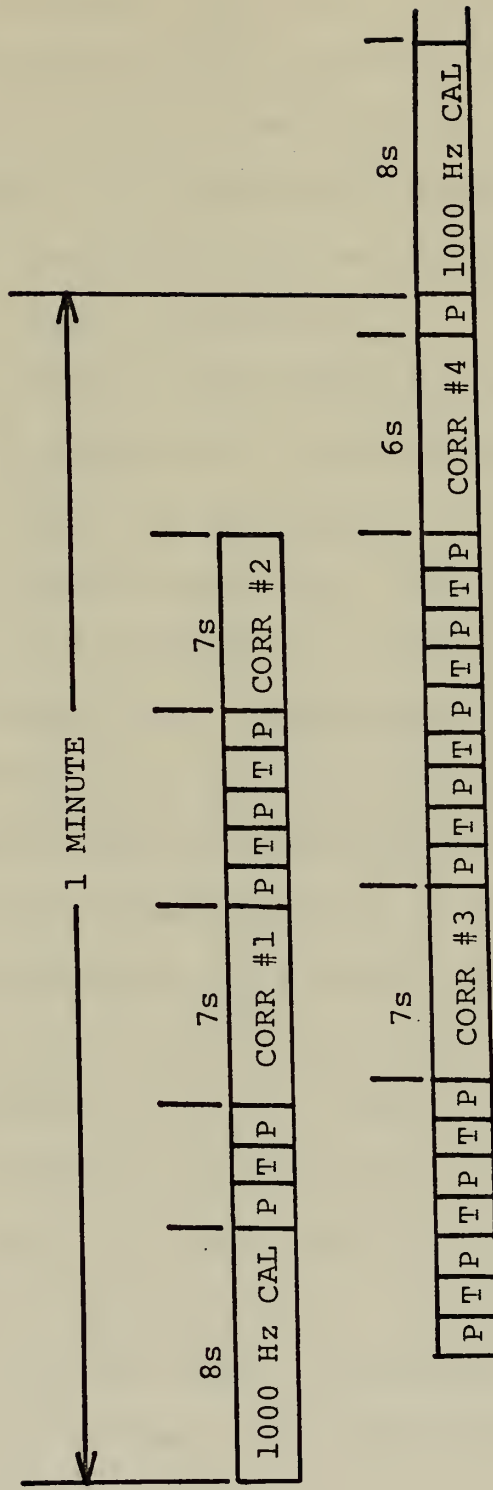


Figure 23. Proposed Differential Omega Message Format

two, divide by ten, counters so that a 1 Hz signal is then fed to the binary counters. The binary counter has the capability of counting up to 4095 seconds. Since the read only memory (ROM) used in the commutator can only accept the binary equivalent of 1023 different binary numbers at its input terminals, only the first ten outputs of the binary counter were used, A_0 through A_9 .

The ROM is a device that causes any combination of its four outputs, 01 through 04, to be activated by any combination of its inputs, A_0 through A_9 . A sample of the ROM programming is shown in Figure 25. ROM binary output 1, 0001, corresponds to LOP correction 1, binary output 2,0010, to LOP correction 2 and so on. Binary output 5,0101, corresponds to the 1000 Hz tone used for calibration and identification and binary 0,0000, corresponds to no tone for the pause. Since the ROM can accept up to 1023 binary inputs, this is equivalent to 1023 seconds or 17 min 3 seconds. This means that the ROM can operate for seventeen one minute cycles before any of the input's numbers repeats itself. The three seconds left over are used to reset the binary counters. Count 1021 and 1022 will be the same as a pause and 1023 will be binary 6,0110. This will reset the binary counters to zero and allow the process to repeat again for the next 17 minutes. For the complete ROM truth table see Appendix A.

The output of the ROM must be converted from binary to decimal numbers. The decimals numbers then correspond to the following list:

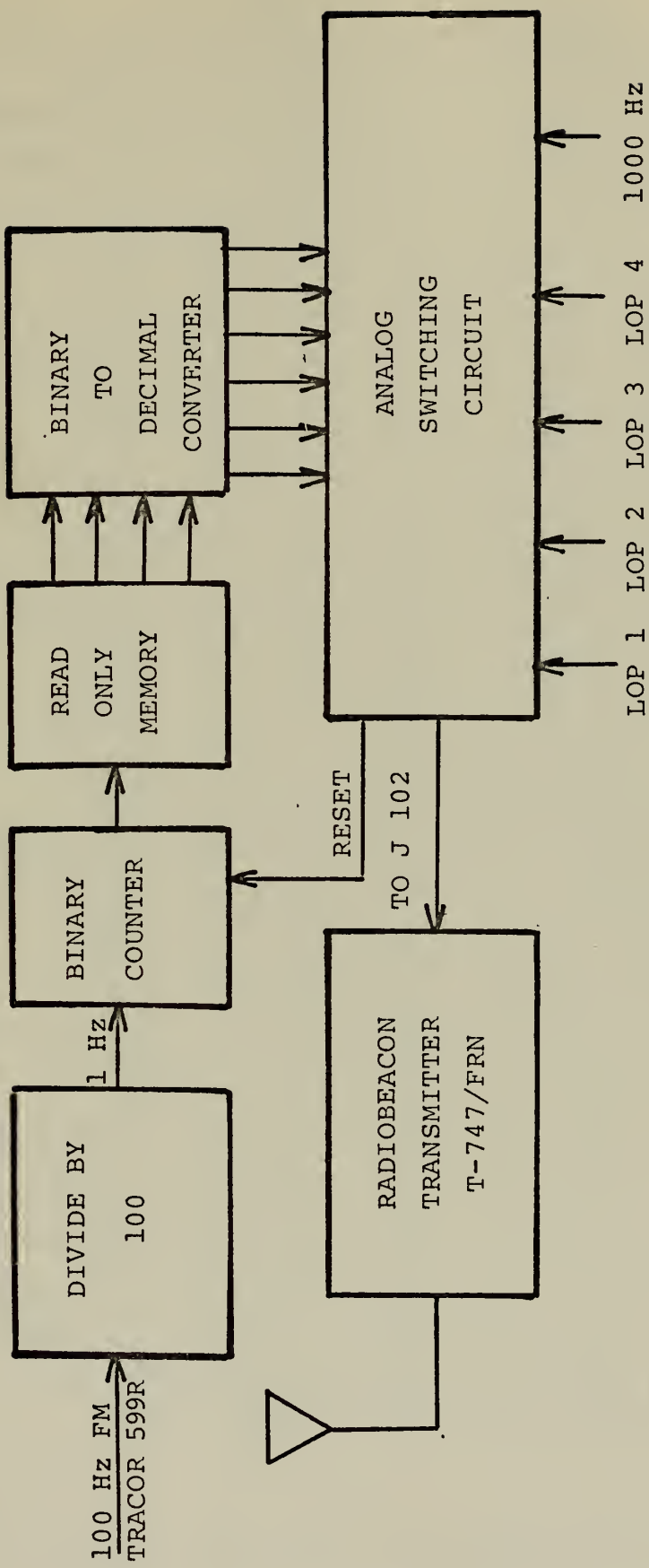


Figure 24. Block Diagram of Commutator Circuit.

Word	OUTPUT				Word	OUTPUT			
	O ₄	O ₃	O ₂	O ₁		O ₄	O ₃	O ₂	O ₁
0					70				
1					71				
2					72				
3					73				
4					74				
5					75				
6					76				
7					77				
8					78				
9					79				
10					80				
11					81				
12					82				
13					83				
14					84				
15					85				
16					86				
17					87				
18					88				
19					89				
20					90				
21					91				
22					92				
23					93				
24					94				
25					95				
26					96				
27					97				
28					98				
29					99				
30					100				
31					101				
32					102				
33					103				
34					104				
35					105				
36					106				
37					107				
38					108				
39					109				
40					110				
41					111				
42					112				
43					113				
44					114				
45					115				
46					116				
47					117				
48					118				
49					119				
50					120				
51					121				
52					122				
53					123				
54					124				
55					125				
56					126				
57					127				
58					128				
59					129				
60					130				
61					131				
62					132				
63					133				
64					134				
65					135				
66					136				
67					137				
68					138				
69					139				

Diagram illustrating the structure of a Read Only Memory Truth Table. The table is organized into vertical columns representing words and horizontal rows representing output bits O₄ through O₁. The table is divided into sections by brackets on the left and right sides. The sections are labeled as follows:

- CALIBRATION TONE (Top section)
- ID LOP #1
- LOP #1 CORRECTION
- ID LOP #2
- LOP #2 CORRECTION
- ID LOP #3
- LOP #3 CORRECTION
- ID LOP #4
- LOP #4 CORRECTION
- CALIBRATION TONE (Bottom section)
- ID LOP #1
- LOP #1 CORRECTION

Arrows point from the labels to their corresponding sections in the table. The table contains 140 rows of data, starting from word 0 and ending at word 69.

Figure 25. Sample from Read Only Memory Truth Table.

<u>ROM Output Binary Number</u>	<u>Decimal Equivalent</u>	<u>Function</u>
0001	1	LOP #1
0010	2	LOP #2
0011	3	LOP #3
0100	4	LOP #4
0101	5	1000 Hz calibration
0110	6	Reset
0000	0	Pause

From the binary to decimal converter all the pulses go to inverter circuits except number 6. The reason for this is that the outputs of the binary to decimal converter are all at plus 5 volts until that particular output is selected by the ROM, then it drops to zero volts. The inverter changes the outputs to zero volts until selected, then the output goes to 5 volts. The reset pulse doesn't go through an inverter since the reset pins of the binary counters require 5 volts there at all times. When the 5 volts is removed then the counters reset. Since the six output of the binary to decimal converter is at 5 volts until selected, then this output can be connected to the reset pins of the binary counters and will cause them to reset when output 6 is selected by the ROM.

After going through the inverter circuit the next step is the level translator to increase the voltage of the signal enough to operate the FET (Field Effect Transistor) switches. Each of the audio signals generated in the Omega

LOP corrector (described later) is fed into its own FET switch and all the outputs of the FETs are connected together and go to J102, the input jack of the audio modulation circuit of the transmitter. When the proper LOP has been selected by the ROM and decoded, then the switch corresponding to the LOP selected is allowed to feed through the FET to J102. All other FETs appear as open circuits to their signals. If no switch is selected then a pause occurs, i.e., there will be no audio modulation of the carrier. This portion of the circuit is the equivalent of five switches in parallel. This completes the commutator circuitry. The complete schematic for the commutator is contained in Appendix B.

2. LOP Differential Correction Circuit

As first envisioned, the LOP correction circuit was as shown in Figure 26. The Omega receiver output was a DC voltage that was directly proportional to the phase in cec of the LOP to which the receiver was tuned. This voltage was fed to a subtractor circuit. A second signal provided by a stable DC source was also fed to the subtractor circuit. This was the reference to which the Omega signal was to be compared. The difference between the reference and the Omega receiver was an indication of the error of the Omega LOP from the correct value. This error voltage was then fed to a voltage controlled oscillator (VCO) which was used to generate an audio tone corresponding to the correction signal.

a. Voltage Controlled Oscillator (VCO)

Before any construction could begin on the overall device, the frequency vs voltage characteristics of the VCO had to be obtained. The schematic diagram for the VCO is as shown in Figure 27. Using the formula

$$f_o = \frac{2(v^+ - v_c)}{R_1 C_1 v^+} \quad (44)$$

and a value of v^+ of 12 volts, $v_c = 10.5$ volts, $R_1 = 4K$ ohms C_1 was determined to be $0.0625 \mu F$.

The circuit was built and tested and the results are shown in Figure 28. The linearity of frequency versus voltage was extraordinary. Frequency was measured to the nearest cycle and v_c , the control voltage, to the nearest millivolt. There were no observed non-linear regions in the graph within the designed range of 500-1500 Hz.

b. Subtractor Circuit

After determining the characteristics of the VCO, the next circuit attacked was the subtractor circuit. Using the circuit shown in Figure 29, the device was built and tested and found to have an offset voltage error. At the same time that the voltage offset error problem was being solved, it was realized that subtraction of the Omega signal from the reference voltage and its application to the VCO would cause the VCO to generate an audio frequency proportional to the error not the correction as desired. As an example assume that the voltage at the control terminal

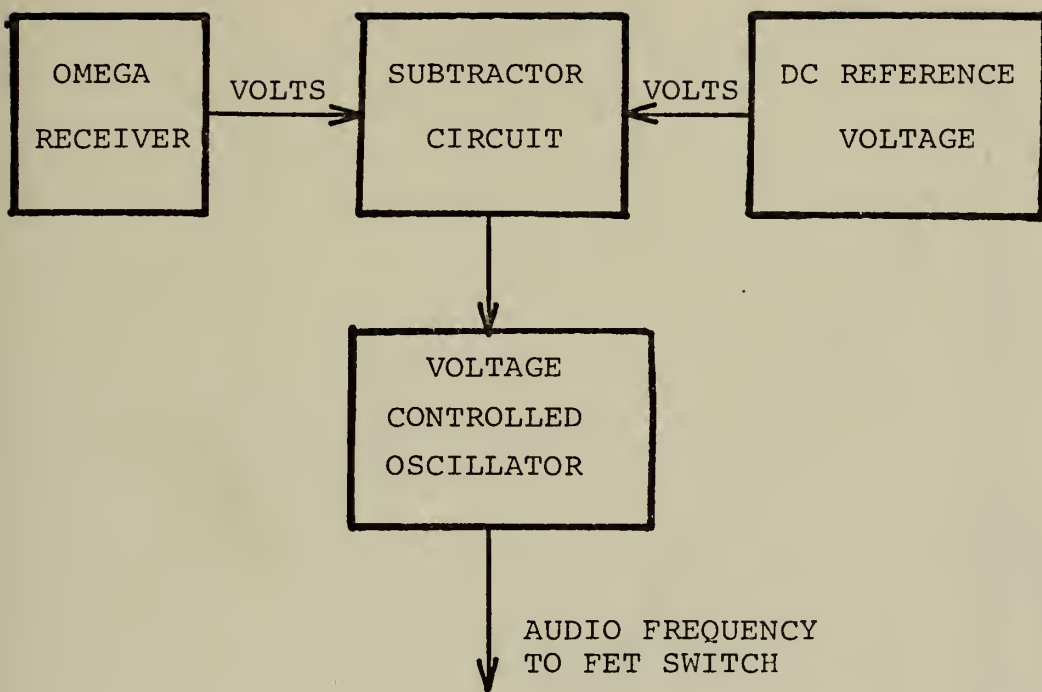


Figure 26. Block Diagram of LOP Correction Generator.

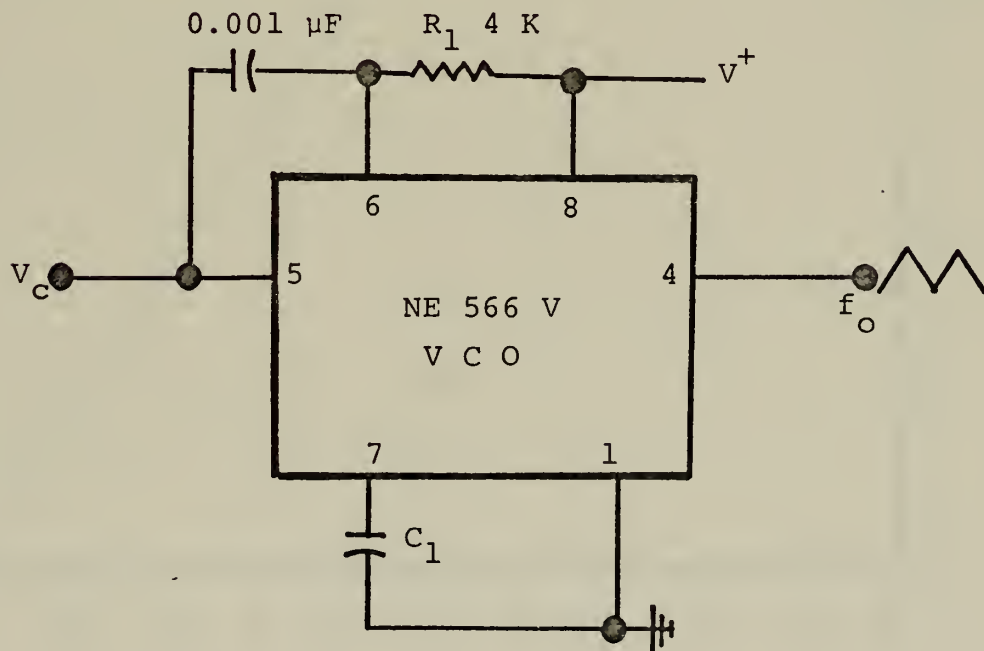


Figure 27. Circuit Diagram for VCO.

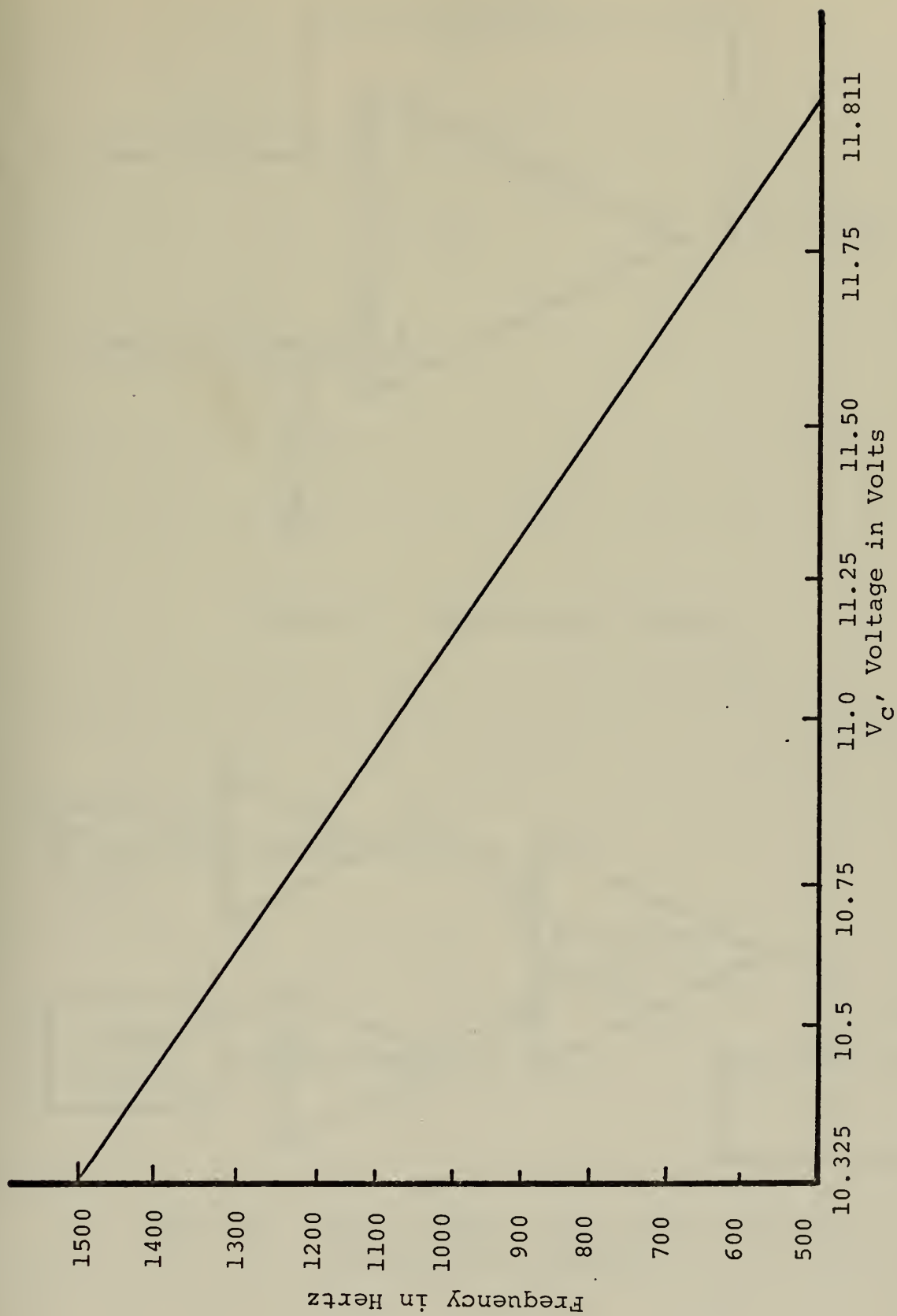


Figure 28. Frequency Versus Voltage of VCO.

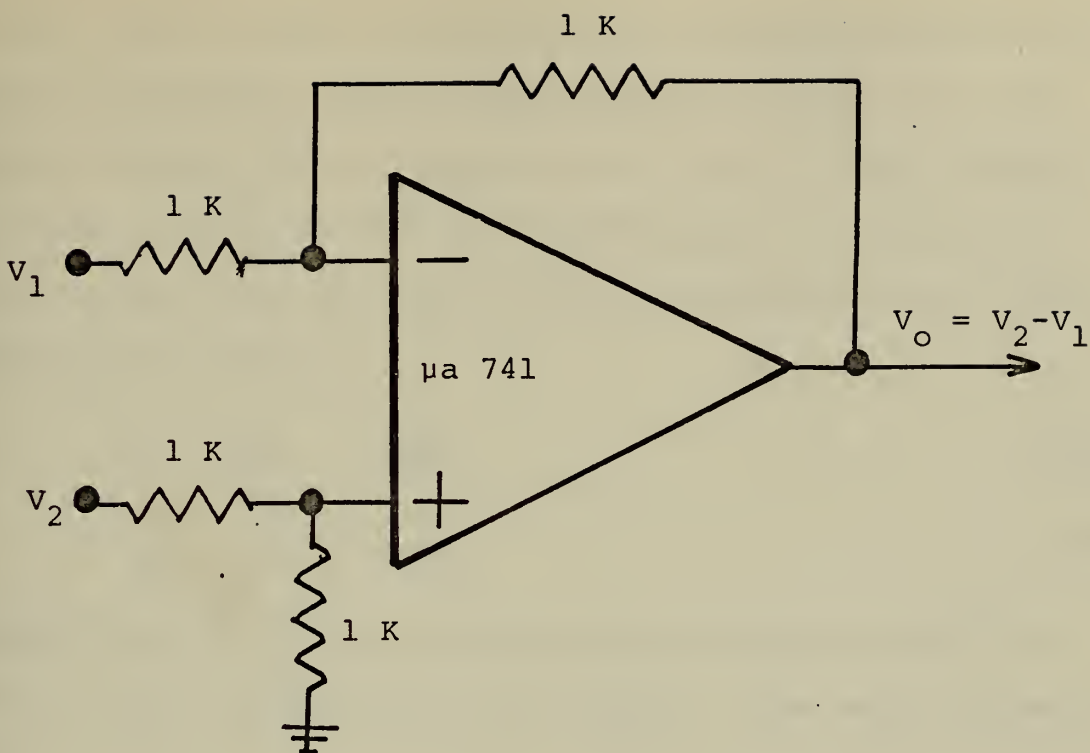


Figure 29. Subtractor Circuit.

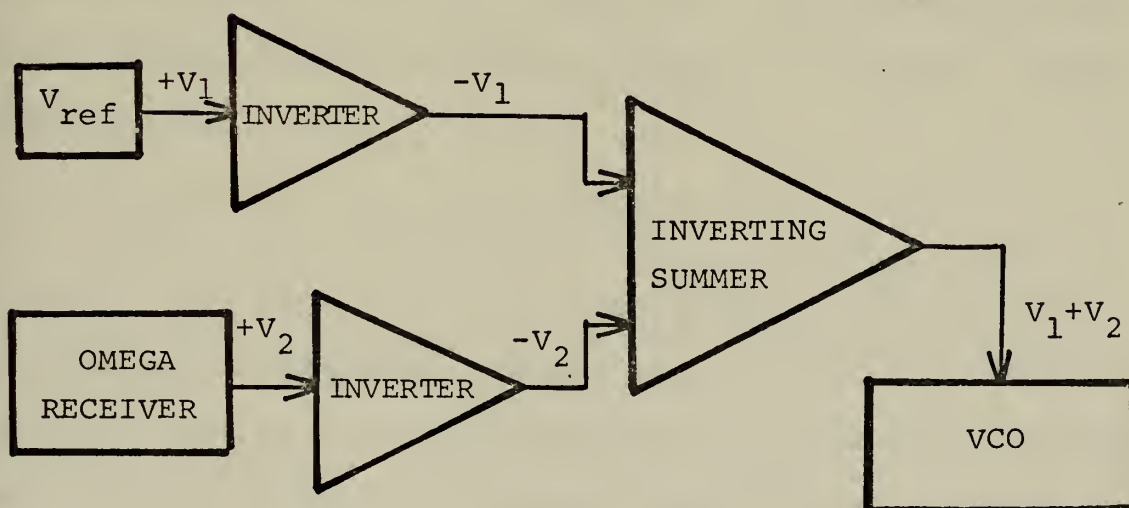


Figure 30. Block Diagram of Differential Omega Corrector Using Adder.

of the VCO, V_C , must be equal to 10.5 volts for the VCO to generate 1000 Hz. Also assume that the voltage from the Omega receiver varies linearly from 0 to 1.0 volts corresponding to 0 cec and 100 cec respectively. To determine what voltage must be used for the DC reference when using a subtractor circuit,

$$V_C = V_{REF} - V_{OMEGA} \quad (45)$$

$$V_{REF} = V_C + V_{OMEGA} \quad (46)$$

Assume that the correct LOP through the monitor site is 50 cec; this corresponds to 0.5 volts. Thus using equation (46)

$$V_{REF} = 10.5 + 0.5 = 11.0 \text{ volts}$$

So if the Omega receiver is actually receiving 50 cec then the VCO generates 1000 Hz as required. Now assume that the Omega reading rises to 60 cec or $V_{OMEGA} = 0.6$ volts. Using equation (45)

$$V_C = 11.0 - 0.6 = 10.4 \text{ volts}$$

As can be seen from Figure 28, a decrease in voltage means an increase in frequency. Assume that a V_C of 10.4 volts generates 1100 Hz. This corresponds to a correction for the Omega LOP of +10 cec. This is an incorrect result since if the Omega receiver shows 60 cec it is 10 cec above the correct value and therefore the correction is -10 cec not +10 cec as generated using the subtractor circuit.

If an adding circuit replaced the subtractor circuit in Figure 26, then the applicable equations are

$$V_C = V_{REF} + V_{OMEGA} \quad (47)$$

$$V_{REF} = V_C - V_{OMEGA} \quad (48)$$

Using the same assumptions as before (correct LOP 50 cec), and equation (48)

$$V_{REF} = 10.5 - 0.5 = 10.0 \text{ volts}$$

Using equation (47)

$$V_C = 10.0 + 0.5 = 10.5 \text{ volts}$$

This is the correct voltage to generate 1000 Hz as required when the received Omega value is equal to the correct value. Assume again that the Omega reading rises to 60 cec or $V_{OMEGA} = 0.6$ volts. Using equation (47)

$$V_C = 10.0 + 0.6 = 10.6 \text{ volts}$$

As before an increase in voltage corresponds to a decrease in VCO frequency. Assuming a V_C of 10.6 volts equals 900 Hz then this corresponds to -10 cec, the proper magnitude and direction of a correction for an Omega reading which is 10 cec too high.

From these results the circuit in Figure 30 was devised. Upon careful consideration of this newly proposed circuit, it was seen that the same effect could be obtained if V_{REF} were a voltage floating with respect to the ground of the Omega receiver. By floating the negative terminal

of the reference voltage it could be placed at the positive terminal of the Omega receiver output voltage. This would be the equivalent of placing two batteries in series, thus forming an adder circuit. By using a floating voltage it was possible to eliminate the two inverters and the inverting adder from the circuit in Figure 30 thereby eliminating three possible sources of nonlinearities. The chances for errors occurring in the summing circuit were high since the output would be close to 11 volts--definitely not a small scale signal and probably approaching the nonlinear portion of the operational amplifier's characteristics.

c. Voltage Reference Circuit

Since the subtractor and adder circuits had been eliminated, the next step was the design of the voltage regulator circuit. It was required that the voltage sources be extremely stable. The voltage of V_C , the VCO control voltage, ranged from 10.325 to 11.811 volts for a frequency change of from 1500 to 500 Hz respectively. This range is only 1.486 volts or 1.486×10^{-3} volts/cycle. Since accuracy to the nearest cycle of audio correction frequency was desired, this meant that the voltage references had to have a stability of better than 1.486 mv. The voltage regulator selected claims to have a long term stability of 0.1%/1000 hr or 10 mv/1000 hrs if $V_{out} = 10.0$ volts. 1000 hours is over one month so this specification is not too important since the correction devices will at manned radiobeacon stations and will be checked three or four times daily by watchstanders

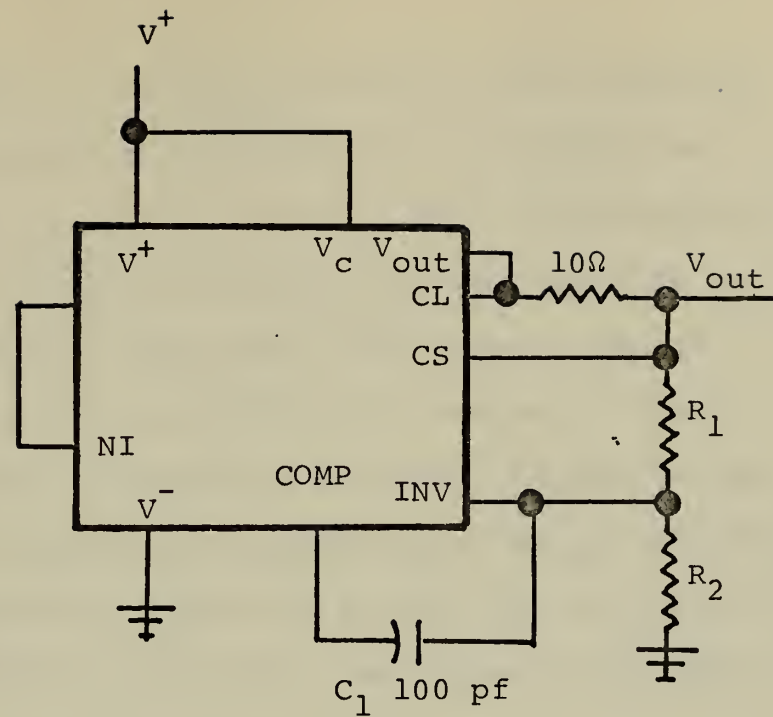


Figure 31. Schematic of Voltage Regulator Circuit.

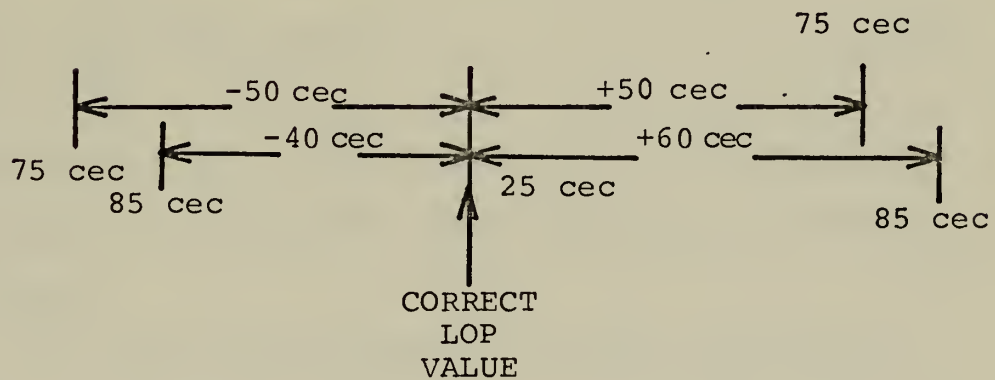


Figure 32. Example of Cyclic Nature of Omega Corrections.

for proper operation. Another parameter of the selected regulator is a temperature coefficient of 0.002%/°C or 0.2 mv/°C assuming $V_{out} = 10.0$ volts. The radiobeacons are generally housed in manned building and therefore the temperature would probably show only a few degrees change thereby eliminating this parameter as a source of error.

In order to provide a floating voltage it was necessary to use a separate regulated power supply floating with respect to building ground to provide the 18.0 volt V^+ for the circuit shown in Fig. 31. The values of R_1 and R_2 are calculated from the formulas

$$R_1 = \left(\frac{V_{out}}{V_{ref}} \right) (2000) \text{ ohms} \quad (49)$$

$$R_2 = \frac{2000}{\frac{V_{out}}{V_{ref}} - 1} \text{ ohms} \quad (50)$$

V_{ref} is typically 1.58 to 1.68 volts and must be measured for each circuit to obtain the proper V_{ref} for the actual circuit on hand.

If a particular Omega LOP passing through the monitor site were exactly 50 cec only one voltage regulator circuit would be needed. If the Omega LOP were any other value than 50 cec, assume 25 cec, then two voltage references are required because of the following:

<u>Omega LOP Received</u>	<u>LOP Correction Required</u>	<u>Frequency Generated Using One Voltage Regulator</u>
25 cec	0	1000 Hz
50 cec	-25 cec	750 Hz
75 cec	-50 cec	500 Hz
15 cec	+10 cec	1100 Hz
5 cec	+20 cec	1200 Hz
85 cec	+40 cec	400 Hz (Incorrect)

The last value in the list 400 Hz is incorrect. By examination of Figure 32 it can be seen that 85 cec corresponds to an error of -40 cec or +60 cec. Since ±50 cec was selected as the bounds for the LCP error by Goodman [7], it was also used as one of the basic premises of this thesis. As can be seen by the above example and Figure 32 any reading greater than 75 cec would result in an incorrect correction frequency being generated for an assumed LOP of 25 cec if only one voltage reference were used. The general equations to determine the upper and lower limits of the Omega readings from the correct values, assuming a ±50 cec excursion are:

Correct LOP less than 50 cec--

$$\text{Correct LOP} + 50 \text{ cec} = \text{upper limit} \quad (51)$$

$$0 \text{ cec} = \text{lower limit}$$

Correct LOP greater than 50 cec--

$$\text{Correct LOP} - 50 \text{ cec} = \text{lower limit} \quad (52)$$

$$100 \text{ cec} = \text{upper limit}$$

The Omega receiver circuitry itself takes care of switching from 100 to 0 cec when phase increases through 100 cec and 0 to 100 cec when phase decreases through 0 cec.

There must be some means of switching another voltage source into the circuit when V_{OMEGA} exceeds the limit set by equation (51) or (52). The switching can be accomplished by a voltage comparator using the circuit shown in Figure 33. A comparator circuit is basically an open loop operational amplifier with no degenerative feedback and a gain of perhaps as much as 10^5 . A difference between V_{OMEGA} and V_{COMPREF} of one millivolt would be enough to drive the output of the comparator into saturation ($\pm V_{\text{cc}}$). This causes very sharp switching when V_{OMEGA} reaches V_{COMPREF} with no gradual output voltage change at the comparator as V_{COMPREF} approaches V_{OMEGA} . When V_{COMPREF} is greater than V_{OMEGA} the output of the comparator is $+V_{\text{cc}}$. When V_{COMPREF} is less than V_{OMEGA} the output is $-V_{\text{cc}}$.

The output of the comparator is fed to a voltage follower in order to isolate the comparator circuit from the heavy drain caused by the relay. The input resistance of the voltage follower is nominally 400 MEGohms while its output resistance is much less than one ohm. The output voltage of the voltage follower is an exact duplicate of its input voltage hence the name voltage follower. When the comparator--voltage follower output is $+V_{\text{cc}}$, meaning that V_{COMPREF} is greater than V_{OMEGA} , then the diode is forward biased and the relay is closed allowing V_{REF1} to be used in

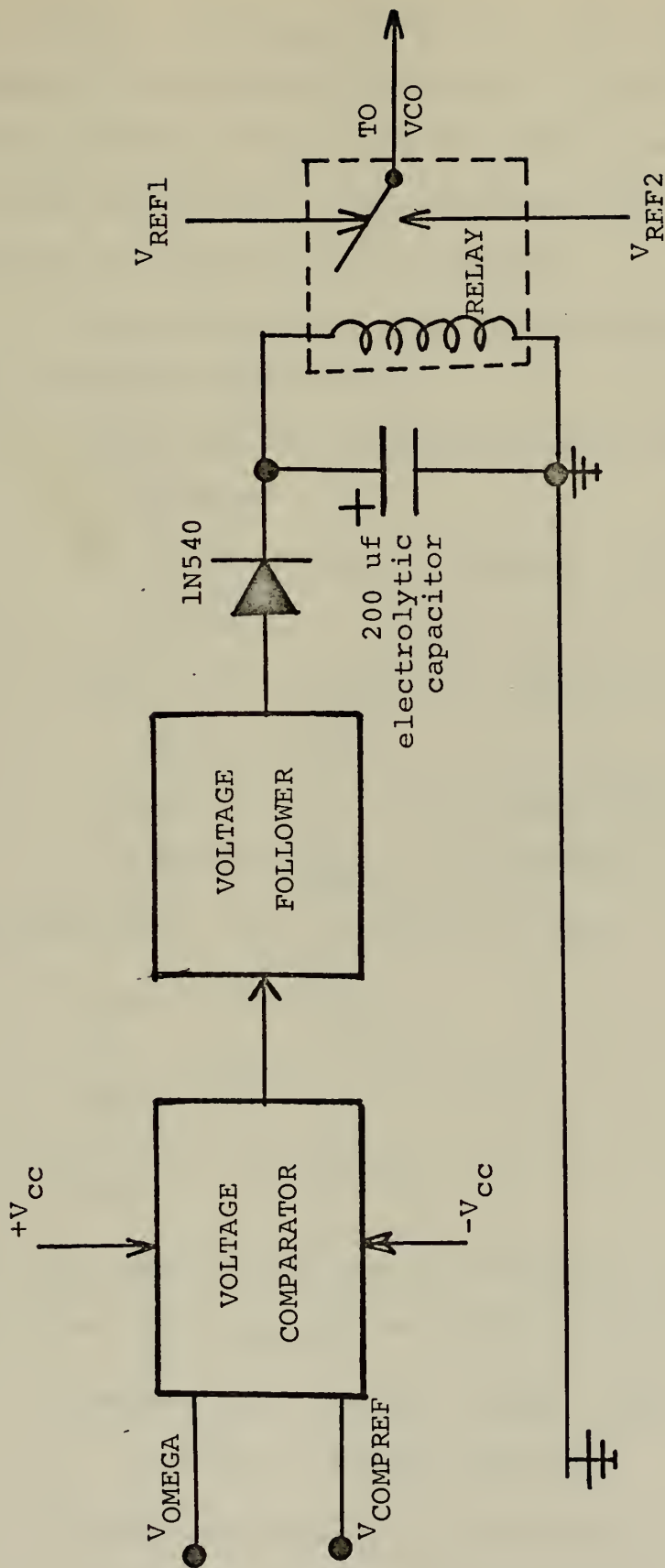


Figure 33. Voltage Comparator Switching Circuit.

the VCO circuit. If V_{OMEGA} is greater than V_{COMPREF} then the output of the comparator--voltage follower is $-V_{\text{cc}}$ so the diode is reverse biased and the relay opens connecting V_{REF2} to the VCO circuit. The capacitor in parallel with the relay is to eliminate relay chatter.

As an example to help clarify the need for two voltages reference assume that:

- (a) V_c of the VCO must be 10.5 volts to generate 1000 Hz
- (b) V_c of 10 volts = 1500 Hz, V_c of 11.0 volts = 500 Hz
- (c) 0 cec = V_{OMEGA} of 0 volts, 100 cec = V_{OMEGA} of 1.0 volts
- (d) The correct value of the LOP of interest is 25 cec ($V_{\text{OMEGA}} = 0.25$ volts.)

Then using equation (48) to solve for V_{REF}

$$V_{\text{REF}} = V_c - V_{\text{OMEGA}} \quad (48)$$

$$V_{\text{REF1}} = 10.5 - 0.25 \text{ volts}$$

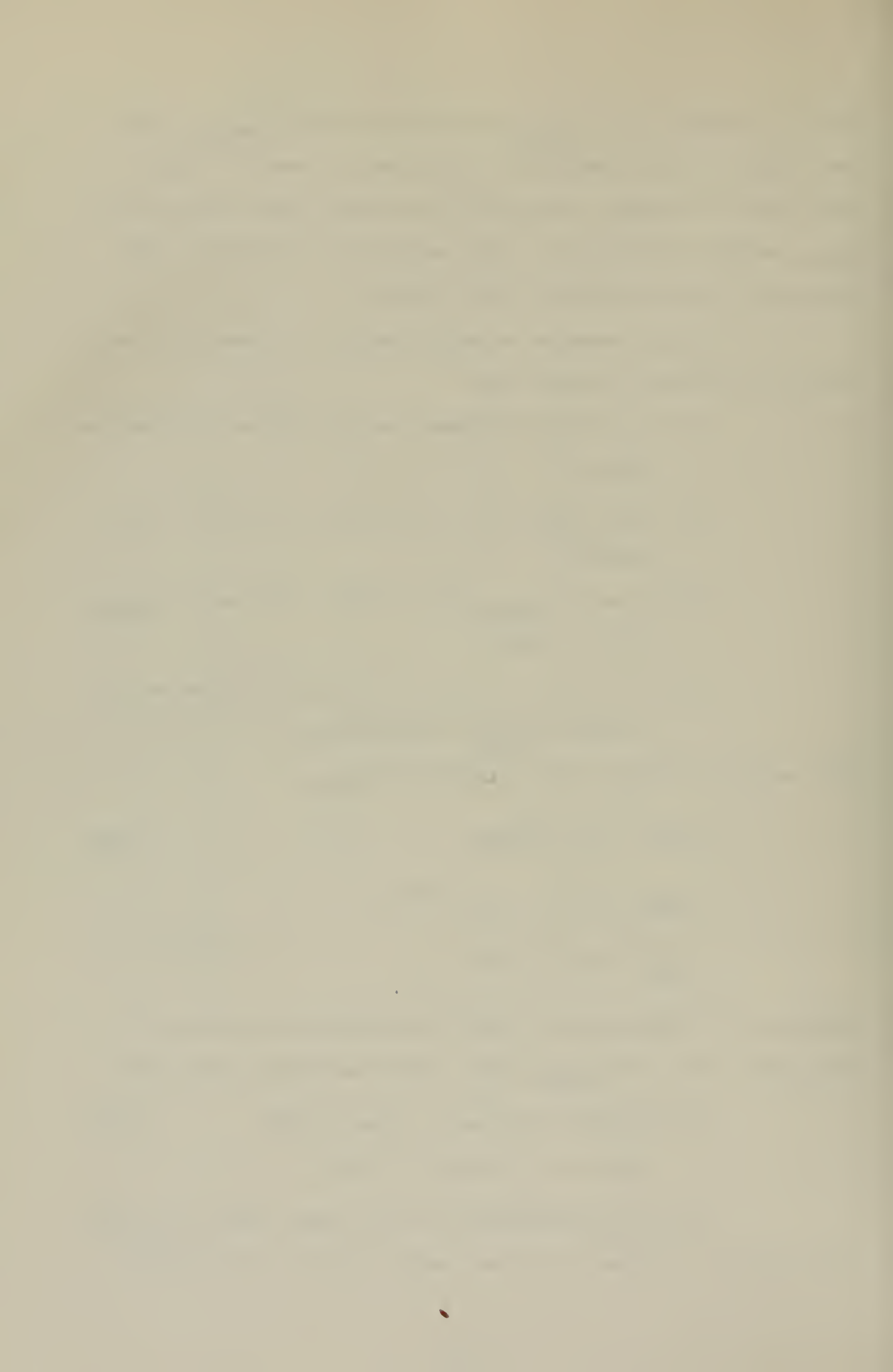
$$V_{\text{REF1}} = 10.25 \text{ volts}$$

Equation (51) must now be used to determine the value of the upper limit of V_{OMEGA} above which switching must occur

$$\text{Correct LOP} + 50 \text{ cec} = \text{upper limit} \quad (51)$$

$$25 \text{ cec} + 50 \text{ cec} = 75 \text{ cec}$$

75 cec corresponds to 0.75 volts, thus $V_{\text{COMPREF}} = 0.75$ volts. A value of 75 cec could require a correction



of either +50 cec or -50 cec since it is the end point either way from 25 cec as shown in Figure 32. Therefore to determine the value of V_{REF2} given that 75 cec equals a +50 cec correction (forcing V_C to equal 10.0 volts so that the VCO will generate 1500 Hz or +50 cec);

$$V_{REF2} = V_C - V_{OMEGA}$$

$$V_{REF2} = 10.0 - 0.75 \text{ volts}$$

$$V_{REF2} = 9.25 \text{ volts}$$

Now if V_{OMEGA} is less than 0.75 volts then V_{REF1} equals 10.25 volts will be used as the voltage reference for the VCO and if V_{OMEGA} is greater than 0.75 volts, V_{REF2} equals 9.25 volts will be used as the reference.

d. Final Differential Omega Correction Circuit

Figure 34 shows the LOP correction circuit in its final form. The Omega signal, V_{OMEGA} is first routed to the voltage comparator circuit where it is compared to $V_{COMPREF}$ to see which of two voltage sources, V_{REF1} or V_{REF2} , will be switched by the relay to the adder circuit. The adder circuit merely consists of the floating reference voltages, V_{REF1} or V_{REF2} being placed in series with the grounded V_{OMEGA} and their combined sum then being fed as V_C to the VCO. The output of the VCO goes through a voltage follower circuit to buffer the output from the effects of the transmitter. This was found necessary because when the VCO was connected to the receiver, the frequency of the VCO changed 20 Hz. The VCO has its own voltage regulator

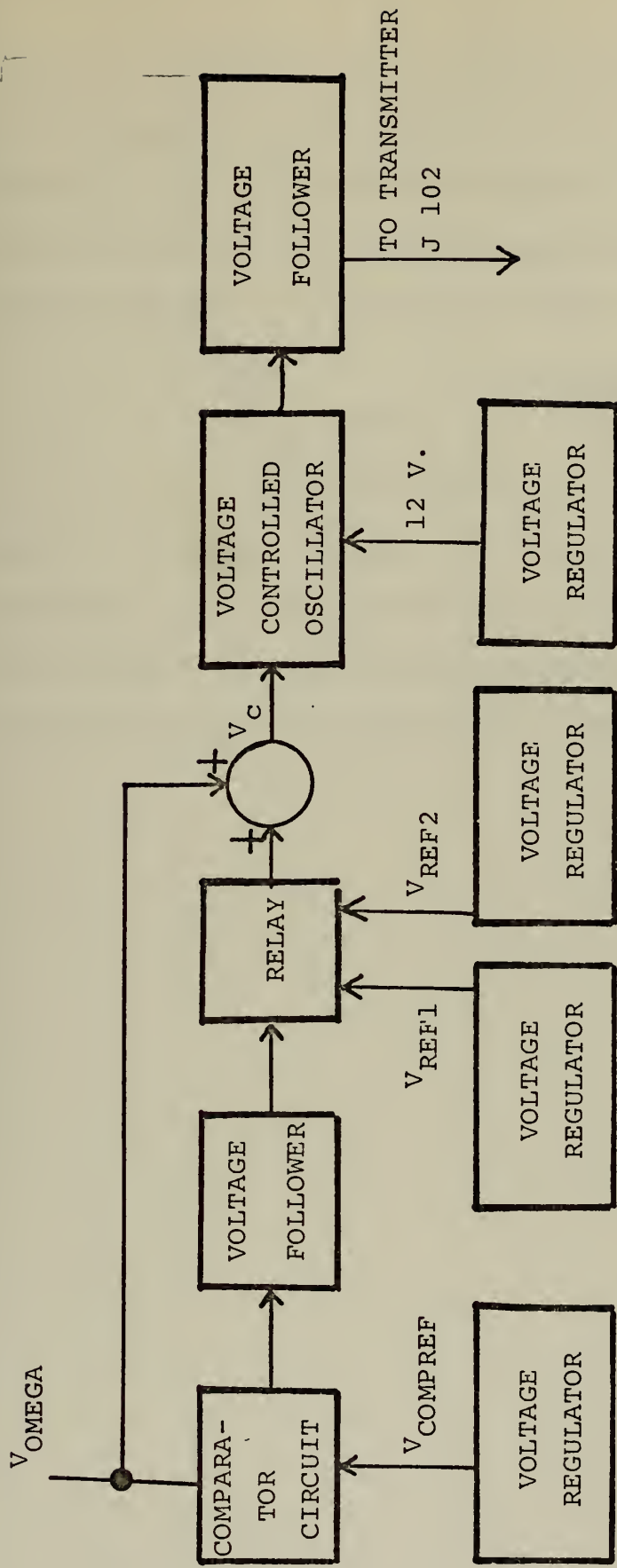


Figure 34. Block Diagram of Differential Omega LOP Corrector.

circuit providing it is a V^+ of 12 volts. The VCO requires its own power supply because, as can be seen from solving equation (44), the output frequency is extremely dependent on the value of V^+ . Solving equation (44) for the differential change in f_o versus V^+ gives:

$$\left. \frac{\partial f_o}{\partial V^+} \right|_{\begin{array}{l} f_o = 1000 \\ V^+ = 12 \text{ volts} \end{array}} = \frac{0.58 \text{ Hz}}{\text{millivolt}}$$

Only a 2 millivolt change in V^+ results in a 1.06 Hz change in output frequency or 0.1 cec when converted to LOP correction terms. For the complete schematic diagram of the differential Omega LOP corrector see Appendix C.

V. TESTING AND ANALYSIS

A. RESULTS OF TESTING WITHOUT TRANSMITTER

When construction of the differential Omega LOP corrector was completed the next step was a thorough testing of the device. It was decided to test initially the device without using the radiobeacon transmitter. This would give an indication of the accuracy of the corrector without errors from interfacing it with the transmitter. The first tests were conducted using the equipment as arranged in Figure 35. The output of the Omega receiver was recorded on the red channel of a dual channel strip chart recorder moving at 0.1 inches per minute. The chart paper was ten inches wide and divided into 1 inch major and 0.1 inch minor divisions. Zero scale corresponded to zero cec and full scale corresponded to 100 cec, thus each minor division was 1 cec. The Omega receiver output was also fed to the differential Omega LOP corrector where it was used to generate the audio correction frequency. The audio correction frequency was fed to a Hewlett Packard 5210A analog frequency meter. This meter has a recorder output which was fed to the blue channel of the chart recorder. Zero scale on the blue channel corresponded to 500 Hz and full scale corresponded to 1500 Hz. Thus each minor division corresponded to 10 Hz.

Figure 36 shows a sample of a chart recording for 2 March 1972. It graphically illustrates the magnitude of phase

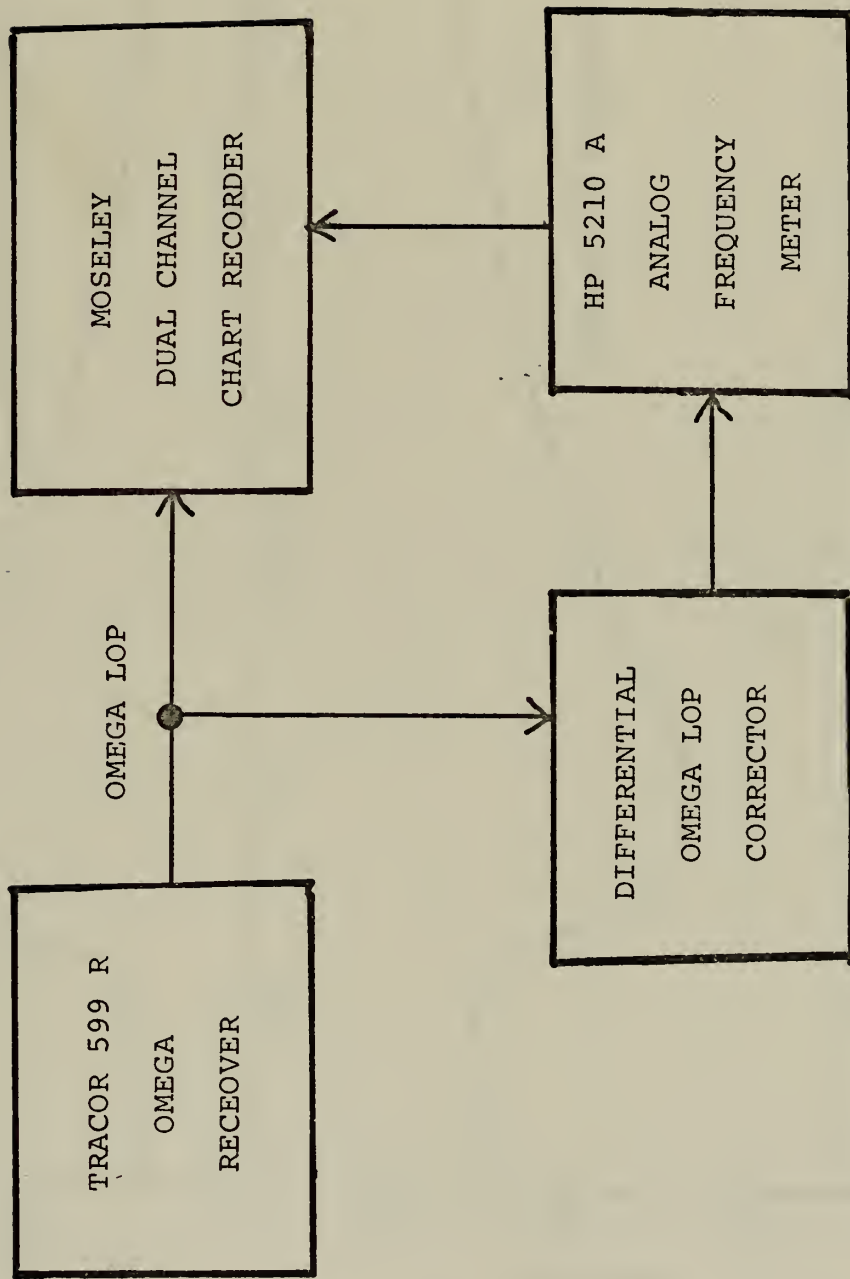


Figure 35. First Differential Omega LOP Corrector Test Layout Without Transmitter.

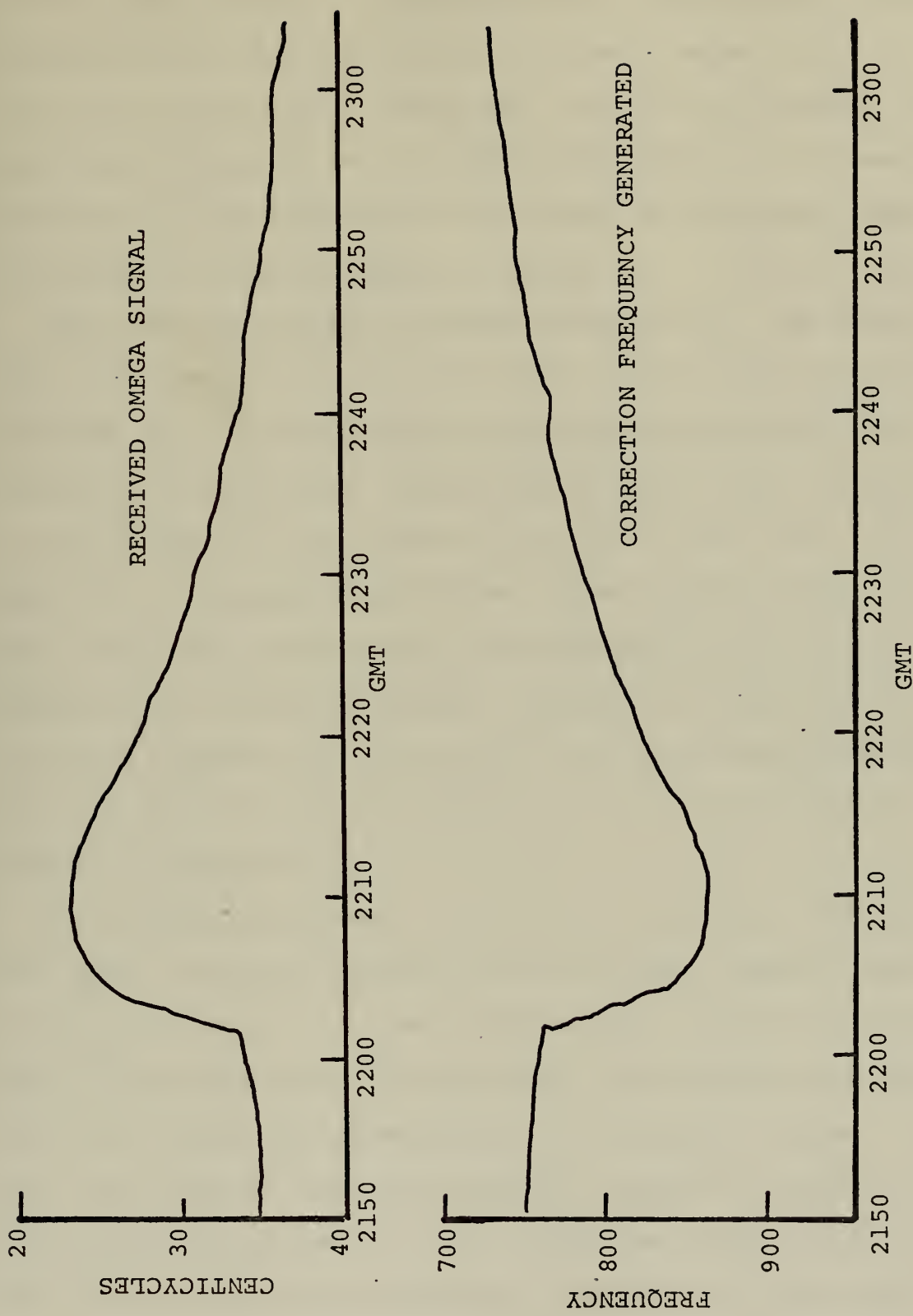


Figure 36. Effect of Solar Flare on Phase of Omega Signal and Differential Omega LOP Corrector, 2 March 1972.

change due to a small anomalous disturbance. There is a sudden phase decrease of approximately 10 cec in five minutes, probably due to a solar flare. The lower curve is the output of the differential Omega LOP corrector as recorded from the analog frequency meter. This curve shows an increase in frequency of 100 Hz which is the change in frequency required to correct a 10 cec decrease in phase.

The data was normally analyzed once a day. The charts were read every ten minutes and the received Omega LOP was recorded as well as the frequency being generated by the corrector at that time. Both recorded lines were interpolated to the nearest 0.1 of a minor division or 0.01 inch. An Omega LOP or frequency measurement read to the nearest 0.01 inch resulted in accuracies to the nearest 0.1 cec for the former and 1 Hz for the latter. These two numbers were then placed on computer data cards and run through the Naval Post-graduate School's IBM 360 computer. The program used is located in Appendix D.

The computer program calculated the difference between the Omega LOP being received and the correct value. Based on this difference, it then computed what required frequency the differential Omega LOP corrector should have been generating to correct the received LOP to the proper value. After this the computer read the frequency actually generated from the data card and computed the difference between what the LOP corrector generated and what it should have generated. This difference resulted in a frequency error which was

converted to cec error by dividing by ten (Δ frequency 1000 Hz = Δ cec 100). The average value of the cec error was obtained using equation (53)

$$\text{Average error cec} = \frac{\sum_{i=1}^n (\text{errcec})_i}{n} \quad (53)$$

The standard deviation of the cec error was obtained using equation (54).

$$\sigma_{\text{error cec}} = \left[\frac{n \left(\sum_{i=1}^n (\text{errcec})_i^2 \right) - \left(\sum_{i=1}^n (\text{errcec})_i \right)^2}{n^2} \right]^{\frac{1}{2}} \quad (54)$$

where errcec_i is the individual error of each data point in cec and n is the number of observations made. A sample computer printout is contained in Appendix E.

The assumed Omega LOP through the antenna location used for this experiment was obtained from Mr. E. R. Swanson of NELC, San Diego. The Trinidad-Hawaii (B-C) 10.2 kHz LOP for this location is 8.5 cec.

Figure 37 is a summary of the results of the computer output. It contains results for V_{REF1} and V_{REF2} . The need for two reference voltages was explained earlier. V_{REF1} was used for received Omega signals of less than 58.5 cec. Above 58.5 cec V_{REF2} was switched into the circuit instead of V_{REF1} .

In the case of non-correlated lines of position, the standard deviation of the fix error is usually taken as the

DATE	V_{REF1}			V_{REF2}		
	σ_{errrec}	Average $errrec$	$\sigma_{fixerror}$ cec	σ_{errrec}	Average $errrec$	$\sigma_{fixerror}$ cec
			yds		yds	yds
18-19 FEB 72	0.16	0.21	0.24	38	0.28	0.55
19-20 FEB 72	0.18	0.39	0.27	43	0.22	-0.07
24-25 FEB 72	0.21	-0.18	0.31	50	0.21	0.10
1-2 MAR 72	0.26	0.11	0.39	62		
2-3 MAR 72	0.21	-0.06	0.31	50	0.27	-0.32
8-9 MAR 72	0.23	0.12	0.34	54	0.28	-0.12
11-12 MAR 72	0.37	0.21	0.55	88		
13-14 MAR 72	0.29	0.31	0.43	69	0.11	0.16
14-15 MAR 72	0.24	-0.23	0.36	58	0.19	0.41
Average of Above data	0.24	0.10	0.36	58	0.22	0.09
					0.32	51

Figure 37. Summary of Accuracy of Differential Omega Corrector Using Strip Chart Recorder without Transmitter.

square root of the sum of the squares of the two LOP errors divided by the sine of the crossing angle between the two LOPs [19]. The crossing angle was shown earlier to never be less than 60° , and 72° may be assumed as a typical value. Assuming both LOPs can be corrected to the same accuracy, then the standard deviation of the fix can be determined from equation (56).

$$\sigma_{\text{fix error}} = \frac{\sigma_{\text{errcec}} \sqrt{2}}{\sin 72^\circ} \quad (55)$$

$$\sigma_{\text{fix error}} = (\sigma_{\text{errcec}}) (1.49) \quad (56)$$

Equation (56) gives the fix error in cec which can be converted to yards by multiplying by 160 ($1\text{cec} = 480 \text{ ft.} = 160 \text{ yds}$ on the baseline). The σ_{fixerror} was 58 yards for V_{REF1} and 51 yards for V_{REF2} .

After 16 March 1972, a new data acquisition technique was employed (see Fig. 38). The analog frequency meter was replaced by a Hewlett Packard digital frequency meter. The Omega receiver voltage, V_{OMEGA} , was measured by a Hewlett Packard digital voltmeter. Instead of recording the data on an analog strip chart, the data was then recorded on three inch wide adding machine paper by a Hewlett Packard 560A digital recorder. The paper printout was not in binary numbers but ordinary decimal numbers. The frequency was recorded to the nearest Hz and V_{OMEGA} to the nearest 0.10 cec. The paper tape information was then transcribed to data cards and the same computer program above was used to analyze the

data. Data points were obtained every six minutes by a clock operated cam. This cam fed a signal to the frequency meter causing it to sample the frequency. When the frequency meter completed its one second count, it commanded the printer to print the frequency and the digital voltmeter reading. Figure 38 contains the results of the computer runs. During the period covered by Figure 39, 16-25 March 1972, σ_{fixerror} of V_{REF1} was 21 yards and V_{REF2} was 30 yards. The reduction of σ_{fixerror} from Figure 37 to Figure 39 was attributed to the fact that the data interpolation was being done automatically instead of manually.

B. RESULTS OF TESTING WITH TRANSMITTER

After sufficient data had been collected to determine what the accuracy of the differential Omega LOP corrector was by itself, it then had to be tested as a transmitter modulator (see Fig. 40). The output of the corrector was fed to J102, the audio modulation input jack of the T-747A/FRN radiobeacon transmitter. The transmitter was connected to a dummy antenna. A wire antenna for the AN/WRR-3A low frequency receiver was placed near the dummy antenna and the stray emissions were picked off and used as receiver input signals. The signals were demodulated and the audio output of the receiver was fed to the digital frequency meter. The same cam timer as before resulted in data points being recorded every six minutes. The output of the printer was typed onto data cards and run through the computer. The results are shown in Figure 41.

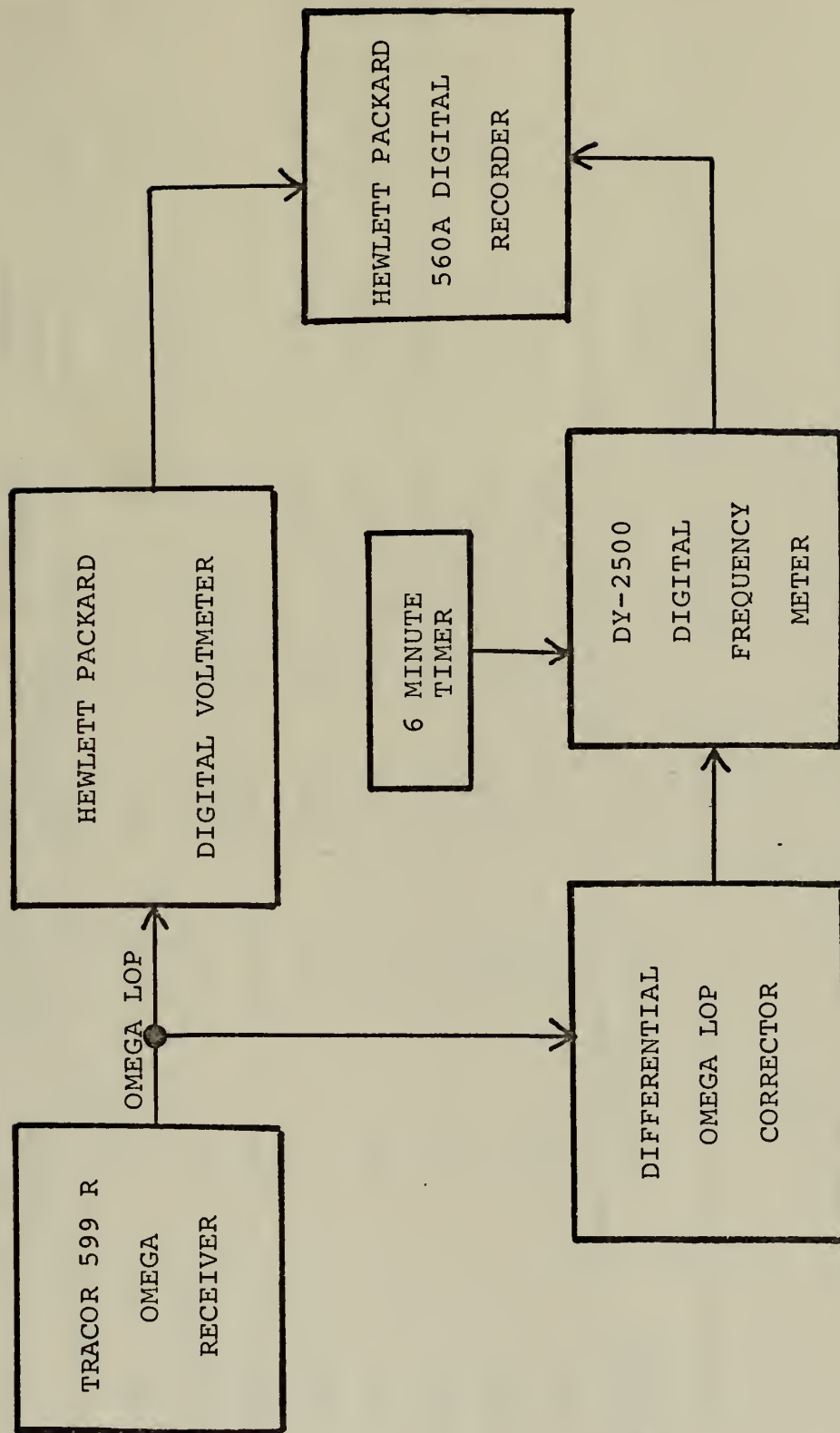


Figure 38. Second Differential Omega LOP Corrector Test Layout Without Transmitter.

DATE	V _{REF1}			V _{REF2}		
	σ_{errrec}	Average errrec	$\sigma_{fixerror}$ cec yds	σ_{errrec}	Average errrec	$\sigma_{fixerror}$ cec yds
16-17 MAR 72	0.10	-0.02	0.15	24	0.09	0.02
17-18 MAR 72	0.08	-0.08	0.12	19	0.13	0.31
18-19 MAR 72	0.14	-0.14	0.21	34		
20-21 MAR 72	0.10	-0.01	0.15	24	0.10	-0.01
21-22 MAR 72	0.08	-0.15	0.12	19	0.17	-0.29
22-23 MAR 72	0.12	0.11	0.18	29	0.21	-0.15
23-24 MAR 72	0.06	0.00	0.09	14	0.16	-0.22
24-25 MAR 72	0.07	0.06	0.10	15	0.07	-0.57
Average of Above data	0.09	-0.03	0.13	21	0.13	-0.13
						0.19
						30

Figure 39. Summary of Differential Omega Corrector Accuracy Using Digital Recorder Without Transmitter.

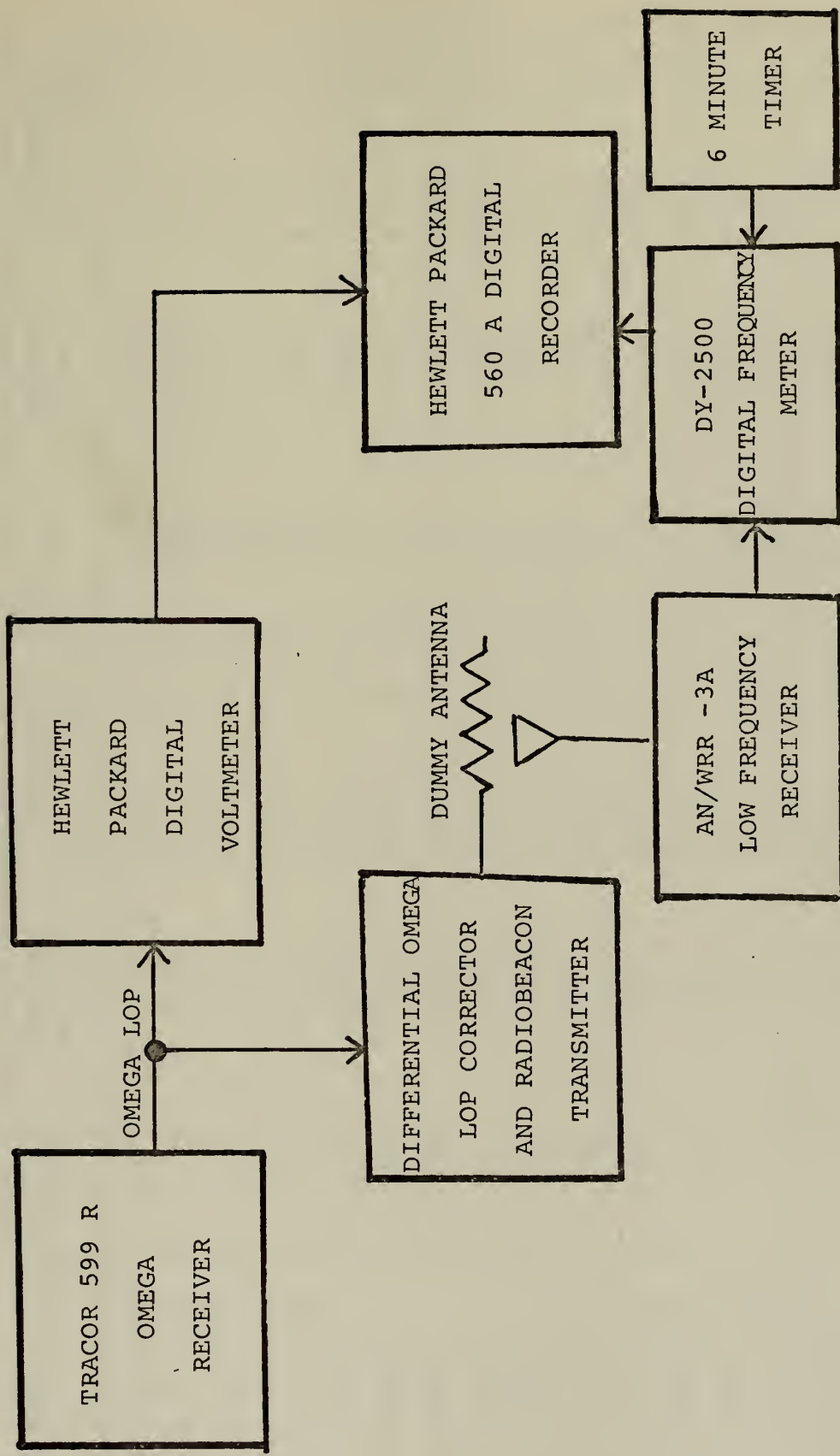


Figure 40. Differential Omega LOP Corrector Test Circuit with Transmitter.

DATE	V _{REF1}			V _{REF2}		
	σ_{errrec}	Average errrec	$\frac{\sigma_{fixerror}}{cec}$	σ_{errrec}	Average errrec	$\frac{\sigma_{fixerror}}{cec}$
			yds		cec	yds
27-28 MAR 72	0.09	-0.05	0.14	21	0.21	-0.03
28-29 MAR 72	0.08	0.01	0.12	19	0.19	-0.08
29-30 MAR 72	0.11	0.01	0.16	26	0.22	-0.21
30-31 MAR 72	0.07	-0.02	0.10	16	0.06	0.05
31 MAR-1 APR	0.07	-0.04	0.10	16	0.07	0.05
1-2 APR 72	0.10	-0.09	0.15	24	0.10	-0.08
2-3 APR 72	0.07	0.04	0.10	16	0.07	-0.03
3-4 APR 72	0.08	-0.09	0.12	19	0.08	0.00
4-5 APR 72	0.07	-0.12	0.10	16	0.13	-0.01
5-6 APR 72	0.11	0.10	0.16	26	0.13	-0.08
10-11 APR 72	0.08	-0.17	0.12	19	0.12	-0.16
12-13 APR 72	0.11	-0.13	0.16	26	0.27	0.07
14-15 APR 72	0.10	-0.06	0.15	24	0.22	0.08
16-17 APR 72	0.13	0.19	0.19	30	0.21	0.15
18-19 APR 72	0.12	-0.24	0.18	29	0.14	-0.16
19-20 APR 72	0.14	0.09	0.21	32	0.22	-0.16
Average of Above data	0.10	-0.04	0.15	24	0.15	-0.03
					0.22	35

Figure 41. Summary of Accuracy of Differential Omega Corrector with Transmitter.

Unexpectedly, there was very little loss of information by using the transmitter-receiver combination. The $\sigma_{fixerror}$ for V_{REF1} was 24 yards and V_{REF2} was 35 yards. This was only a 4 yard (0.2 cec) increase over operation without the transmitter for V_{REF1} and a 5 yard (0.03 cec) increase for V_{REF2} .

C. ANALYSIS OF RESULTS

1. Test Results

The circular probable error (CPE) is considered to be the radius of a circle, centered at the mean position of a group of measurements, that encloses 50 percent of the measurements.

$$CPE = \frac{1.18 \sigma_{errcec}}{\sin \text{ crossing angle}} \quad (57)$$

Ninety-five percent of the fixes will lie within a circle of radius:

$$95\% \text{ circular error} = \frac{2.45 \sigma_{errcec}}{\sin \text{ crossing angle}} \quad (58)$$

Using equation (57) and (58) and the averages of Figure 41 the results are:

$$CPE V_{REF1} = \frac{(1.18)(0.10)}{(0.95)} = 0.12 \text{ cec} = 19 \text{ yards}$$

$$CPE V_{REF2} = \frac{(1.18)(0.15)}{0.95} = 0.19 \text{ cec} = 30 \text{ yards}$$

$$\text{Average CPE} = 25 \text{ yards}$$

$$95\% \text{ Circular error } V_{REF1} = \frac{2.45(0.1)}{0.95} = 0.25 \text{ cec} = 41 \text{ yards}$$

$$95\% \text{ Circular error } V_{REF2} = \frac{2.45(0.15)}{0.95} = 0.39 \text{ cec} = 62 \text{ yards}$$

Average 95% Circular error = 52 yards

These results mean that at the monitor site, an erroneous Omega fix can be corrected to within a circle of 52 yards radius 95% of the time and a circle of 25 yards radius 50% of the time. This is a tremendous improvement over the generally conceded 1 to 2 mile error of ordinary Omega using skywave correction tables.

2. Digitizing Errors

Anytime a digital measurement is made inevitably some errors arise. Accuracies of digital devices are generally held to be \pm one in the last digit read. The standard deviation of a digital device assuming that the likelihoods that the device will read one high, one low or right on are equal gives:

$$\sigma = \left(\frac{n^2 - 1}{12} \right)^{\frac{1}{2}} \quad (59)$$

where $n = 3$ in this case.

$$\sigma = \left(\frac{9 - 1}{12} \right)^{\frac{1}{2}}$$

$$\sigma = (0.75)^{\frac{1}{2}}$$

$$\sigma = 0.866 \text{ counts}$$

$$\sigma_{cec} = 0.0866 \text{ or } 0.09 \text{ cec}$$

This means that 0.09 cec or 14 yards of the error for one LOP attributable to the differential Omega corrector could be due to digitizing error and not error in the corrector device itself. This would mean that the digitizing error by itself could cause a CPE of 0.11 cec or 18 yds and a 95% circular error 0.23 cec or 37 yds. It is felt that while there is some digitizing error in the results presented in Figure 41, 0.09 cec is too large a value. The probability of being one count high is not necessarily the same as being one count low, and neither is the same as the probability of being right on but in general each is smaller. This would reduce the standard deviation of the digitizing error to something smaller than 0.09 cec but it is an undeterminable amount since the exact probabilities of each of the digitizing errors cannot be obtained.

3. Receiver Errors

All the results discussed previously have been using the assumption that the receiver at the monitor site and the mobile receiver would read the same if they were placed side by side and fed from the same antenna. This however is not the case for the receivers used in this experiment, the Tracor 599R. NELC conducted tests on three 599R receivers and concluded that they could be expected to agree to within 1 cec about half the time; to within 2 cec most of the time and to within 3 cec essentially all the time. These are not statistically analyzed results but are results of an intuitive analysis by the author of Ref. 22 [22]. Based on this

information, if Tracor 599R receivers were used as the monitor receiver and the mobile receiver, and both were receiving the same station and were theoretically on the same phase difference, the LOPs obtained would agree within 160 yds half the time, 320 yards most of the time and within 480 yds essentially all the time. This leads one to believe that in any experiment using two receivers, extensive analysis of their measurement errors should be undertaken first. If two receivers had been used in this experiment the 95% circular error of 52 yards would have been lost in the errors caused by the disparities between the two receivers. Tests conducted on two Tracor 599R receivers at the Naval Postgraduate School showed that when both receivers were tracking the same signal an error of as much as one cec occurred (see Fig. 42). Additional tests to show the difference between two channels on the same receiver tracking the same signal resulted in an error between the two channels of as much as 1.5 cec (see Fig. 43).

If Tracor 599R Omega receivers were again used as monitor and mobile receivers and both were receiving the same station but were theoretically on different phase LOPs, there could be as much as 1.4 cec difference between the two readings. This error is caused by what is known as S-curve error. S-curve error is caused by the receiver not displaying the correct phase for the phase fed into it. For example if a 0 cec signal were fed into the receiver it might read 0.3 cec. If a 50 cec signal were fed in, the

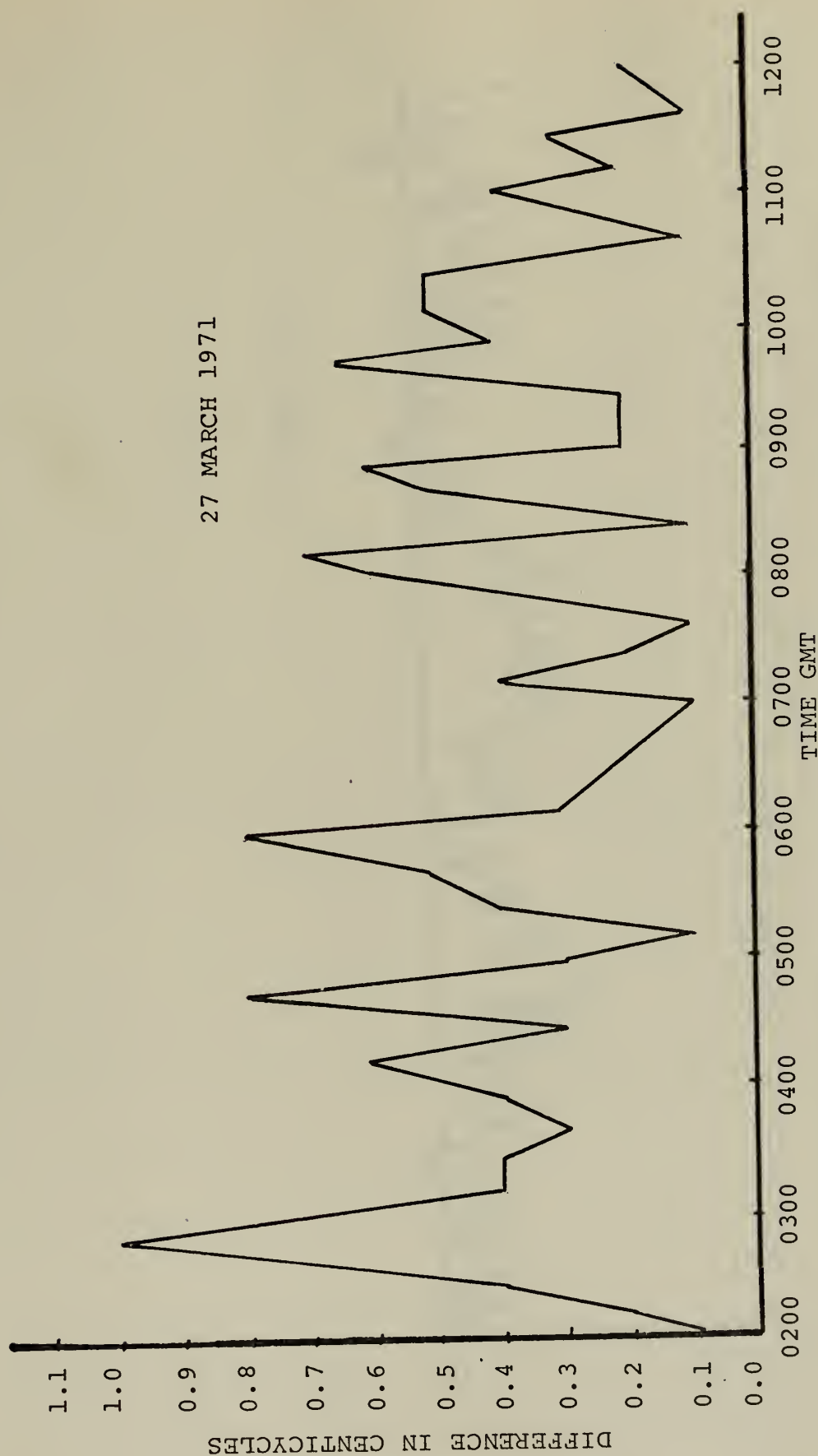


Figure 42. Difference Between Two Tracor 599R Receivers Tracking the Same Signal (Trinidad-Hawaii).

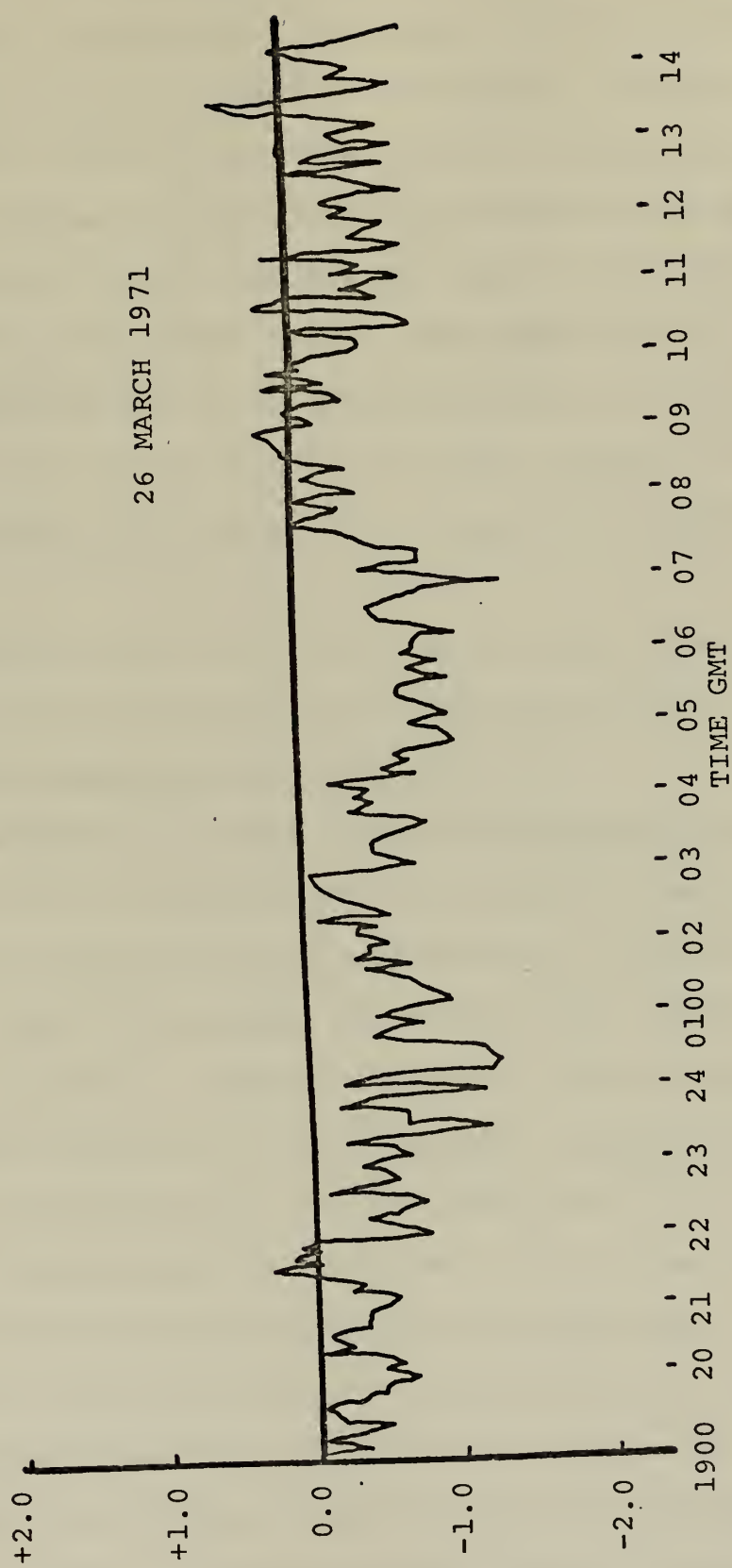


Figure 43. Difference Between Two Channels on the Same Tracor 599R Tracking the Same Signal.

receiver might read 50.8 cec and so on. The reason for this error being called S-curve error is because the shape of the curve of error vs input is generally "S" shaped. S-curve error is different from the error described in the preceding paragraph because there the signals being compared were the same phase whereas in this paragraph the signals have different phases. S-curve errors on the three NELC Tracor receivers ran from 0.6 to 1.4 cec peak to peak [22]. S-curve errors are believed to be caused by low level leakage of the internally generated 1 kHz signal in or around the tracking filters.

It should be noted that the receiver errors described in this section cannot be removed by differential Omega.

4. LOP Errors Caused by Ship Velocity

A ship moving at 15 knots along the baseline between two stations, X and Y is covering 8.34 yards/sec. The time difference between the stop of X's transmission and start of Y's could be over four seconds due to the Omega signal format shown in Figure 2. Therefore the ship could travel 25.36 yards toward station Y in four seconds. Assume that if the ship were standing still and the phase of X = 50 cec and Y = 25 cec, the phase difference then, X-Y = 25 cec. Now assume the ship is moving and station X's phase was received as 50 cec and stored until Y comes on the air. When Y's transmission arrives, the phase will not be 25 cec as before but will be 24.84 cec because the vessel has moved 25.36 (0.16 cec) toward Y during the four second interval

between X's and Y's transmissions. Thus X-Y = 25.16 cec causing a 25.36 yd. error in the LOP. This type of error can easily be removed by providing a biasing voltage for the readout circuit that can be adjusted to remove the error from each LOP. The bias voltage would be proportional to the velocity of the ship perpendicular to the LOPs in use and could be either positive or negative depending on whether the vessel was traveling toward or away from the Omega station.

D. ADVANTAGES AND DISADVANTAGES OF USING THE COAST GUARD RADIOBEACON AS A DIFFERENTIAL OMEGA CORRECTION TRANSMITTER

1. Advantages

The primary reason for the implementation of the CG radiobeacon differential Omega system is cost. The radio-beacon net is a fact of life, it is here and operating. The Omega system will be operational world-wide by the end of 1974. The use of the radiobeacon as a means of transmitting corrections would allow one system, Omega, to be used for both mid-ocean and coastal navigation.

As far as shipboard users are concerned, the only additional items needed for the minimum differential Omega installation would be a radiobeacon receiver and a frequency meter. Any ship using Omega as a navigation aid would undoubtably have a LF receiver aboard. The proposed system could be used by sophisticated computer oriented users, or the unsophisticated navigator without changing the message format.

The Raydist and Lorac systems both suffer from the fact that not only are expensive transmitter sites (three or four per chain) required every 200 n.mi. up and down the coast, but a continued operating cost would be incurred. The user would also be required to purchase special receivers in order to use these systems. In addition the range of these systems is reduced at night.

The Sercel system and Micro-Omega also require additional transmitter sites (one per station) to be built--with their continued operating cost--plus special receiving units on the ships. No cost figures are available for the Micro-Omega system hardware. The Sercel differential correcting receiver and standard Omega receiver will cost approximately one-third more than the Sercel Omega receiver alone. The receiver will cost approximately \$5000 without the differential correction receiver.

Loran A statitons cost \$250,000 each per year to operate. When the Omega system becomes operational with all stations at full power, it appears superfluous to continue operating Loran A stations. Estimated operating costs for Loran A over the next 30 years is 360 million dollars for the U.S. alone [24]. Loran C operation costs are even higher and furthermore the receivers cost at least \$20,000 for an automatic tracking receiver compared to \$4000 to \$7000 for an Omega receiver.

2. Disadvantages

One definite disadvantage common to all differential Omega systems is the basic lane ambiguity problem suffered

by the Omega system itself. The proposed radiobeacon system, the Sercel system and Micro-Omega are alike in that they cannot help solve the ambiguity problem. Raydist and Lorac are also subject to the lane ambiguity problems of Omega only on a smaller scale. Of course Loran A and C suffer no ambiguities so they have the advantage over Omega in this respect.

The Sercel and Micro-Omega systems have the advantage of being inherently automatic and therefore simpler for the navigator to operate. Demands on the attention of the navigator are likely to be greatest when he needs the additional accuracy of differential Omega and the simpler the system is to operate the better. Corrected position data should be available for convenient visual readout. For this reason an automatic system would be favored. This advantage for the Sercel and Micro-Omega systems would be eliminated in the automatic shipboard installation using the radiobeacon system described earlier. Whereas the Sercel and Micro-Omega systems are real time correction schemes, the radiobeacon LOP correction information could be as much as one minute old.

The use of the proposed continuous differential Omega transmissions from a radiobeacon will disrupt the radiobeacon chain transmission technique. This will require the reallocation of the frequencies in the radiobeacon band to allow the differential Omega transmission station to transmit continuously. The frequency reallocation would

permit the remaining radiobeacon transmitters to operate as they are presently but on different frequencies than the differential Omega station. An additional cost necessary to implement the proposed system would be the purchase of a power amplifier for the differential Omega radiobeacon station. The purpose of this amplifier would be to boost the range of the radiobeacon from its present 125 n.mi. to 200 n.mi. or more.

As the radiobeacons transmit in the low frequency range, receivers are subjected to a great deal of atmospheric noise particularly during thunder storms. The ground wave is rapidly attenuated and night and skywave interference can occur between the ground and skywaves.

The disadvantages presented above however are far outweighed by the economic and operational advantages of implementing the system using the presently installed radiobeacons.

VI. SUMMARY

The Omega navigation system will be implemented world-wide by the end of 1974. This system, using only eight transmitters, will be capable of providing navigators their choice of either 10 or 15 lines of position anywhere in the world. The Omega system will be able to secure world-wide navigation with only eight stations because the very low frequencies (10-14 kHz) employed show very little attenuation, good stability and excellent predictability. However VLF frequencies are subject to unpredictable (anomalous) effects caused primarily by the sun. Differential Omega is the process of observing the anomalous effects and disseminating correction information to users in the differential area. Persons using the differential information can theoretically expect to have fix accuracies of 0.26 to 0.5 n.mi. at 200 n.mi. from the monitor site. The error decreases as the distance to the monitor site decreases. These errors are a great improvement over the generally expected 1 to 2 n.mi. fix errors associated with the use of ordinary Omega and published skywave correction tables.

The presently operating system of U.S. Coast Guard radiobeacons was proposed by Goodman and McKaughan as a logical and inexpensive method of transmitting differential Omega information to users nearby. Their proposed systems were examined and improvements suggested. In addition, two

other differential Omega systems were examined and their advantages and disadvantages discussed. It was concluded that the radiobeacon system provided the most economic method of implementing a differential Omega system.

Other coastal navigation systems were also examined but the use of differential Omega along with Omega appears to be the best solution since it can provide both mid-ocean and coastal navigation information with a minimum expenditure for both the user and the government. The radiobeacon system has another great advantage in that the differential information can be extracted from the radiobeacon using as sophisticated a system as the user can afford--starting with only an analog frequency meter, through a more expensive digital frequency meter, then to a special purpose computer and on to a sub-routine on a large shipboard computer for the highly sophisticated user.

A differential Omega LOP device was built and tested in a closed loop transmission system to determine its accuracy. A CPE of 25 yards and a 95% circular error of 52 yards were obtained at the monitor site. These results were analyzed and it was found that up to 18 yds of the CPE and 37 yds of the 95% circular error could be attributed to digitizing errors in the measuring equipment.

Receiver errors are a major source of error in trying to optimize a differential Omega system. It was shown that receiver errors can be on the same order of magnitude as the spatial correlation errors out to distances of about 100 n.mi.

and are a considerable percentage in size of the spatial correlation error out to much greater distances. The receiver errors are added to the errors predicted by the spatial correlation model causing gross errors compared to the errors of the differential Omega LOP corrector constructed for this thesis. For this reason it has been concluded that to derive the maximum benefit from the use of differential Omega that a receiver with an S-curve error and a repeatability error of no larger than 0.1 cec will be required for use both at the monitor and mobile sites. Ship velocity errors can be removed by the addition to the receiver of LOP velocity correctors.

It is strongly felt that any decision on a differential Omega system should be delayed until the entire 8 station Omega system is operating at the rated 10 kW of power. Only then can an intelligent decision as to the full capabilities of Omega and differential Omega be made. To dismiss the many advantages of the use of differential Omega based on the presently available low power station would be a serious error.

Future research efforts should include actual "on the air" testing in some location where there is an accurate navigation system available against which to measure the proposed system's error. This study should include both day and night testing to identify the errors caused by the interference caused by skywaves as well as low signal to noise ratios for the radiobeacon signal.

The system proposed in this thesis limits the correction information to only ± 50 cec. Fifty centicycles is not adequate correction in all cases. For example, from 0030-0415 GMT, 1-15 April 1972 the skywave correction is greater than -50 cec for the geographic position of the Naval Postgraduate School using Trinidad-Hawaii (B-C) at 10.2 kHz. If the error in the LOP exceeds 50 cec then the sign of the correction message abruptly changes as the increasing error goes through 50 cec. This can cause an error of one complete lane for a vessel which moments ago had its ambiguity problem solved. Future researchers should consider some means of identifying these occurrences.

The correction message is presently restricted to one minute lengths. This was done originally in order to allow the differential Omega transmission to fit into the one minute transmission segments presently being used by the five transmitter radiobeacon chains. However this restriction has since been removed because it was realized that differential Omega transmissions spaced five minutes apart were not sufficiently accurate. The correction message should now be examined by future researchers from the standpoint of the best format from the users point of view. Any changes made to the format proposed in this thesis should strike a balance between user acceptability and minimum time between correction messages for any particular LOP. The minimum time criterion is in order to reduce the errors arising during normal, rapid phase changes during the

day-night, night-day transition period. Any new message format can easily be incorporated into the commutator circuit designed in thesis by changing the read only memory truth table.

One last area of future research could be the design of the special purpose computer to be used in the automatic differential Omega correction system on board larger ships.

APPENDIX A

READ ONLY MEMORY TRUTH TABLE

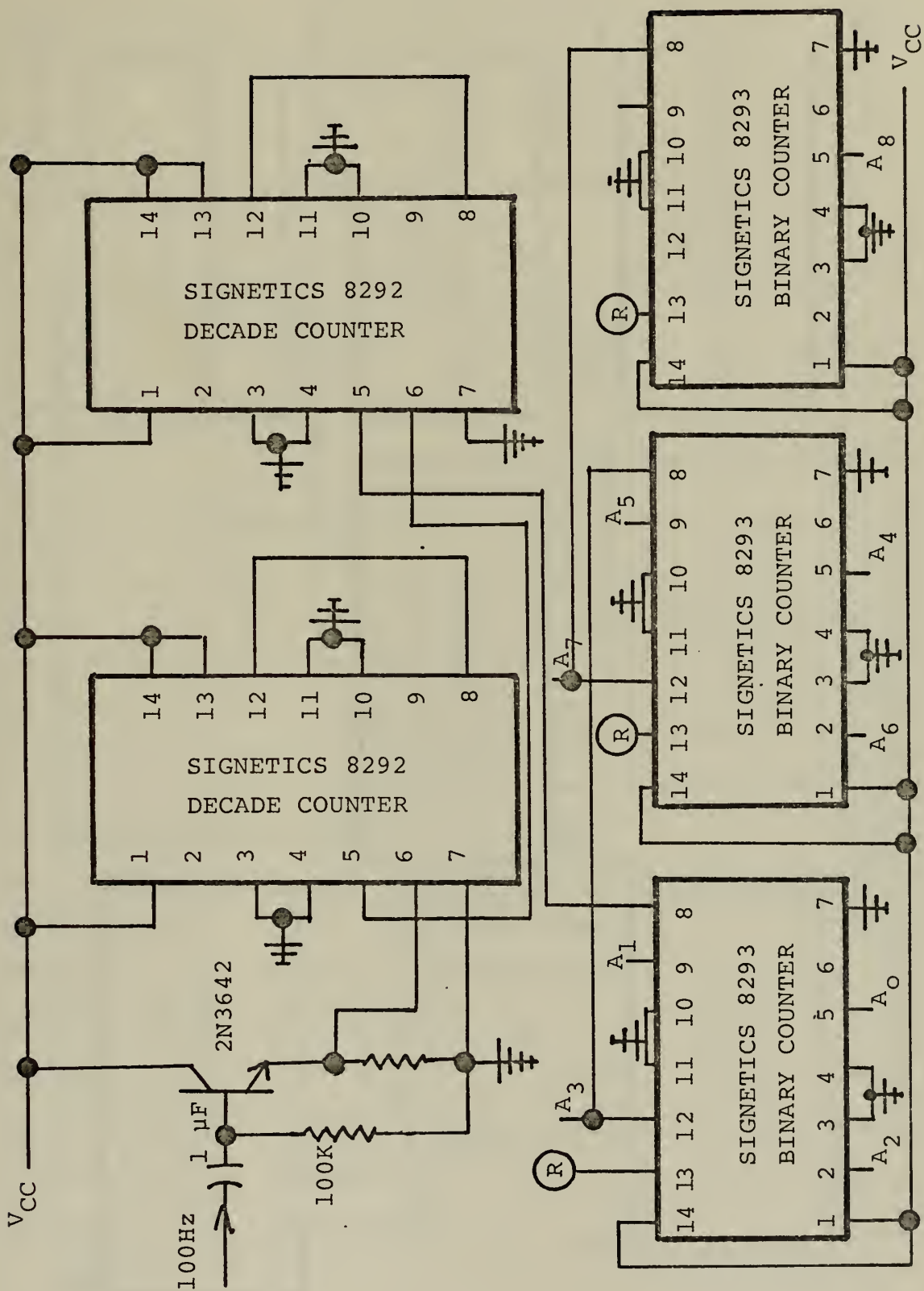
Word	OUTPUT																		
	O ₄	O ₃	O ₂	O ₁		O ₄	O ₃	O ₂	O ₁		O ₄	O ₃	O ₂	O ₁		O ₄	O ₃	O ₂	O ₁
0					70					140					210				
1					71					141					211				
2					72					142					212				
3					73					143					213				
4					74					144					214				
5					75					145					215				
6					76					146					216				
7					77					147					217				
8					78					148					218				
9					79					149					219				
10					80					150					220				
11					81					151					221				
12					82					152					222				
13					83					153					223				
14					84					154					224				
15					85					155					225				
16					86					156					226				
17					87					157					227				
18					88					158					228				
19					89					159					229				
20					90					160					230				
21					91					161					231				
22					92					162					232				
23					93					163					233				
24					94					164					234				
25					95					165					235				
26					96					166					236				
27					97					167					237				
28					98					168					238				
29					99					169					239				
30					100					170					240				
31					101					171					241				
32					102					172					242				
33					103					173					243				
34					104					174					244				
35					105					175					245				
36					106					176					246				
37					107					177					247				
38					108					178					248				
39					109					179					249				
40					110					180					250				
41					111					181					251				
42					112					182					252				
43					113					183					253				
44					114					184					254				
45					115					185					255				
46					116					186					256				
47					117					187					257				
48					118					188					258				
49					119					189					259				
50					120					190					260				
51					121					191					261				
52					122					192					262				
53					123					193					263				
54					124					194					264				
55					125					195					265				
56					126					196					266				
57					127					197					267				
58					128					198					268				
59					129					199					269				
60					130					200					270				
61					131					201					271				
62					132					202					272				
63					133					203					273				
64					134					204					274				
65					135					205					275				
66					136					205					276				
67					137					207					277				
68					138					208					278				
69					139					209					279				

Word	OUTPUT				Word	OUTPUT				Word	OUTPUT				Word	OUTPUT			
	O ₄	O ₃	O ₂	O ₁		O ₄	O ₃	O ₂	O ₁		O ₄	O ₃	O ₂	O ₁		O ₄	O ₃	O ₂	O ₁
280					350					420					490				
281					351					421					491				
282					352					422					492				
283					353					423					493				
284					354					424					494				
285					355					425					495				
286					356					426					496				
287					357					427					497				
288					358					428					498				
289					359					429					499				
290					360					430					500				
291					361					431					501				
292					362					432					502				
293					363					433					503				
294					364					434					504				
295					365					435					505				
296					366					436					506				
297					367					437					507				
298					368					438					508				
299					369					439					509				
300					370					440					510				
301					371					441					511				
302					372					442					512				
303					373					443					513				
304					374					444					514				
305					375					445					515				
306					376					446					516				
307					377					447					517				
308					378					448					518				
309					379					449					519				
310					380					450					520				
311					381					451					521				
312					382					452					522				
313					383					453					523				
314					384					454					524				
315					385					455					525				
316					386					456					526				
317					387					457					527				
318					388					458					528				
319					389					459					529				
320					390					460					530				
321					391					461					531				
322					392					462					532				
323					393					463					533				
324					394					464					534				
325					395					465					535				
326					396					466					536				
327					397					467					537				
328					398					468					538				
329					399					469					539				
330					400					470					540				
331					401					471					541				
332					402					472					542				
333					403					473					543				
334					404					474					544				
335					405					475					545				
336					406					476					546				
337					407					477					547				
338					408					478					548				
339					409					479					549				
340					410					480					550				
341					411					481					551				
342					412					482					552				
343					413					483					553				
344					414					484					554				
345					415					485					555				
346					416					486					556				
347					417					487					557				
348					418					488					558				
349					419					489					559				

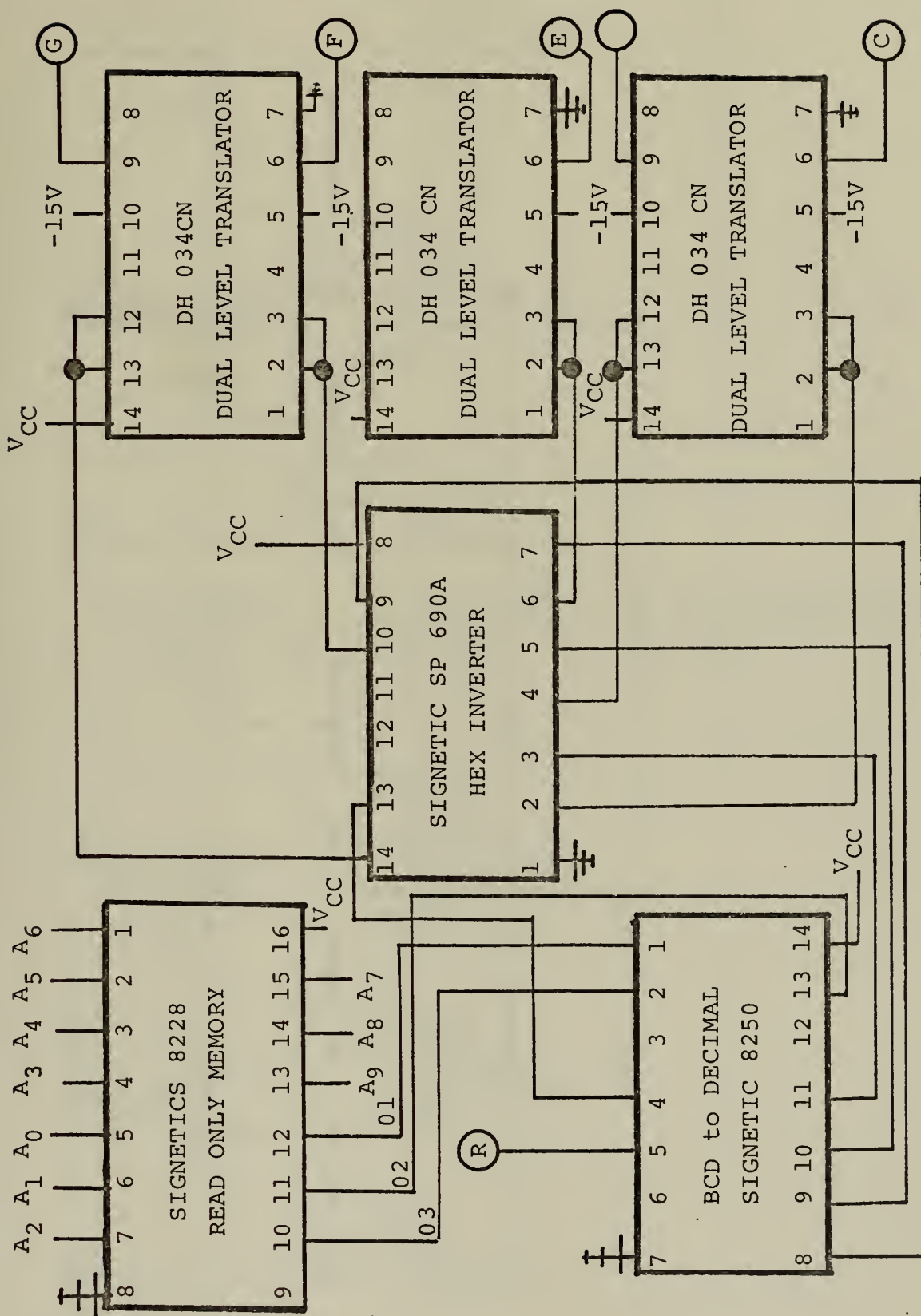
Word	OUTPUT				Word	OUTPUT				Word	OUTPUT				Word	OUTPUT			
	O ₄	O ₃	O ₂	O ₁		O ₄	O ₃	O ₂	O ₁		O ₄	O ₃	O ₂	O ₁		O ₄	O ₃	O ₂	O ₁
560					630					700					770				
561					631					701					771				
562					632					702					772				
563					633					703					773				
564					634					704					774				
565					635					705					775				
566					636					706					776				
567					637					707					777				
568					638					708					778				
569					639					709					779				
570					640					710					780				
571					641					711					781				
572					642					712					782				
573					643					713					783				
574					644					714					784				
575					645					715					785				
576					646					716					786				
577					647					717					787				
578					648					718					788				
579					649					719					789				
580					650					720					790				
581					651					721					791				
582					652					722					792				
583					653					723					793				
584					654					724					794				
585					655					725					795				
586					656					726					796				
587					657					727					797				
588					658					728					798				
589					659					729					799				
590					660					730					800				
591					661					731					801				
592					662					732					802				
593					663					733					803				
594					664					734					804				
595					665					735					805				
596					666					736					806				
597					667					737					807				
598					668					738					808				
599					669					739					809				
600					670					740					810				
601					671					741					811				
602					672					742					812				
603					673					743					813				
604					674					744					814				
605					675					745					815				
606					676					746					816				
607					677					747					817				
608					678					748					818				
609					679					749					819				
610					680					750					820				
611					681					751					821				
612					682					752					822				
613					683					753					823				
614					684					754					824				
615					685					755					825				
616					686					756					826				
617					687					757					827				
618					688					758					828				
619					689					759					829				
620					690					760					830				
621					691					761					831				
622					692					762					832				
623					693					763					833				
624					694					764					834				
625					695					765					835				
626					696					766					836				
627					697					767					837				
628					698					768					838				
629					699					769					839				

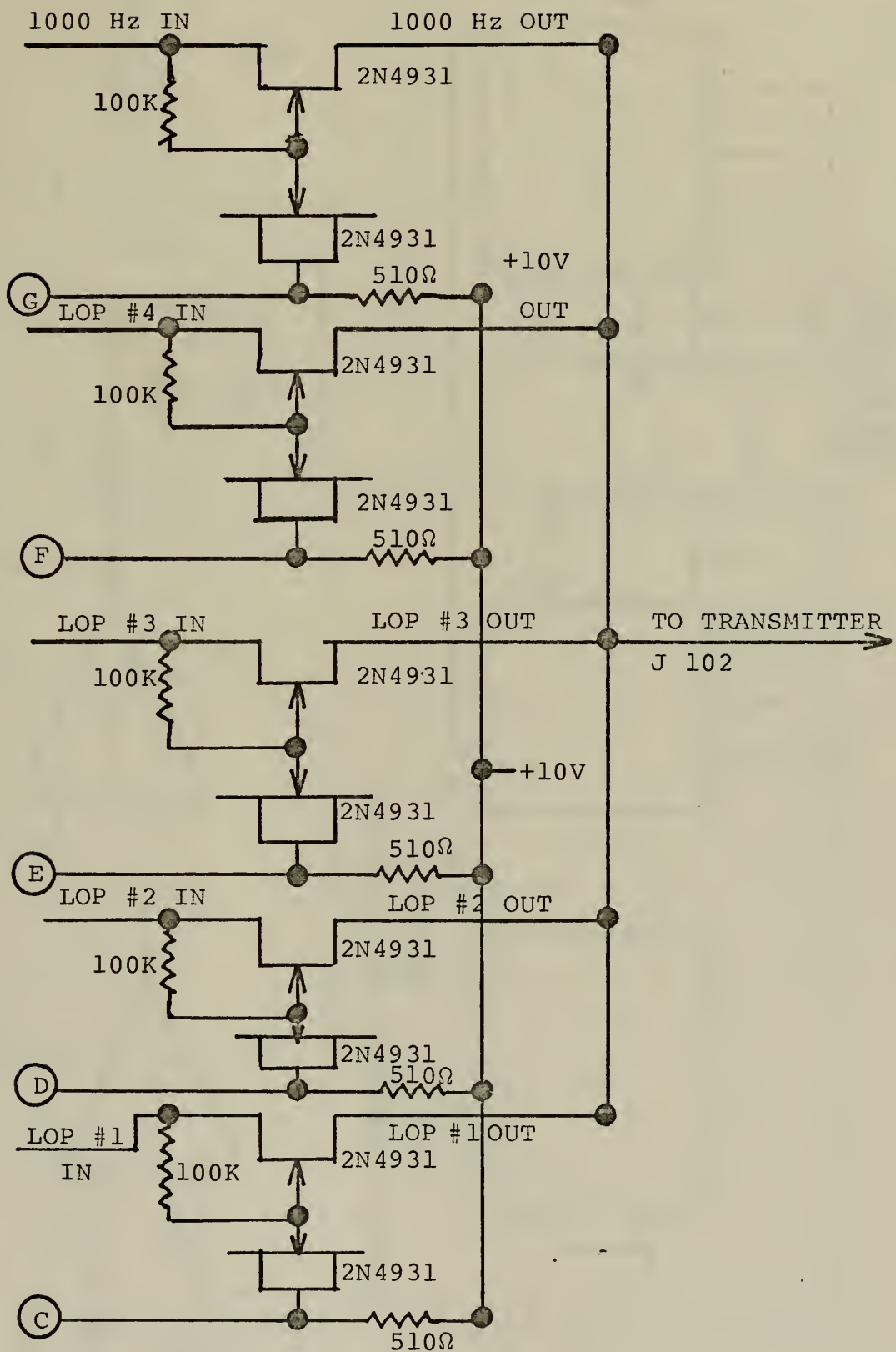
Word	OUTPUT				Word	OUTPUT				Word	OUTPUT				Word	OUTPUT			
	O ₄	O ₃	O ₂	O ₁		O ₄	O ₃	O ₂	O ₁		O ₄	O ₃	O ₂	O ₁		O ₄	O ₃	O ₂	O ₁
840					910					980									
841					911					981									
842					912					982									
843					913					983									
844					914					984									
845					915					985									
846					916					986									
847					917					987									
848					918					988									
849					919					989									
850					920					990									
851					921					991									
852					922					992									
853					923					993									
854					924					994									
855					925					995									
856					926					996									
857					927					997									
858					928					998									
859					929					999									
860					930					1000									
861					931					1001									
862					932					1002									
863					933					1003									
864					934					1004									
865					935					1005									
866					936					1006									
867					937					1007									
868					938					1008									
869					939					1009									
870					940					1010									
871					941					1011									
872					942					1012									
873					943					1013									
874					944					1014									
875					945					1015									
876					946					1016									
877					947					1017									
878					948					1018									
879					949					1019									
880					950					1020									
881					951					1021									
882					952					1022									
883					953					1023									
884					954														
885					955														
886					956														
887					957														
888					958														
889					959														
890					960														
891					961														
892					962														
893					963														
894					964														
895					965														
896					966														
897					967														
898					968														
899					969														
900					970														
901					971														
902					972														
903					973														
904					974														
905					975														
906					976														
907					977														
908					978														
909					979														

APPENDIX B
COMMUTATOR CIRCUIT



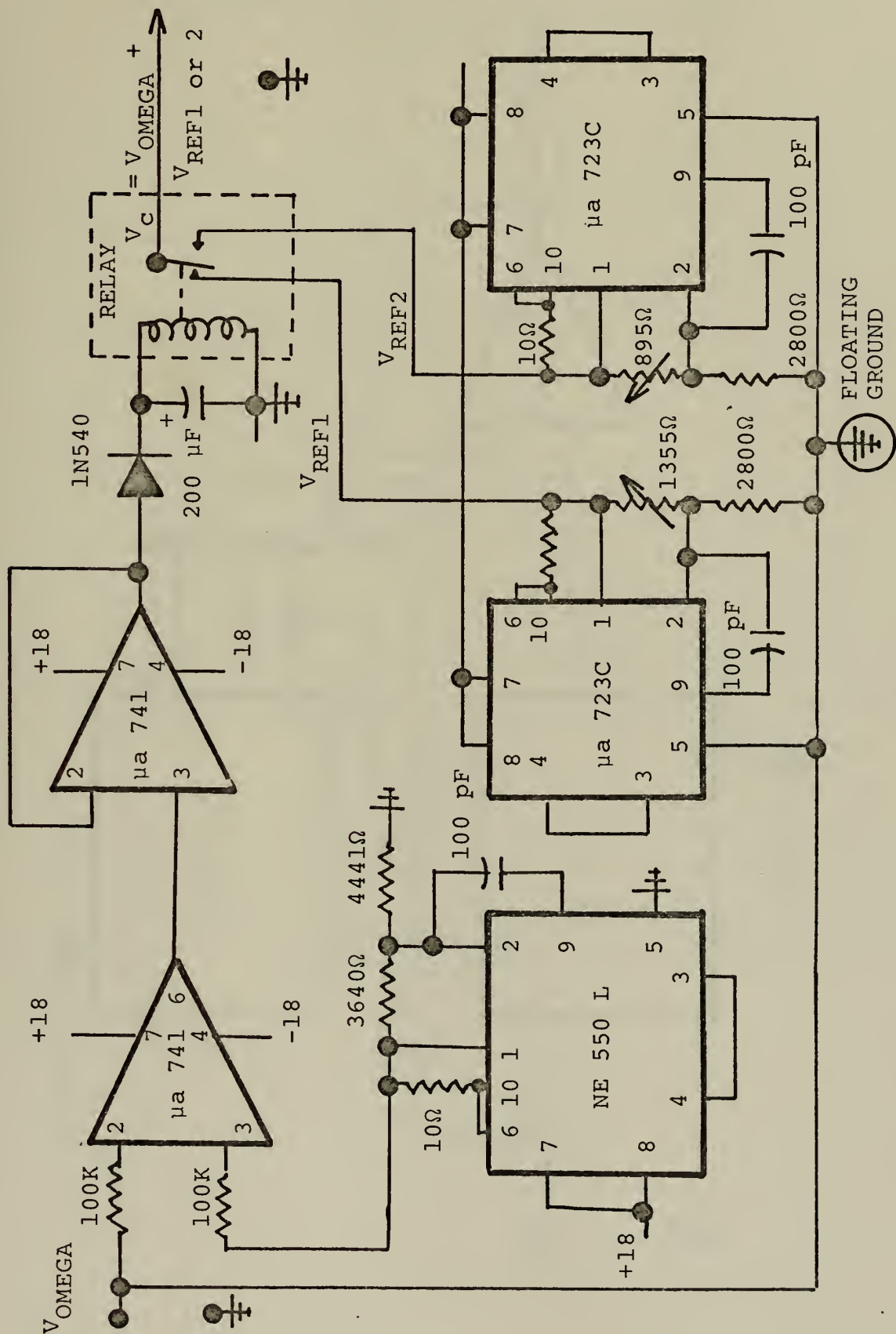
APPENDIX B
COMMUTATOR CIRCUIT

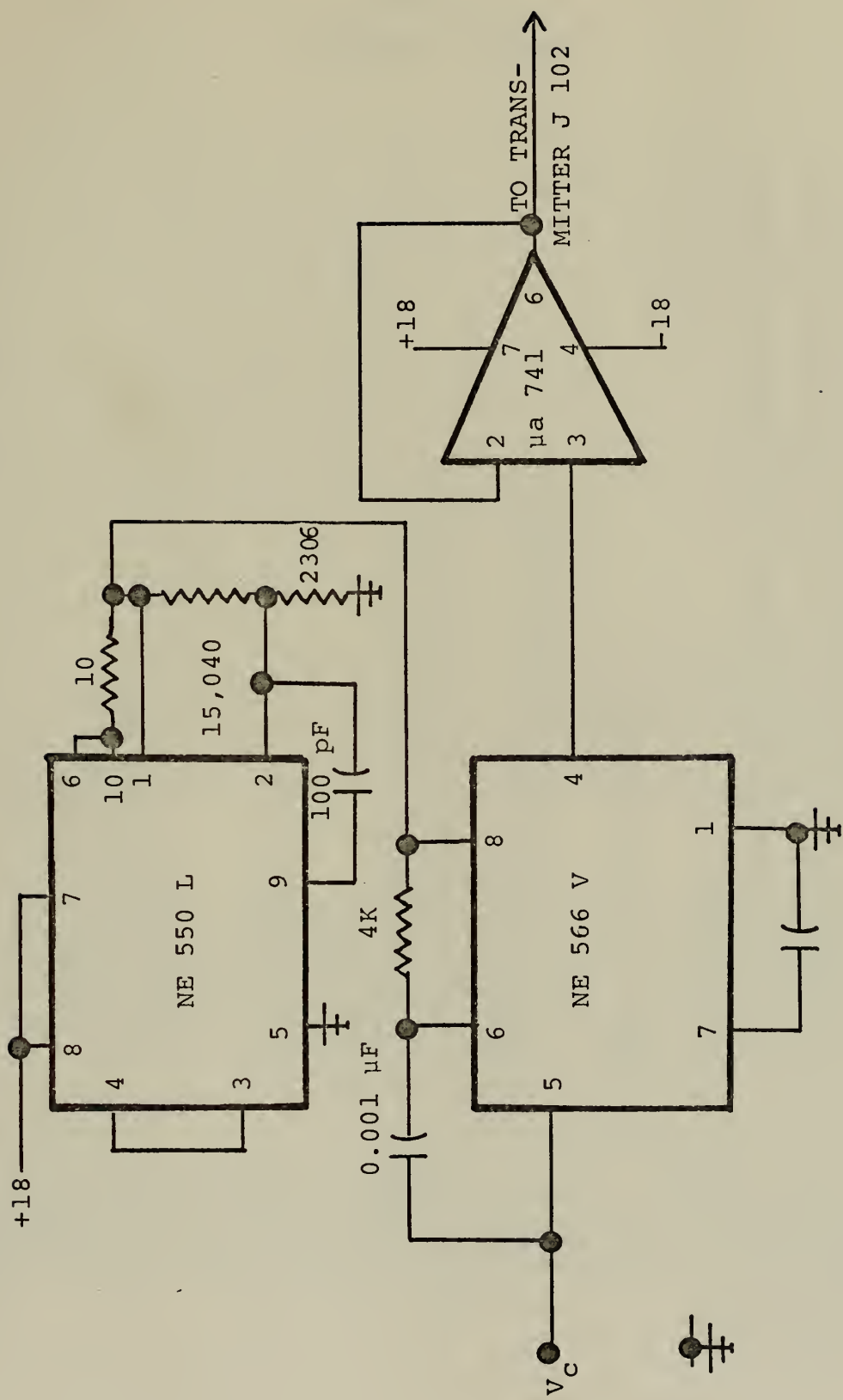




APPENDIX C

DIFFERENTIAL OMEGA LOP CORRECTOR CIRCUIT





DIMENSION NMEDAT(20)

```

3  NM=0
    SUMSX=0.0
    READ(5,1000) (NMEDAT(I), I=1,20)
    WRITE(6,2000) (NMEDAT(I), I=1,20)

4  READ(5,1010) OMEGA,FRQSYN,NEND,NAND
    IF(OMEGA.GE.58.0) GO TO 5
    OMEGAI = OMEGA-8.0
    COFREQ = 1000-OMEGAI*10
    GO TO 10
    OMEGAI = 108.0-OMEGA
    COFREQ = OMEGAI*10+1000
    IF(OMEGA.GT.58.0.OF.OMEGA.LE.8.0) GO TO 11
    FRQERR = FRQSYN-COFREQ
    GO TO 12
    FRQSYN = FRQSYN + 1000
    FRQERR = FRQSYN-COFREQ
    ERRCEC = FRQEP/10
    IF(ERRCEC.GT.1.0.OR.ERRCEC.LT.-1.0) GO TO 16
    WRITE(6,2040) OMEGA,FRQSYN,OMEGAI,COFREQ,ERRCEC
    GO TO 7
    SUMSX = SUMSX+ERRCEC
    SUMSX = SUMSX+(ERRCEC**2)
    N=N+1
    WRITE(6,2020) OMEGA,FRQSYN,OMEGAI,COFREQ,ERRCEC
    IF(NEND.NE.99) GO TO 4
    DN=DN
    EXPV = SUMX/DN
    VARY = (DN*SUMSX-(SUMX**2))/(DN**2)
    SD = VARY**0.5
    WRITE(6,2030) EXPV,SD
    FORMAT(20A4)
    1000 FORMAT(F10.1,F10.0,F11.0)
    1010 FORMAT(1H1,25X,20A4//)
    2000 FORMAT(33X,OMEGA,9X,FRQSYN',10X,'OMEGAI',9X,'COFREQ',9X,'ERRCEC
    1      ')
    2020 FORMAT(31X,5(1PE10.3,5X))
    2030 FORMAT(11X,'NSRGO-ERRCEC AVERAGE ERRCEC = ',F5.2,6X,'STD DEV ERRCEC = ',F6.2
    1      )
    2040 FORMAT(11X,'NSRGO-ERRCEC GT 1.0',5(1PE10.3,5X))
    IF(NAND.EQ.99) GO TO 3
    STOP
END

```


LOW DIFFERENTIAL OMEGA WITH TRANS 1612Z 30 MARCH 72 TO 1612Z 31 MARCH 72

APPENDIX E

COMPUTER PRINTOUT

OMEGA	FRQSYN	COFREQ	ERRCEC
1.820E-01	8.980E-02	1.020E-01	8.980E-02
1.760E-01	9.040E-02	9.600E-00	9.040E-02
1.610E-01	9.190E-02	8.150E-00	9.190E-02
1.450E-01	9.350E-02	6.500E-00	9.350E-02
1.320E-01	9.470E-02	5.200E-00	9.480E-02
1.210E-01	9.590E-02	4.100E-00	9.590E-02
1.020E-01	9.780E-02	2.200E-00	9.780E-02
8.800E-00	9.920E-02	8.000E-01	9.920E-02
7.400E-00	1.006E-03	-6.000E-01	1.006E-03
6.000E-00	1.019E-03	-2.000E-00	1.020E-03
4.000E-00	1.040E-03	-4.000E-00	1.040E-03
2.600E-00	1.054E-03	-5.400E-00	1.054E-03
2.000E-01	1.077E-03	-7.600E-00	1.076E-03

AVERAGE ERRCEC = -0.02

STD DEV ERRCEC = 0.07

OMEGA	FRQSYN	COFREQ	ERRCEC
9.020E-01	1.179E-03	1.178E-03	1.000E-01
9.040E-01	1.176E-03	1.176E-03	0.0
9.060E-01	1.174E-03	1.174E-03	0.0
9.080E-01	1.172E-03	1.172E-03	0.0
9.110E-01	1.168E-03	1.169E-03	-1.000E-01
9.140E-01	1.163E-03	1.163E-03	0.0
9.170E-01	1.161E-03	1.163E-03	0.0
9.200E-01	1.156E-03	1.155E-03	1.000E-01
9.220E-01	1.157E-03	1.153E-03	-1.000E-01
9.250E-01	1.151E-03	1.151E-03	0.0
9.290E-01	1.147E-03	1.147E-03	0.000E-01
9.330E-01	1.142E-03	1.141E-03	1.000E-01
9.390E-01	1.138E-03	1.138E-03	0.0
9.420E-01	1.137E-03	1.136E-03	1.000E-01
9.449E-01	1.137E-03	1.129E-03	1.000E-01
9.510E-01	1.120E-03	1.122E-03	1.000E-01
9.580E-01	1.123E-03	1.119E-03	1.000E-01
9.610E-01	1.120E-03	1.111E-03	1.000E-01
9.690E-01	1.112E-03	1.105E-03	1.000E-01
9.750E-01	1.106E-03	1.010E-03	1.000E-01
9.790E-01	1.102E-03	1.097E-03	0.0
9.830E-01	1.094E-03	1.092E-03	2.000E-01
9.890E-01	1.094E-03	1.092E-03	2.000E-01

AVERAGE ERRCEC = 0.055

STD DEV ERRCEC = 0.06

BIBLIOGRAPHY

1. Albee, P. R. and Bates, H. F., "VLF Observations at College, Alaska, of Various D-Region Disturbance Phenomena," Planetary and Space Science, Vol. 13, p. 175-206, March 1965.
2. Asche, G. P., "Implementation Status of the Omega Navigation System," Proceedings ION Omega Symposium, Washington, D.C., November 1971.
3. Cawley, John, Review of Marine Navigation Systems and Techniques, NObsr-81564-SS-050, January 1965.
4. Crombie, D. D., The Propagation of VLF Signals over Long Distances, NBS course in radio propagation, Lecture no. 30, Summer 1961.
5. Crombie, D. D., Chilton, C. J., and Jean. A. G., Phase Variations in VLF Propagation, NBS course in radio propagation, Lecture no. 32, Summer 1961.
6. D'Appolito, Joseph A., and Kasper, Joseph F., Jr., "Predicted Performance of an Integrated Omega/Inertial Navigation System," Proceedings 1971 National Aerospace Electronics Conference, Dayton, Ohio, May 1971.
7. Goodman, G. R., A Proposed Differential Omega System, M.S.E.E. Thesis, Naval Postgraduate School, Monterey, California, 1969.
8. Hastings, Charles E., and Barkely, A. Clifford, "Automatic Real Time Omega Accuracy Enhancement," Journal of Institute of Navigation, Vol. 18, No. 2, Summer 1971.
9. Jean. A. G., VLF Propagation-II, NBS course in radio propagation, Lecture no. 11, Summer 1961.
10. Kasper, J. F., Jr., "A Skywave Correction Adjustment Procedure for Improved Omega Accuracy," Paper presented to the ION National Marine Meeting, U.S.C.G. Academy, 12 October 1970.
11. Kasper, Joseph F., Jr., "Evaluation of Omega Configurations for Airways System Operations," Proceedings of ION Marine Meeting, April 1971.

12. Kasper, Joseph F., Jr., "Omega Utilization by Non-Military Subscribers," Proc. ION Omega Symposium, Washington, D.C., November 1971.
13. McKaughan, M. E., Analysis of a Proposed Differential Omega System, M.S.E.E. Thesis, Naval Postgraduate School, Monterey, California, 1970.
14. Nard, Georges, "Results of Recent Experiments with Differential Omega," Proceedings ION Omega Symposium, Washington, D.C., November 1971.
15. Naval Electronics Laboratory Center Technical Document 26, Omega Propagation Correction Technique Study, by Nortronics a division of Northrop Corp., March 1968.
16. Naval Electronics Laboratory Report 1207, Project Fishbowl Effects on Omega VLF Transmissions, by C. J. Casselman, R. L. Denton and J. J. Wilson, December 1963.
17. Naval Electronics Laboratory Center Technical Note, TN-1375, Remarks on the Propagation of 10.2 kHz Electromagnetic Waves: The Effects of Bearing, Total Magnetic Field Strength, Dip Angle of the Magnetic Field and Ground Conductivity, by E. R. Swanson, March 1968.
18. Naval Electronics Laboratory Center Technical Report, TR 1781, Diurnal Phase Variation at 10.2 kHz, by E. R. Swanson and W. R. Brandford, August 1971.
19. Naval Electronics Laboratory Technical Note TN-1767, Experimental Research Results on the Accuracy of Differential Omega and of VLF DF System, by E. E. Gossard and C. G. Norgard, November 1970.
20. Naval Research Laboratory, Accuracy Studies of the Differential Omega Technique, by K. Luken, J. W. Brogden and W. D. Meyers, June 1970.
21. Naval Electronics Laboratory Center Technical Report, TR 1757, Omega Synchronization and Control, by E. R. Swanson and C. P. Kugel, March 1971.
22. Naval Electronics Laboratory Center Technical Note, TN-1529, Accuracy Tests on Tracor 3-599R Omega Receivers, by J. E. Britt, August 1969.
23. Pierce, J. A., Palmer, W., Watt, A. D., and Woodward, R. H., Omega, A World Wide Navigation System, P&B Pub. No. 886B, Pickard and Burns Electronics, 2nd ed., May 1966.

24. Pierce, J. A. and Woodward, R. H., "The Development of Long-Range Hyperbolic Navigation in the United States," Journal of the Institute of Navigation, Vol 18, No 1, Spring 1971.
25. Scientific Management Associates, Inc., Differential Omega Feasibility Test, NObsr-95105, June 1967.
26. Sechrist, C. F., Jr., "VLF Anomalies Observed at State College, Pa., During the U.S. 1962 High-Altitude Nuclear Tests," Radio Science, Vol. 68D, No. 1, pp. 125-133, January 1964.
27. Straker, T. W., "The Ionospheric Reflection of Radio Waves of 16 kHz Over Short Distances," IEE, part C, Jan 1955.
28. Swanson, E. R., Omega (personal communication).
29. Tibbals, M. L., "Omega Navigation System," paper presented before NATO Study Group 2 Conference, NATO Building, Paris, France 1-10 April 1967.
30. Tracor, Inc. Report 67-135-U, Final Technical Report, Differential Omega Test and Evaluation Program, 18 January 1967.
31. U.S. Naval Oceanographic Office, "Omega Skywave Correction Tables," H. O. Publication No. 224 (101-C), Jan 1972.
32. Watt, A. D., VLF Radio Engineering, 1st ed., Pergamon Press, 1967.
33. Westfall, W. D., "Diurnal Changes of Phase and Group Velocity of VLF Radio Waves," Radio Science, Vol. 2, No. 1, pp. 119-125, January 1967.

INITIAL DISTRIBUTION LIST

	No. Copies
1. Defense Documentation Center Cameron Station Alexandria, Virginia 22314	2
2. Library, Code 0212 Naval Postgraduate School Monterey, California 93940	2
3. Commandant U.S. Coast Guard NASSIF Building 400 Seventh Street, S.W. Washington, D.C. 20591	1
4. Professor C. E. Menneken, Code 023 Dean of Research Naval Postgraduate School Monterey, California 93940	5
5. Assistant Professor R. W. Adler, Code 52ab Department of Electrical Engineering Naval Postgraduate School Monterey, California 93940	1
6. LCDR R. L. Vence, Jr. USCG Communication Staff NASSIF Building 400 Seventh Street, S.W. Washington, D.C. 20591	2

UNCLASSIFIED

Security Classification

DOCUMENT CONTROL DATA - R & D

(Security classification of title, body of abstract and indexing annotation must be entered when the overall report is classified)

1. ORIGINATING ACTIVITY (Corporate author)	2a. REPORT SECURITY CLASSIFICATION Unclassified
Naval Postgraduate School Monterey, California 93940	2b. GROUP

3. REPORT TITLE

IMPLEMENTATION AND TESTING OF A PROPOSED DIFFERENTIAL OMEGA SYSTEM

4. DESCRIPTIVE NOTES (Type of report and, inclusive dates)

Electrical Engineer's Thesis; June 1972

5. AUTHOR(S) (First name, middle initial, last name)

Robert Lawrence Vence, Jr.; Lieutenant Commander, U.S. Coast Guard

6. REPORT DATE June 1972	7a. TOTAL NO. OF PAGES 148	7b. NO. OF REFS 33
8a. CONTRACT OR GRANT NO.	9a. ORIGINATOR'S REPORT NUMBER(S)	
b. PROJECT NO.		
c.		
d.	9b. OTHER REPORT NO(S) (Any other numbers that may be assigned this report)	

10. DISTRIBUTION STATEMENT

Approved for public release; distribution unlimited.

11. SUPPLEMENTARY NOTES	12. SPONSORING MILITARY ACTIVITY Naval Postgraduate School Monterey, California 93940
-------------------------	---

13. ABSTRACT

Omega is a very low frequency (VLF) navigation system which will give world-wide coverage with eight stations when fully implemented. Using published skywave correction tables accuracies of 1 to 2 n.mi. are attainable. Through the use of differential Omega, correction information can be disseminated to users in the vicinity of a monitor site. Differential Omega accuracies are directly proportional to distance from the monitor site and are 0.26 - 0.5 n.mi. at 200 n.mi. from the monitor site.

A system using U.S. Coast Guard radiobeacons as the differential information transmitter was proposed by Goodman and McKaughan. Their proposals were examined and improvements suggested. Two additional differential Omega systems being proposed by civilian contractors were also examined.

The interface between an Omega receiver and the radiobeacon was built and tested. The device produced a CPE of 25 yds. (0.16 cec) and a 95% circular error of 52 yds. (0.32 cec) at the monitor site for LOPs crossing at 72° which is a marked improvement over accuracies that can be attained using skywave correction tables.

DD FORM 1 NOV 65 1473

(PAGE 1)

S/N 0101-807-6811

147

UNCLASSIFIED
Security Classification

A-31408

UNCLASSIFIED

Security Classification

KEY WORDS	LINK A		LINK B		LINK C	
	ROLE	WT	ROLE	WT	ROLE	WT
OMEGA						
HYPERBOLIC NAVIGATION						
DIFFERENTIAL OMEGA						
RELATIVE OMEGA						
RADIOBEACON						
VLF PROPAGATION						
VLF PHASE ANOMALIES						

10 FEB 74 23091
7 FEB 77 24688
10 MAR 77 24688
6 MAR 79 25441

Thesis 134925
V365 Vence
c.1 Implementation and
 testing of a proposed
 differential omega sys-
 tem. 23091
10 FEB 74 24688
7 FEB 77 24688
10 MAR 77 25441
6 MAR 79

Thesis 134925
V365 Vence
c.1 Implementation and
 testing of a proposed
 differential omega sys-
 tem.

